

LATERAL SEISMIC VELOCITY GRADIENTS ON GEORGES BANK,
U.S. ATLANTIC CONTINENTAL MARGIN: A COMPARISON
OF SEISMIC COMMON DEPTH POINT (CDP) MOVEOUT
VELOCITY WITH SONIC AND CHECKSHOT
VELOCITIES FROM TEN
EXPLORATORY WELLS.

by

MD. NOOR ALAM

November, 1988.

ProQuest Number: 10783424

All rights reserved

INFORMATION TO ALL USERS

The quality of this reproduction is dependent upon the quality of the copy submitted.

In the unlikely event that the author did not send a complete manuscript and there are missing pages, these will be noted. Also, if material had to be removed, a note will indicate the deletion.



ProQuest 10783424

Published by ProQuest LLC (2018). Copyright of the Dissertation is held by the Author.

All rights reserved.

This work is protected against unauthorized copying under Title 17, United States Code
Microform Edition © ProQuest LLC.

ProQuest LLC.
789 East Eisenhower Parkway
P.O. Box 1346
Ann Arbor, MI 48106 – 1346

T-3667

A thesis submitted to the Faculty and the Board of Trustees of the Colorado School of Mines in partial fulfillment of the requirements for the degree of Master of Science (Geophysics).

Golden, Colorado
Date 11/11/88

Signed: Md. Noor Alam
Md. Noor Alam

Approved: John A. Grow
Dr. John A. Grow
Thesis Advisor, and

Alfred H. Balch
Professor A. H. Balch
Thesis Advisor

Golden, Colorado
Date 11/11/88

P. R. Romig
Professor Phillip R. Romig
Professor and Head,
Department of Geophysics

ABSTRACT

The tectonic evolution of a passive margin creates distinctive crustal structures, and sedimentary distribution patterns. The primary structural elements of the Georges Bank basin are typical of passive continental margins. The sedimentary column underneath Georges Bank is mainly a thick sequence of Jurassic age overlain by a much thinner section of Cretaceous to Cenozoic age. Paleoenvironment of the Jurassic period favoured the development of a certain type of sedimentary sequence along the continental margins. The purpose of this study is to identify lithologic sequences and their changes along and across the shelf area in the Georges Bank. Availability of multichannel seismic data, along with checkshot and sonic logs from ten different wells in close proximity favoured an attempt to identify lithologic changes on the basis of CDP moveout velocities, which is conventionally obtained with multichannel seismic data processing. A comparison of velocity data from three different sources also gave an opportunity to check the reliability of the velocities obtained by the conventional velocity analyses. It has been observed that the velocity profiles across and along the margin of the Georges Bank show a systematic increase in velocity in the Jurassic

section from the inner shelf to the outer shelf indicating a lithologic change from a dominantly clastic to a more carbonate sequence represented by dense limestone and dolomites. It was also observed that a careful CDP moveout velocity analyses could provide reliable velocity informations that can be used to identify sedimentary sequences along the passive margins where the drill holes are not available for a reliable velocity survey.

TABLE OF CONTENTS

	page
ABSTRACT.....	iii
LIST OF FIGURES.....	viii
LIST OF PLATES.....	xi
ACKNOWLEDGEMENTS.....	xii
1. INTRODUCTION.....	1
2. GEOLOGY OF THE AREA.....	4
3. DATA ACQUISITION.....	14
3.1 Reflection Seismic Data.....	14
3.2 Digital Well Log Data.....	16
3.3 Velocity Checkshot Data.....	18
4. DATA PROCESSING.....	20
4.1 Seismic Data Processing.....	20
4.2 Digital Well Log processing.....	21
4.2.1 Editing sonic logs.....	24
4.2.2 Editing density logs.....	25
4.2.3 Editing caliper logs.....	25
4.3 Velocity Checkshot Data Processing.....	25
4.4 Synthetic seismogram generation.....	27

TABLE OF CONTENTS(Continued)

	page
5. VELOCITY ANALYSIS.....	34
5.1 Stacking Velocity Analysis.....	37
5.2 Isovelocity plots.....	39
6. INTERPRETATION.....	43
6.1 Seismic stratigraphic interpretation.....	43
6.1.1 Early postrift deposits (Jurassic).....	48
6.1.2 Late postrift deposits (Cretaceous- Tertiary).....	54
6.1.3 Ancient carbonate platform.....	56
6.2 Interval velocity interpretation:.....	57
6.2.1 Common Depth Point (CDP) moveout velocities.....	58
6.2.2 Sonic log velocities.....	61
6.2.3 Checkshot velocities.....	63
6.2.4 Velocity gradients across the shelf.....	66
6.2.5 Velocity gradients along the margin.....	70
7. CONCLUSIONS.....	78
8. REFERENCES.....	81
9. APPENDIXES.....	87
Appendix A. Standerd deviations of CDP moveout velocities.....	88

TABLE OF CONTENTS(Continued)

	page
Appendix B. Checkshot time-depth curves.....	90
Appendix C. Sonic and interval velocity logs...	99
Appendix D. Checkshot and sonic interval velocities.....	107
Appendix E. Velocity-density relationships....	117
PLATES.....	Pocket

LIST OF FIGURES

	page
Figure 2.1: Tectonic map of northeastern United States Atlantic Margin (from Klitgord, K.D., in Grow and Sheridan, 1988).....	6
Figure 2.2: Schematic cross-section through Georges Bank region, showing distribution of sedimentary wedge bound by sea floor and crystalline basement (from Schlee and Klitgord, 1981). Sediment facies relationships are indicated. The wavy line above crystalline basement represents postrift unconformity.....	7
Figure 2.3: Principal multichannel reflection profiles and borehole locations for Georges Bank Basin offshore Massachusetts and Maine (from Poag and Valentine, 1988).....	9
Figure 2.4: Gravity model across Georges Bank Basin along USGS seismic line 19 (Swift et al., 1987)...	10
Figure 4.1: Final stacked section (after 2:1 horizontal summation) of USGS seismic line 209 (gap represents a field tape not readable).....	22
Figure 4.2: Final stacked section (after 2:1 horizontal summation) of USGS seismic line 19.....	23
Figure 4.3: A comparison of the synthetic seismogram with the seismic section of seismic line 209 at the COST G-2 site.....	26
Figure 4.4: Time-depth curve obtained from the checkshots of COST G-2 well.....	28
Figure 4.5: Interval velocities obtained from checkshots time-depth curve of COST G-2 well (at 500 m interval).....	29

LIST OF FIGURES(Continued)

	page
Figure 5.1: Average interval velocities across the shelf along USGS seismic line 209.....	40
Figure 5.2: Average interval velocities across the shelf along the USGS seismic line 19.....	41
Figure 6.1: Interpreted seismic section of USGS seismic line 209 (only the major postrift sedimentary horizons are shown).....	45
Figure 6.2: Interpreted seismic section of USGS seismic line 19 (only the major postrift sedimentary horizons are shown).....	46
Figure 6.3: Strata penetrated in COST G-1 and COST G-2 wells in the Georges Bank (Schlee and Klitgord, 1988).....	50
Figure 6.4(a): Part of the final stacked section of seismic line 12I and 12J that joins line 209 and 19 in the mid-shelf region.....	51
Figure 6.4(b): Part of the final stacked section of seismic line 33 that joins line 209 and 19 in the mid-shelf region.....	52
Figure 6.5: Velocity and the avaraged interval velocity (at 500 m interval) logs obtained from the sonic logs of COST G-2 well.....	62
Figure 6.6: Averaged interval velocities from sonic logs (at 500 m interval) from the nine wells in the Georges Bank Basin.....	64
Figure 6.7: A comparison of checkshot and sonic interval velocities (at 500 m interval) at the COST G-2 site.....	65

LIST OF FIGURES (Continued)

	page
Figure 6.8(a): A comparison of the averaged sonic velocities along a NW-SE section through COST G-1, Exxon-170, Mobil-196, and Shell-218 wells.....	67
Figure 6.8(b): A comparison of the averaged sonic velocities along a NW-SE section through Exxon-153, COST G-2, Tenneco-182, and Shell-218 wells.....	69
Figure 6.8(c): A comparison of the averaged sonic interval velocities along a SW-NE section through COST G-1, Exxon-170, and Exxon-153 wells.....	71
Figure 6.8(d): A comparison of the averaged sonic velocities along a east-west section through COST G-1 and Exxon-153 wells.....	72
Figure 6.8(e): A comparison of the averaged sonic velocities along a NW-SE section through Shell-210, Mobil-196, Tenneco-182, and Conoco-179 wells.....	73
Figure 6.9: Part of the final stacked section of seismic line 12I and 12J, that joins line 209 and 19 in the midshelf region, on which sonic interval velocities have been projected.....	75
Figure 6.10: Part of the final stacked section of seismic line 33 , that joins line 209 and 19 in the midshelf region, on which sonic interval velocities have been projected.....	76

LIST OF PLATES

1. Plate 1. Interpreted seismic section of line 209..Pocket
2. Plate 2. Interpreted seismic section of line 19...Pocket
3. Plate 3. Isovelocity (CDP moveout) plots of
line 209.....Pocket
4. Plate 4. Isovelocity (CDP moveout) plots of
line 19.....Pocket

ACKNOWLEDGEMENTS

There are so many individuals who have helped and encouraged me in this endeavour that I hesitate to consider this an individual accomplishment. I express my heartfelt thanks and gratitude to all of them.

I most gratefully acknowledge the continued guidance and advice extended to me by Dr. John A. Grow, Research Geophysicist, USGS, my thesis co-advisor, throughout this research project and reviewing the draft several times for critical suggestions and necessary modifications. It would not have been possible to complete this research in time without his continued involvement and help. I must also recognize the involvement of Prof. Alfred H. Balch, my thesis advisor, for showing interest in this research and providing direction, advice, and many discussions we had during the entire period of this work. I am also thankful to Dr. Thomas L. Dobecki (Associate Professor) and Dr. Abdelwahid A. Ibrahim (Associate Professor) for carefully reviewing my thesis and many suggestions to improve certain topics of this thesis.

I wish to recognize many individuals like Dr. Myung W. Lee, John J. Millar, Warren Agena, Richard Dick Wiser, and F. Nick Zihlman of the Seismic Stratigraphic Group, Branch of Petroleum Geology, USGS, Denver Federal Center, for their help during the processing of the marine seismic data, and David J. Taylor for his help during the processing of digital well logs and checkshot data. I am also thankful to the USGS, Denver Federal Center, for providing me the seismic data and computer facilities. I also thank Mr. Steve Prensky of USGS for allowing me to use the digital well logs and Mineral Management Services (MMS) for providing the checkshot data.

It would remain incomplete unless I thank Dr. John A. Grow and Renea Ericson for their extra effort in providing me transportation so many times that made my life little easier and comfortable.

INTRODUCTION

The primary structural elements of the Georges Bank Basin region are typical of passive continental margins: shallow basement platform, deep marginal sedimentary basin, and deep ocean basin. The tectonic evolution of a passive margin creates distinctive crustal structures, and sedimentary distribution patterns. The sedimentary column underneath Georges Bank is mainly a thick sequence of interbedded carbonate and evaporite rocks of Jurassic age overlain by a much thinner section of marine siliciclastic sedimentary rocks of Cretaceous and Cenozoic age (Schlee and Klitgord, 1988). In a previous study along seismic line-1 on the Georges Bank (Schlee et al., 1976), a seismic velocity gradient from the inner shelf to the outer shelf was indicated and was interpreted to be due to a gradual change in lithology from a clastic sequence to a more carbonate rich sequence towards the outer shelf. The purpose of this study is to identify lithologic changes along the shelf area on the basis of formation interval velocities as obtained from three different sources, viz., reflection seismic data, sonic logs, and checkshot data. In this study, interval velocities are obtained from the CDP moveout or stacking velocity analysis, sonic logs, and checkshots from

ten different drill holes in the Georges Bank area, and are compared with each other to obtain a picture of the lateral velocity gradients and for a reliable identification of rock types, particularly in the Upper and Middle Jurassic section along the shelf.

USGS seismic lines 209 and 19 pass across the shelf area in the Georges Bank basin and are very close to the ten deep drill holes in the area. In order to obtain the interval velocities from the seismic data, the above mentioned seismic lines have been reprocessed and velocity analyses were computed at every 100th CDP (2500 m apart) from which the RMS velocity functions were obtained, and used for stacking. After stacking, three major reflectors along the shelf region of those two lines were traced and stacking velocities were re-picked at those reflecting horizons. These velocities were used to determine the interval velocities by Dix's (1955) method of converting interval velocities from the RMS velocities.

Interval velocities were obtained from the sonic logs available from nine drill holes in the area. A synthetic seismogram for the COST G-2(Continental Offshore

Stratigraphic Test) well was calculated from the sonic and density logs and was compared with the seismic section of line 209 for age and lithologic correlation (Poag and Valentine, 1988). It was observed that the major unconformities shown on COST G-2 well correlate very well with the synthetic seismogram.

Longer wavelength interval velocities (100 to 500 m) obtained from the checkshots are considered more reliable than sonic velocities. Checkshot data available from the ten different wells were used to compute interval velocities. These interval velocities were then compared with the CDP and sonic log velocities at the COST G-2 site and also projected on the seismic lines 12I, 12J, and 33 to see the change in velocities along the Georges Bank margin. The average interval velocities from the sonic logs show a significant change across the shelf, where as there is a little change along the margin.

GEOLOGY OF THE AREA

The Atlantic continental margin is often referred to as a passive margin because today it is located near the center of the North Atlantic plate and displays little seismic or volcanic activity. The Atlantic continental margin developed during an extensional phase of crustal deformation that began in the later part of Triassic. Its evolution took place in three main stages (Bally,1981):

1) A rifting phase which involved stretching of the lithosphere and thermal uplift of the mantle (this part was characterized by complex horst and graben tectonics);

2) The onset of drifting, which involved the separation of continental lithosphere (oceanic crust was emplaced for the first time and accretion by sea floor spreading across a mid-ocean ridge which filled in the gap between attenuated blocks);

3) A main drifting phase which was dominated by massive subsidence with rates of subsidence that decreased exponentially from the date of the onset drifting, which are driven by thermal cooling of the extended lithosphere.

Phase-1 took place during the late Triassic and early Jurassic and phase-2 began in the early to mid Jurassic (Morgan and Dowdell, 1981).

The Georges Bank Basin is the northernmost sediment filled basement depression on the U.S. Atlantic outer continental shelf (figure 2.1). The axis of this assymmetric trough runs from its shallowest point in the southwest to its deepest point in the northeast. Sediment thickness in the basin ranges from a minimum of about 780 m along eastern and northern edge to a maximum in excess of 8000 m in the deepest areas along the basin axis (Schultz and Grover, 1974 ; Schlee et al., 1976; Schlee and Klitgord, 1988).

Figure 2.2 show a schematic cross section of Georges Bank Basin. The basement is thought to be composed primarily of either crystalline or metasedimentary material. In the Georges Bank region, crystalline basement include Paleozoic and older rocks on the platforms, blockfaulted pre-Mesozoic rocks mixed with Triassic and Jurassic igneous rocks beneath the marginal basin, and Jurassic and younger oceanic crust seaward of the marginal basin. On the Georges Bank,

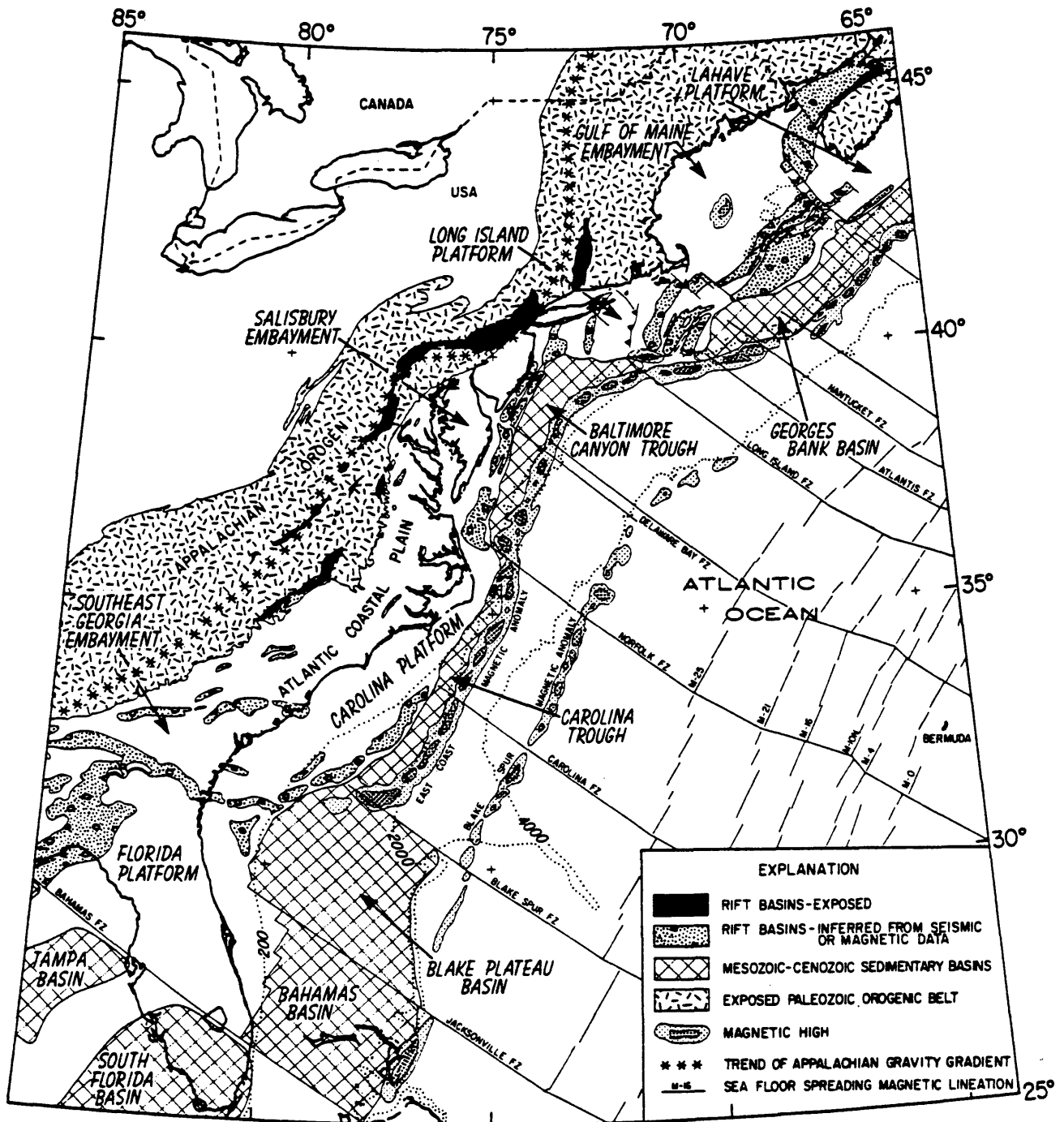


Figure 2.1: Tectonic map of northeastern United States Atlantic Margin (from Klitgord, K.D., in Grow and Sheridan, 1988).

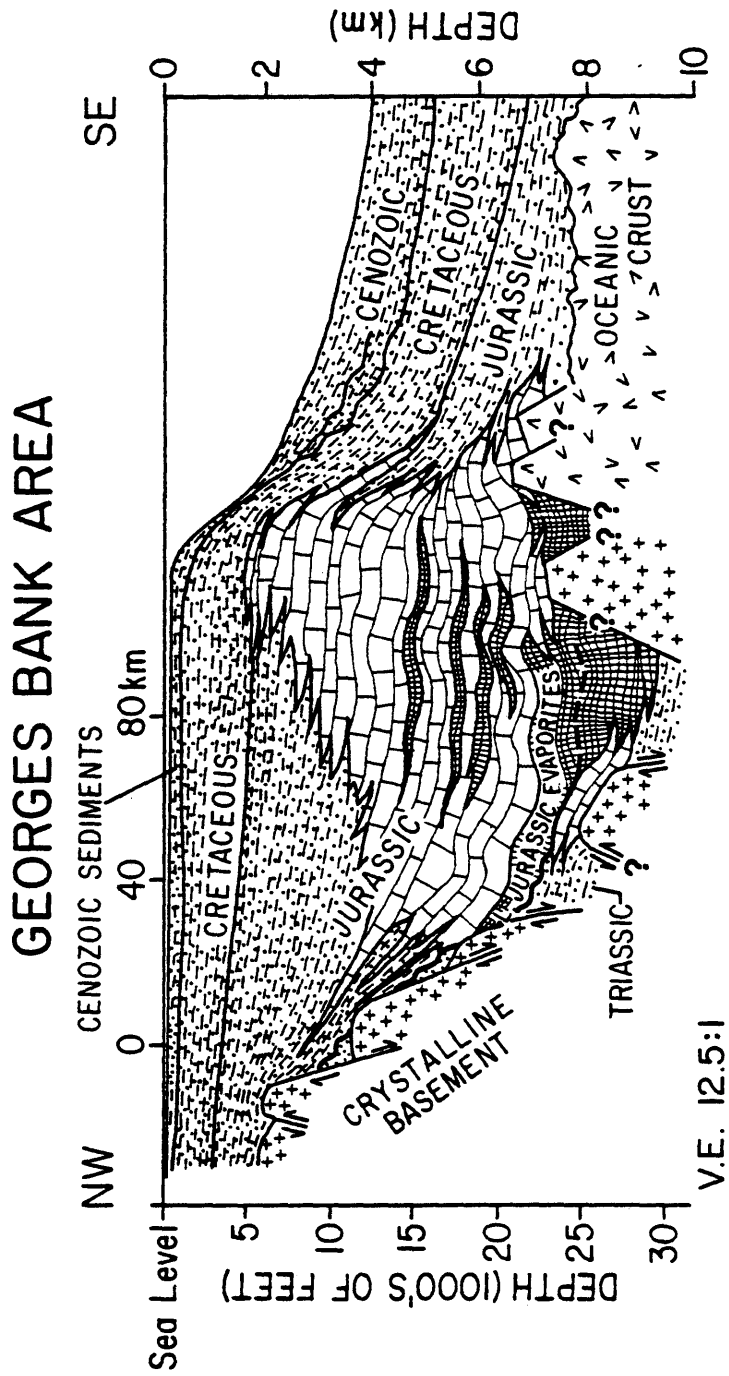


Figure 2.2: Schematic Cross-section through Georges Bank region, showing distribution of sedimentary wedge bound by sea floor and crystalline basement (from Schlee and Klitgord, 1981). Sediment facies relationships are indicated. The wavy line above crystalline basement represents postrift unconformity.

graphitic slate, schist, and phyllite were sampled in the COST G-1 well, which ties with line 1 (figure 2.3). COST G-2 well penetrated through a thick section of post rift sediment and is bottomed in a salt layer which overlies the crystalline basement. Jansa and Wade (1975) reported that the Shell Mohawk-B-93 well, which ties directly into USGS line 12 off Nova Scotia, bottomed in a granitic complex to be of Devonian age.

The Triassic structures in the Gulf of Maine may be filled with continentally derived sediments. Jansa and Wade (1975) reported such basins on the Scotian Shelf being filled with red conglomerate and Shale. Maher and Applin (1974) reported finding roughly the same strata in Triassic basins on the Atlantic Piedmont.

Mattick et al., (1975) suggested that the shelf-edge basement ridge associated with the East Coast Magnetic Anomaly (figure 2.4) acted as a barrier to the Atlantic system during Triassic time and established a shallow, restricted marine environment in the Georges Bank trough. Mattick's idea of a large basement ridge has not held up. It may have started as a small basement high but the carbonate

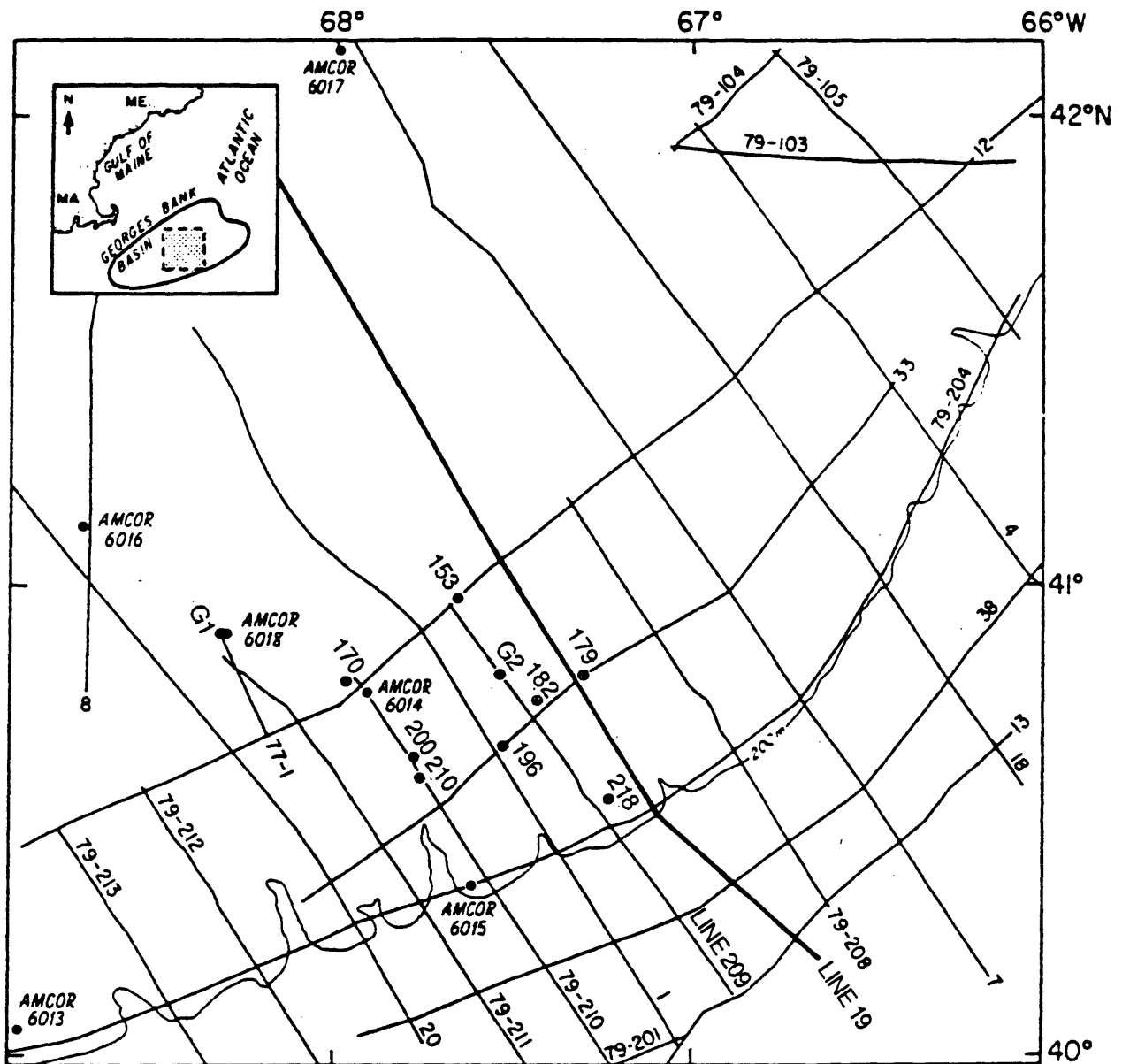


Figure 2.3: Principal multichannel reflection profiles and borehole locations for Georges Bank Basin offshore Massachusetts and Maine (from Poag and Valentine, 1988).

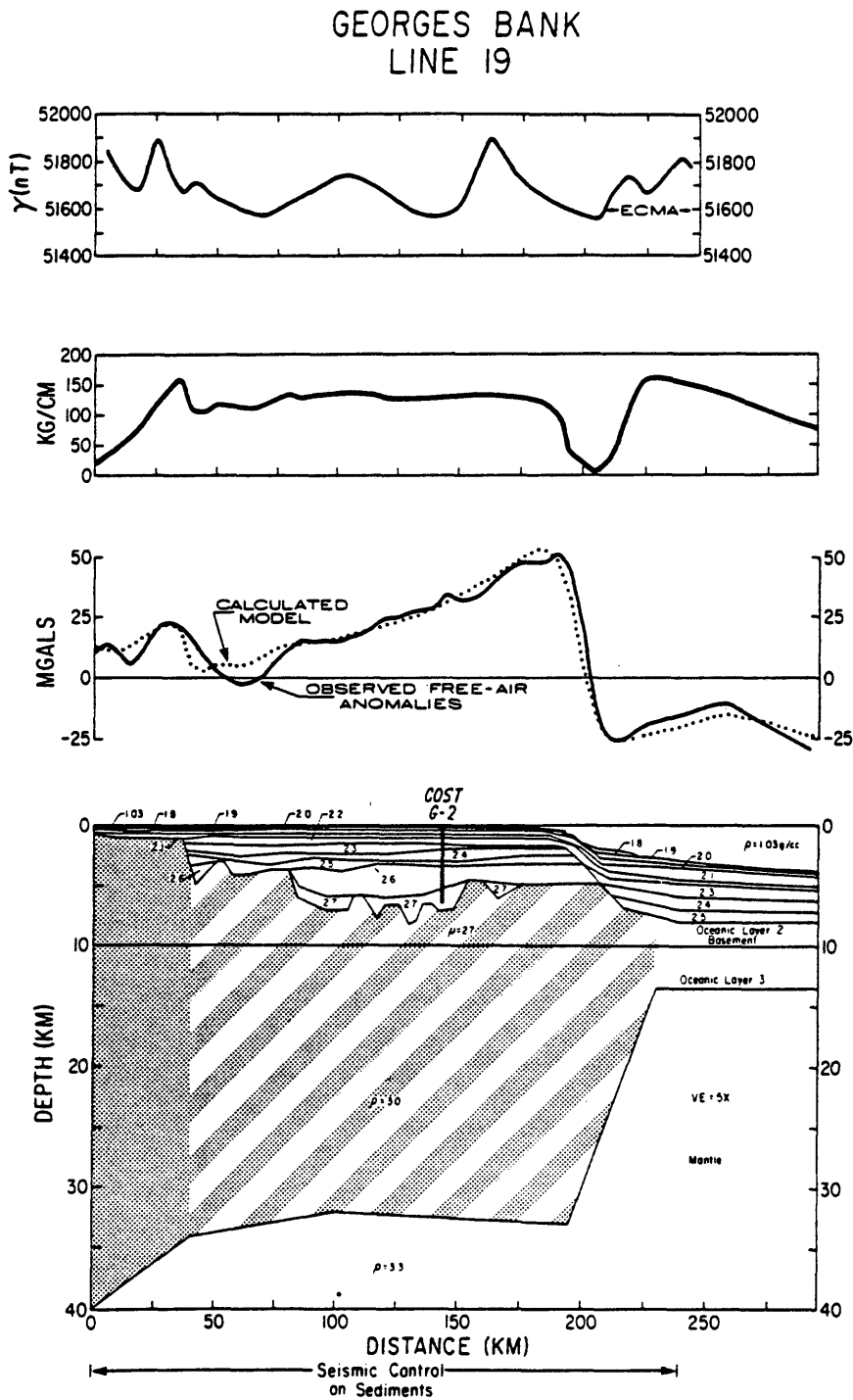


Figure 2.4: Gravity model across Georges Bank Basin along USGS seismic line 19 (from Swift et al., 1987).

bank and reef goes down to at least 6 km depth (Grow et al., 1979). While Lower Jurassic evaporites were probably deposited in the trough (Anderson and Taylor, 1981), sedimentation in the Middle Jurassic probably occurred in a less restricted yet shallow marine environment, parts of which could have been above sea level. This model suggests that thick accumulations of limestone, dolomite, and anhydrite may have formed in the central basin region in Middle Jurassic time, separated from the main Atlantic ocean by a carbonate bank or reef along the outer continental shelf edge as hypothesized by Schlee et al., (1976), and Schlee, J., (1977).

Within the deeper parts of the Georges Bank Trough, Jurassic rocks probably represent an extremely thick section and exhibit mixed lithology. Seismic velocity studies and reflection characters suggest that Jurassic material starts as a clastic sequence at the inner shelf and grades seaward into a dense carbonate sequence with an underlying Jurassic evaporite layer occupying the deepest parts of the basin (figure 2.2). Sherwin and Jansa and Wade (1975) reported the presence, throughout the Scotian Shelf and the Grand Banks, of a thick Jurassic salt layer known as Argo Formation. This salt layer could extend

southward from the Canadian shelf and be present in the Georges Bank Trough. At the base of COST G-2 well this Jurassic salt layer was found to exist at a depth over 6.7 km. Lower Cretaceous sedimentary strata are predominantly clastic, except near the outer shelf edge, while Upper Cretaceous and Cenozoic sedimentary rocks are dominantly clastics (Schlee and cheetham., 1967, Schlee,J.,1977, and Schlee and Klitgord, 1988).

Internal sediment structure in the Georges Bank Trough is controlled by faults and flexures within the basement which formed during the rifting phase. To a minor extent small structural features may be inferred by sedimentologic processes. The sedimentary forms most likely to exert such influence may include carbonate buildups, sandstone lenses due either channel or barrier-bar features, deep evaporite swells, and differential compaction of sediments.

Seismic velocity studies and reflection character indicate that interval velocities of 5.6 to 5.9 km/sec are present between depths of 4 and 7 km on seismic data from beneath the Georges Bank area, increasing toward the southeast (Schlee et al.,1976). These high velocities

would suggest that the sequence below about 2.5 sec (two-way time) on the seismic section (in the mid shelf region) would be composed of dense limestone, dolomite, and anhydrite. A best guess as to the depositional model for these sediments would be a shallow, semi-restricted marine environment. If thick sections of dolomite exist in the carbonate sequence, their presence may indicate that large areas of carbonate-bank deposits had been exposed, resulting in dolomitization. Drill hole data of the COST G-2 well confirms the presence of thick limestone and dolomites in the lower Jurassic section (Schlee and Klitgard, 1988; Poag and Valentine, 1988).

DATA ACQUISITION

3.1: Reflection seismic data.

The U.S. Geological Survey (USGS) collected approximately 6,500 km of 48 channel common-depth-point (CDP) seismic reflection profiles (30 km spacing regional grid and a 10 km grid over outer shelf and upper rise) in the U.S. Atlantic margin. These are now in the public domain (figure 2.3).

To see the seismic velocity gradients along the shelf region, I have chosen two seismic lines in the Georges Bank, viz., line 209 and line 19. The reason for choosing these two lines are primarily due to the close proximity of these lines to the ten deep exploratory wells in the area. COST G-2 well was drilled directly on line 209 and line 19 runs parallel to line 209 and covers a large distance from inner shelf to the outer shelf. It too is very close to the drill holes.

USGS seismic line 209 is about 120 km long and was collected by Prakla-Seismos of the Federal Republic of

Germany in 1979 under a cooperative research project between the USGS and Geological Survey of West Germany (BGR). The recording parameters are as follows:

- i) Instrument used: DFS-V system.
- ii) Record length: 10 seconds.
- iii) Sampling rate: 4 ms.
- iv) Filter: Lowcut-8 hz at 18 db/octave
Highcut-64 hz.
- v) Tape format: SEG-B with gain constant 24 db.
- vi) Cable length: 2400 m
- vii) Cable depth: 15 m
- viii) Geophone group spacing: 50 m.
- ix) Shot point interval: 50 m.
- x) Array depth: 8 m.
- xi) Array volume: 23.45 l.
- xii) Number of traces: 48 channel.
- xiii) Recording density: 800 BPI.
- xiv) Direction: NW to SE.

USGS seismic line 19 is about 240 km long in the NW-SE direction and the data was collected by Geophysical Services Incorporated (GSI) in 1978 under a contract with the USGS. The recording parameters are as follows:

- i) Instrument used: DFS-IV system.
- ii) Record length: 12 seconds.
- iii) Sampling rate: 4 ms.
- iv) Filter: Low-cut: 8 hz at 18db/octave
High-cut: 62 hz
- v) Tape format: SEG-B with gain constant 30db.
- vi) Cable length: 2400 m.
- vii) Geophone group spacing: 50 m.
- viii) Shot point interval: 50 m.
- ix) Array depth: 9 m.
- x) Array volume: 2000 cu in.
- xi) Number of traces: 48 channel.
- xii) Gun delay: 51 ms.
- xiii) Direction: NW to SE.

3.2: Digital well log data

Ten deep exploratory drill holes have been drilled in the Georges Bank basin between 1976 -1982. They are respectively COST G-1, COST G-2 , Exxon-153, Exxon-170, Conoco-179, Tenneco-182, Mobil-196, Shell-200, Shell-210, and Shell-218. All of these wells have been well documented with various kinds of geophysical logs. Mr. Steve Prenskey of USGS has made digital tapes of these logs available. (Note:

Exploratory wells OCS-153, OCS-179 etc., are the Exxon-153 and Conoco-179 wells respectively. I have chosen to use these names for no special reason.)

The continuous velocity logs (CVL) gives the time detail of the velocity layering and is a very good correlation tool and is also useful in computing formation parameters.

The CVL tool consists of an acoustic transmitter and either one or two pressure detectors, with acoustic insulators separating the elements by known fixed distances. The source is usually is an electromechanical device that produces acoustic pulses in the 10-20 khz frequency range. By using a pulse repetition rate about 20 pulses/second and moving the tool slowly up the hole, the set of traveltime measurements produces a nearly continuous measure of transit time, either between transmitter and receiver or between the two receivers, depending on the tool configuration.

The velocity obtained from the CVL measurements is the velocity averaged over the separation distance between the

elements. Errors in the transit-time measurements caused by formation damage during drilling, borehole cavities, and other irregularities, low signal amplitude due to absorption, calibration inaccuracies, and so on, will introduce errors in the time-depth computation. For this reason, the integrated CVL curve usually is tied to a checkshot well survey to produce a time- depth function that is accurate throughout the entire section of the open hole that is being logged. The well logs that are used for the present investigation are as follows:

- i) Sonic logs.
- ii) Density logs, and
- iii) Caliper logs.

3.3: Velocity checkshot data.

Checkshot data from the ten wells have been obtained by Schlumberger and by Birdwell Inc. The checkshot data have been provided by the Mineral Management Service (MMS). The recorded data are not regular and the interval of checkpoints varies between 30 m to about 100 m depending the bore hole condition.

Estimates of velocity in boreholes by shooting a well involve measurements of traveltime of seismic waves from sources at or near the surface to a detector located at various depths in the well. To obtain vertical traveltimes, the measurements must be corrected for angularity and refraction effects, because the source must necessarily be offset from the well bore. Well shooting gives good estimates of the gross velocity layering.

The detector depths below the sea level at which measurements were made are usually called checkpoints. The received signal time at the checkpoints are plotted on a graph. The time-depth pairs (t_i, z_i) is obtained from the time-depth curve and their ratios (z_i / t_i) give the average velocity to the base of the second layer

$$V_{ave,2} = z_i / t_i \dots\dots\dots(3.1)$$

The interval velocity between adjacent checkpoints is obtained by the relation:

$$V_i = \frac{z_i - z_{i-1}}{t_i - t_{i-1}} \dots\dots\dots(3.2)$$

DATA PROCESSING

Computer processing facilities, reflection seismic data, digital well logs and checkshot data from ten boreholes was made available by the USGS at the Denver Federal Center. DISCO software package by Digicon Inc., and a Digital Log Processing System (DLPS) by Cogniseis Inc., has been used for the processing of reflection seismic data, digital well log, and checkshot data respectively.

4.1: Seismic data processing

To obtain the velocity distribution along the seismic line 209 and 19 it was necessary to reprocess these two lines starting from the field tapes. USGS seismic line 209 is about 110 km long and has 2215 shot points at 50 m interval, and the seismic line 19 is about 240 km long with 4820 shot points at a 50 m interval. Both the data sets have undergone similar data processing sequence excepting that with line 19 a prestack Predictive deconvolution was applied and for line 209 Spiking deconvolution was applied.

Seismic data processing sequence for the USGS seismic line 209 and 19 are as follows:

- i) Demultiplexing
- ii) Sorting into CDP gathers
- iii) Pre-stack deconvolution
- iv) Velocity analysis
- v) Stacking
- vi) Filtering
- vii) Horizontal 2:1 stacking
- viii) Interval velocity from NMO or stacking velocities

Final stacked section of line 209 and 19 are shown in figures 4.1 and 4.2 respectively (100 traces /inch); only for upper 6 seconds data were shown. Larger seismic sections for both the lines with their full data length were presented as plates 1 and 2 respectively.

4.2: Digital well log processing

Digital well log data from all the ten wells are on magnetic tapes from which only the sonic, density, and the

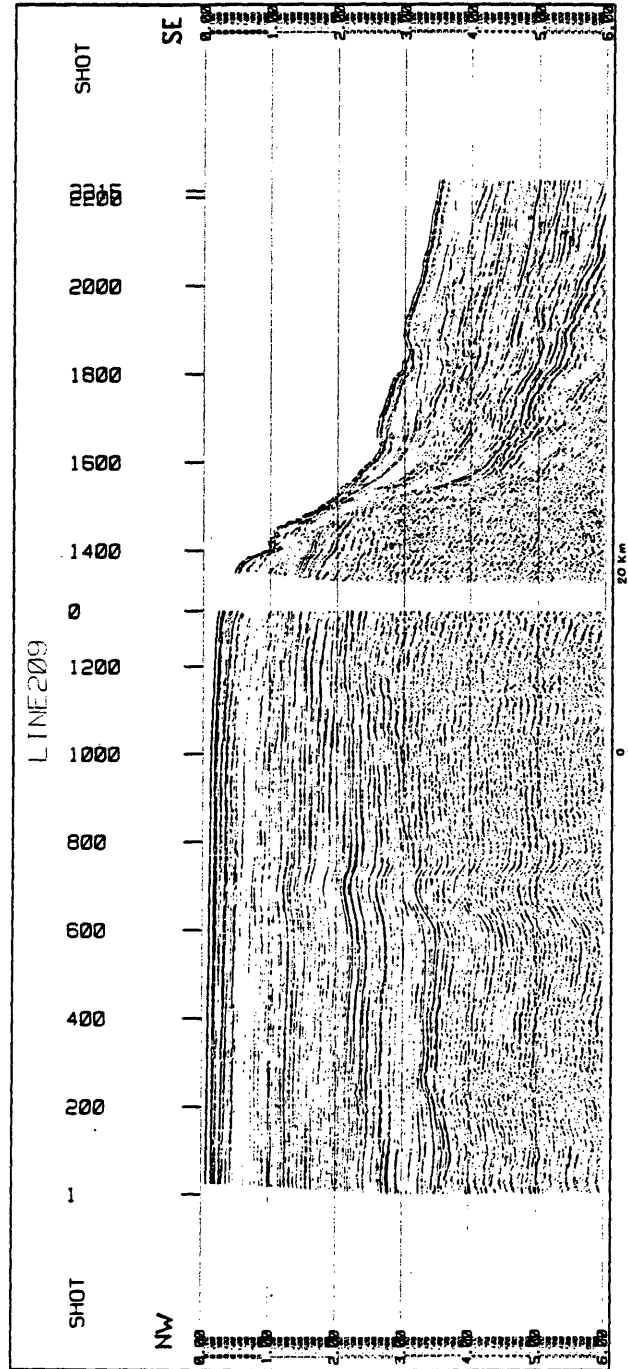


Figure 4.1: Final stacked section (after 2:1 horizontal summation) of USGS seismic line 209 (gap in the middle represents a field tape not readable).

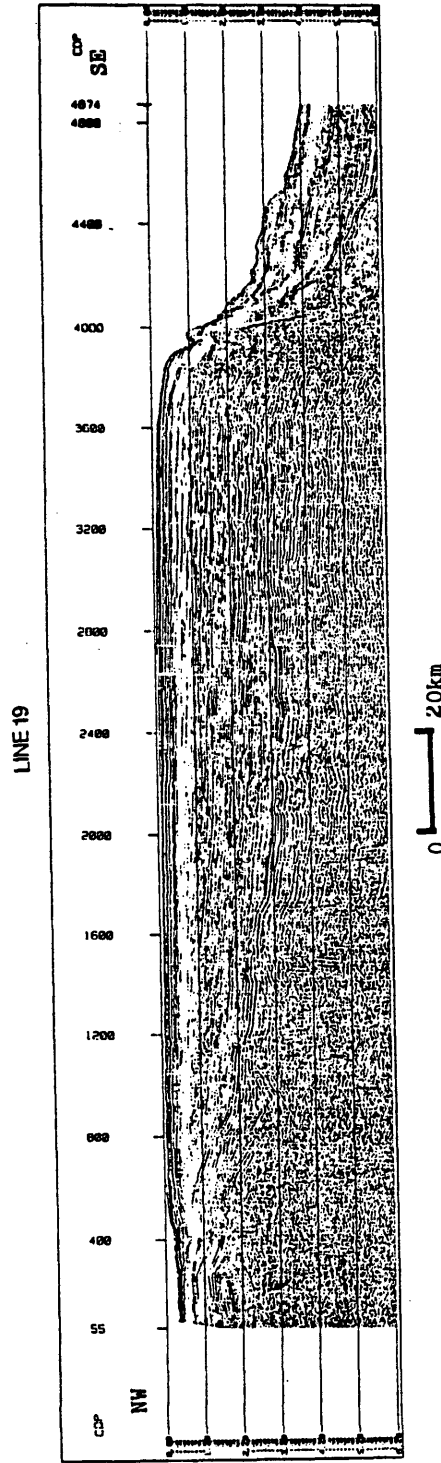


Figure 4.2: Final stacked section (after 2:1 horizontal summation) of USGS seismic line 19.

Caliper logs have been read into the data base for processing (the tape for the OCS-200 well was not readable).

4.2.1: Editing sonic logs. -----

In editing the sonic logs, the maximum and minimum transit time was set at 180 microseconds to 40 microseconds/ft as they represent velocities in the range of 5,555 ft/sec to 25,000 ft/sec, respectively (metric equivalent). The sonic logs were very noisy, particularly near washout zones, cavities, and fracture zones. They were compared with the caliper logs of the respective wells and the anomalies were smoothed or removed by applying personal judgement. Sometimes anomalous transit times more than 180 microseconds/ft and lower than 40 microseconds/ft were observed, and removed as they represent unreasonably low or high velocities, e.g., >200 microseconds represents < 5000 ft/sec and <30 microseconds represents > 33,000 ft/sec. 5000 ft /sec represents the velocity of sonic waves in water and velocities above 25,000 ft/sec are not common in sedimentary formations. All of these logs have started at a certain depth below the surface and therefore have to be filled to the surface to about 300 to 1200 m. An approximate range of

uppermost log values was used to fill the logs up to the surface. In most of the logs the lowermost part represented some inconsistent log values and should be ignored.

4.2.2: Editing density logs.

The density logs have been edited in the same fashion as the sonic logs where the upper and lower density values have been assumed to be around 2 gm/cc to about 3 gm/cc. Only the density log for the COST G-2 well was actually used in this study, for a synthetic seismic response (figure 4.3), since it was drilled directly on line 209.

4.2.3: Editing caliper logs

The caliper logs have been used to determine the magnitude of the washout zones, cavities , or the range of fracture zone in the bore holes so that proper editing could be applied to the sonic and density logs.

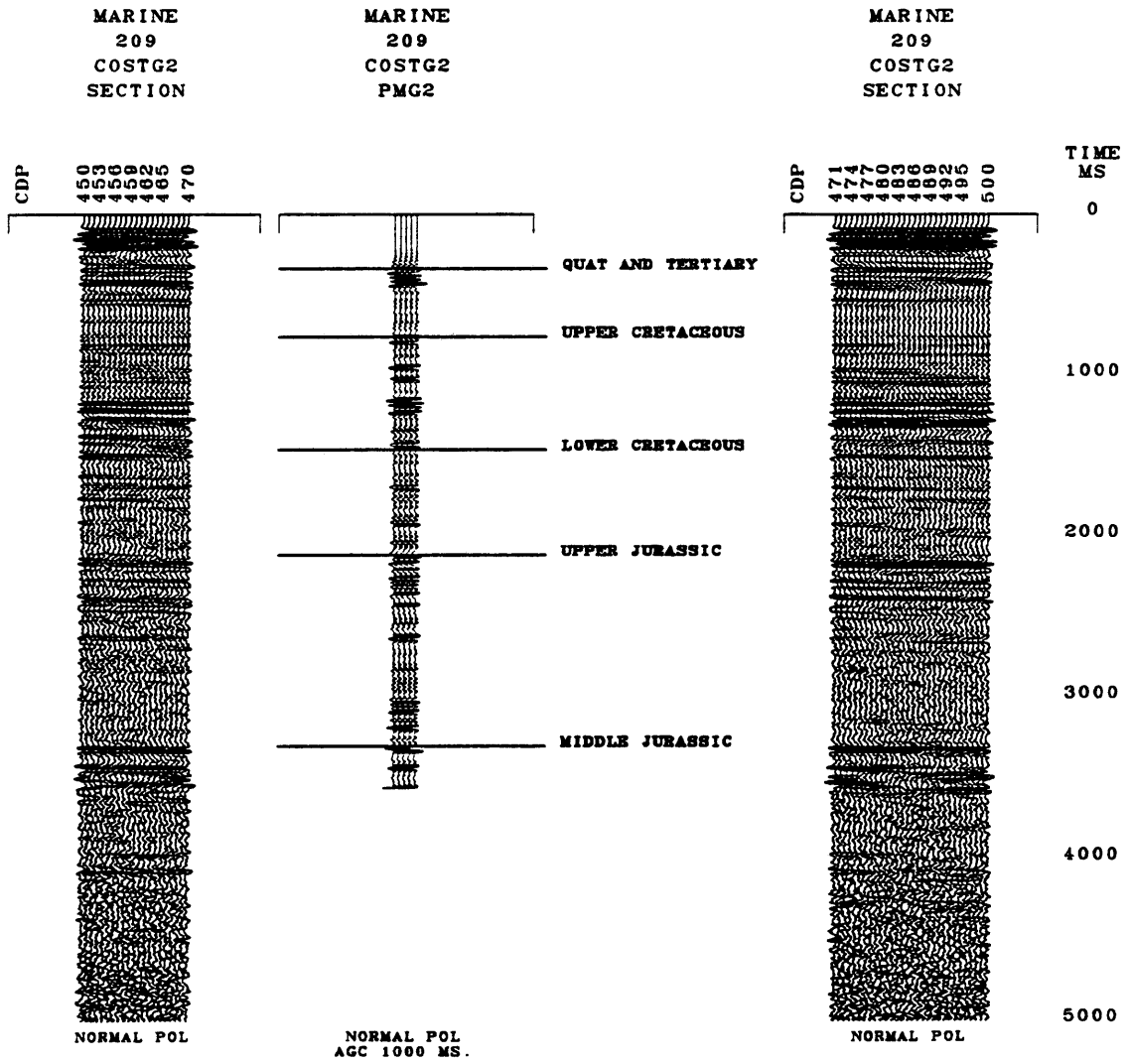


Figure 4.3: A comparison of the synthetic seismogram with the seismic section of line 209 at the COST G-2 site.

4.3: Velocity checkshot data processing

Checkshot data from all the ten wells were collected by the Schlumberger and Birdwell Inc., at uneven intervals of about 30 to 100 m. These time depth data were first entered into the computer to create a data file from which a time-depth curve was obtained. The time-depth curve of COST G-2 well is shown in figure 4.4 and the rest are shown in the appendix A.

These time-depth curves were then used to obtain an interval velocity curve over a 500 m depth interval. The interval velocity curve for COST G-2 well is shown in figure 4.5 and the rest are shown in the appendix B.

4.4: Synthetic seismogram generation

Synthetic seismograms are one of the best possible ways to identify real events in the seismic section by the sonic and density logs from COST G-2 well for correlation with the seismic line 209 and is shown in figure 4.3.

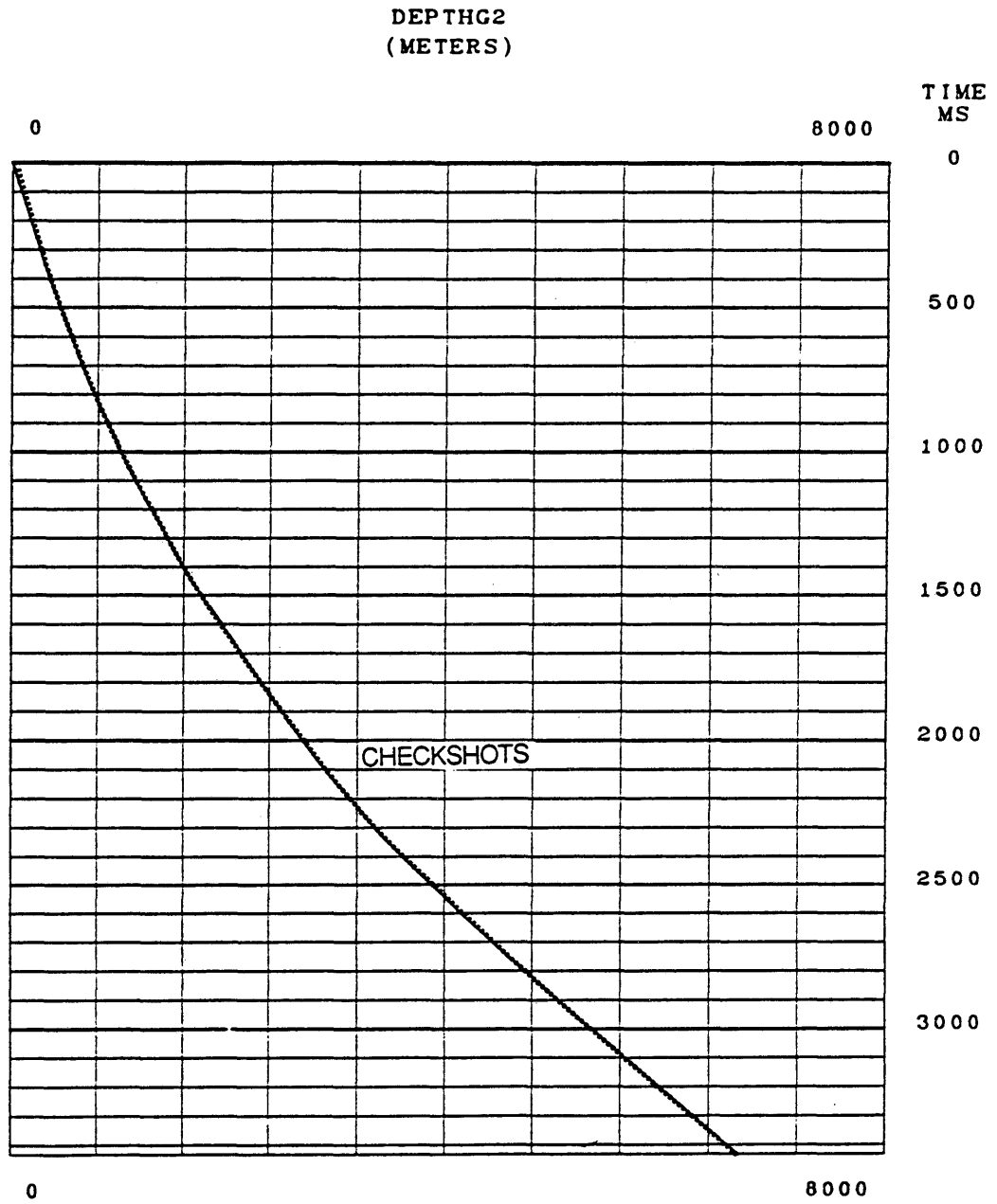


Figure 4.4: Time-depth curve obtained from the checkshots of COST G-2 well.

The continuous velocity log gives the velocity distribution as a function of depth. This is converted to velocity as a function of two-way traveltime. In the discrete layer case the reflection amplitude is determined by the reflection coefficients, as given by

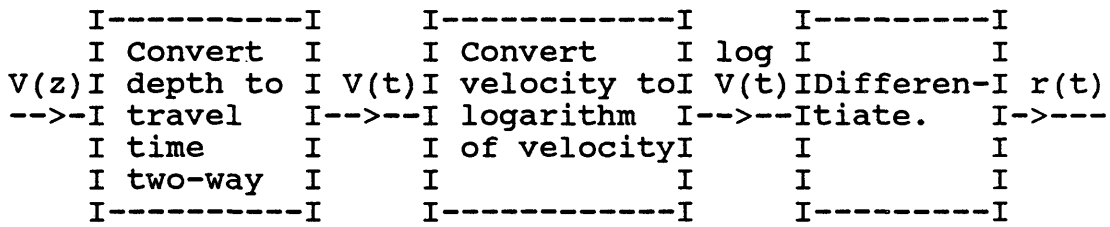
$$R_1 = \frac{p_2 V_2 - p_1 V_1}{p_2 V_2 + p_1 V_1} \dots\dots\dots (4.1)$$

Where R_1 is the reflection coefficient, and V_2 and V_1 are the velocities, and p_2 and p_1 are the densities in the second and the first medium respectively.

In the continuous case the set of reflection coefficients, as given by the equation (4.1) is replaced by the reflectivity function, designated as $r(t)$. The logarithm of velocity as a function of time will be called the velocity function. Then the derivative of that velocity function with respect to time is defined as the reflectivity function,

$$r(t) = \frac{d}{dt} \log V(t) \dots\dots\dots (4.2)$$

If the velocity function is continuous, the reflectivity function will also be continuous. The steps required to convert a velocity log to the reflectivity function are shown by the following block diagram.



where $V(z)$ is the velocity log and $r(t)$ is the reflectivity function (Sengbush et al., 1961).

$$r(t) = \frac{d}{dt} \log V(t) \dots\dots\dots (4.3)$$

The principle behind the generation of synthetic seismogram may be explained by the following relation:

$$s(t) = r(t) * b(t) * h(t) \dots\dots\dots (4.4)$$

Where $s(t)$ is the synthetic seismogram, $b(t)$ is the source pulse, $h(t)$ represents the multiples such as ghosts,

reverberations etc., and "*" represents convolutional process.

In order to generate the synthetic seismogram, the edited sonic and density logs were used to generate

- i) Impedance,
- ii) Velocity, and
- iii) Reflectivity function.

This reflectivity function was used to generate the synthetic seismogram which includes both primaries and multiples. The synthetic seismogram was then filtered with a 8 hz to 45 hz bandpass filter (the same filter used for the reflection seismic data). This synthetic seismogram was compared with the seismic section of line 209 at the COST G-2 well site and is shown in figure 4.3. Numerous reflection events ranging in age from Middle Jurassic to Quaternary are represented in the synthetic seismogram. All the major reflection events (line 209) correlate very well with the synthetic seismogram (figure 4.3), suggesting that the processing of the seismic profile (line 209) is of good quality. Other events in the synthetic seismogram

represent lithological changes (due to a change in acoustic impedance) within the major group of formations separated by the basin wide unconformities.

VELOCITY ANALYSIS

Good estimates of velocity as a function of depth are of paramount importance in the interpretation of seismic data. The time-honoured technique of shooting a well for velocity gives good estimates of the gross velocity layering. Fine detail is provided by continuous velocity logs. These two methods provide good, accurate information in the wells. In frontier areas where no wells are available, however, it is necessary to estimate the velocity from the normal moveout of seismic reflection profiles. The widespread use of horizontal stacking has led to an abundance on velocity data that have proved useful for lithologic studies, in addition to their primary purpose of enhancing the stack to increase the primary- -to-multiple ratio and to improve the signal to noise ratio.

Velocity estimation from surface seismic measurements using 'dt' analysis based on normal moveout has been done for many years (Green,1938; Steele,1941; Gardner,1947; Brustad,1953; Pfleuger,1954; Slotnik,1959). Weaknesses in these techniques are:

- i) Small errors in 'dt' measurements result in large errors in 'V' and consequently in the calculated depth.

ii) Straight line paths in media with uniform velocity are often assumed, rather than using least-time paths in layered media that obey Snell's law.

A very significant breakthrough in precision of estimating interval velocities from surface measurements was Dix's (1955) expanding spread technique. By expanding the distance between the source and detectors in such a way that large horizontal separation between source and detector is achieved while illuminating only the subsurface coverage of a symmetrical split-spread, the slope of the reflection

arrivals in (T_x^2, x^2) space can be determined with

considerable accuracy; this slope, which is related to the velocity distribution, applies in the vicinity of the midpoint of the split-spread.

Under the assumption of horizontal layering (no dip), Dix(1955) showed that the least time path through layered media for small offsets leads to the concept of the rms velocity, V_{rms} velocity. The rms velocity in the n-layer case is given by the following equation:

$$V_{rms,n} = \frac{\sum_{i=1}^n T_i V_i^2}{\sum_{i=1}^n T_i} \dots (5.1)$$

where T_i is the two-way traveltime and V_i is the interval velocity in the i th layer. The importance of the rms velocity, which is a mathematical quantity devoid of physical meaning, is that the interval velocity layering is measurable from the rms velocity distribution. The interval velocity in the n th layer is obtained by subtracting the equation for the rms velocity in the $(n-1)$ th layer case from the rms velocity in the n th layer case. The result is

$$V_{rms,n}^2 \sum_{i=1}^n T_i - V_{rms,n-1}^2 \sum_{i=1}^{n-1} T_i = T_n V_n^2 \dots (5.2)$$

The interval velocity in the n th layer, V_n , is then

$$V_n = \left(V_{rms,n}^2 \sum_{i=1}^n T_i - V_{rms,n-1}^2 \sum_{i=1}^{n-1} T_i \right) / T_n \dots (5.3)$$

All quantities on the right-hand side are measurable

from the data; the rms velocities are the slopes of

reflection arrival time in (T_x^2, X_x^2) space, and $\sum_i T_i$ are

the arrival times of the events.

Expanding spreads proved to be very useful for accurately determining interval velocities from which gross lithology could be deduced and for identifying multiples (Musgrave, 1962). The introduction of horizontal stacking procedures (Mayne, 1962) gave rise to techniques for velocity estimation directly from data that are being collected routinely.

5.1: Stacking velocity analysis

The determination of velocities in seismic reflection processing is inexact in many cases. Although the final time processed stacked section may look acceptable (in fact it may be the best possible product), the errors introduced sometimes cause the stacking velocity functions to differ greatly from actual velocities.

To determine stacking velocity functions, analyses are performed at a spatial sampling rate, and the analyses themselves can only determine a range of velocities for a given reflector. Normal moveout velocity analyses were made at every 2.5 km along the entire length of the seismic lines 209 and 19. The velocity functions obtained at each of the group of CDP's analysed was used for stacking the CDP gathers at the corresponding locations. The CDP gathers in between two subsequent CDP groups analysed was stacked by the extrapolation between two consecutive CDP groups being analysed for velocity.

Most processing done on reflection seismic data is carried out and displayed as a function of two-way reflection time. This is convenient since this is how the data are recorded. Since the purpose of this investigation was to see the trends of interval velocities within the major sedimentary units across from the inner-shelf to the outer-shelf, stacking velocity functions have been smoothed to include the stacking velocities only at the major sedimentary horizons along the shelf. This was done to see the interval velocity trends only and was not used to stack the data. This smoothed set of velocity functions was then used to obtain interval velocities for the major lithologic

units. Isovelocity plots for stacking velocities and a cross sectional plot of the interval velocities along the shelf of seismic line 209 and 19 are shown in plate 3 and 4, and figures 5.1 and 5.2 respectively.

5.2: Isovelocity plots

Since it has been shown that the stacking velocities are in suspect, one should first plot up a graph of isovelocity lines, commonly referred to as an isovelocity plot. This is a plot of lines connecting points of equal RMS velocity in cross-sectional form similar to that of the conventional seismic section, i.e., surface location as the abscissa and two-way traveltime as the ordinate (plate 3 and 4).

From the isovelocity plot the interpreter can easily make comparisons to the actual seismic section in order to determine if the velocities used are consistent with the geologic appearance of the seismic data. For example, unless faulting is readily apparent in the seismic data, the isovelocity plot should not be expected to exhibit large time jumps in its contours. If large time discrepancies are

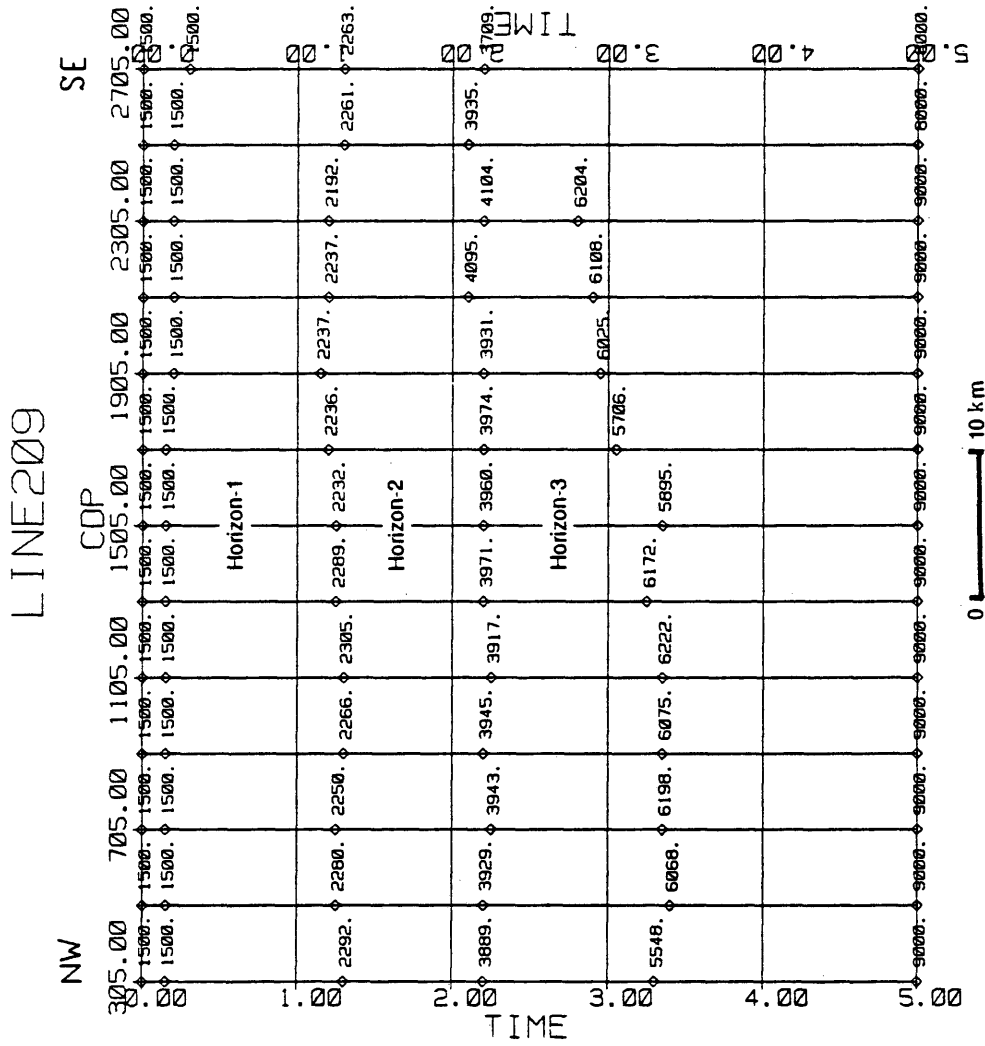


Figure 5.1: Average interval velocities (CDP moveout) across the shelf along the USGS seismic line 209 (averaged over 5 points).

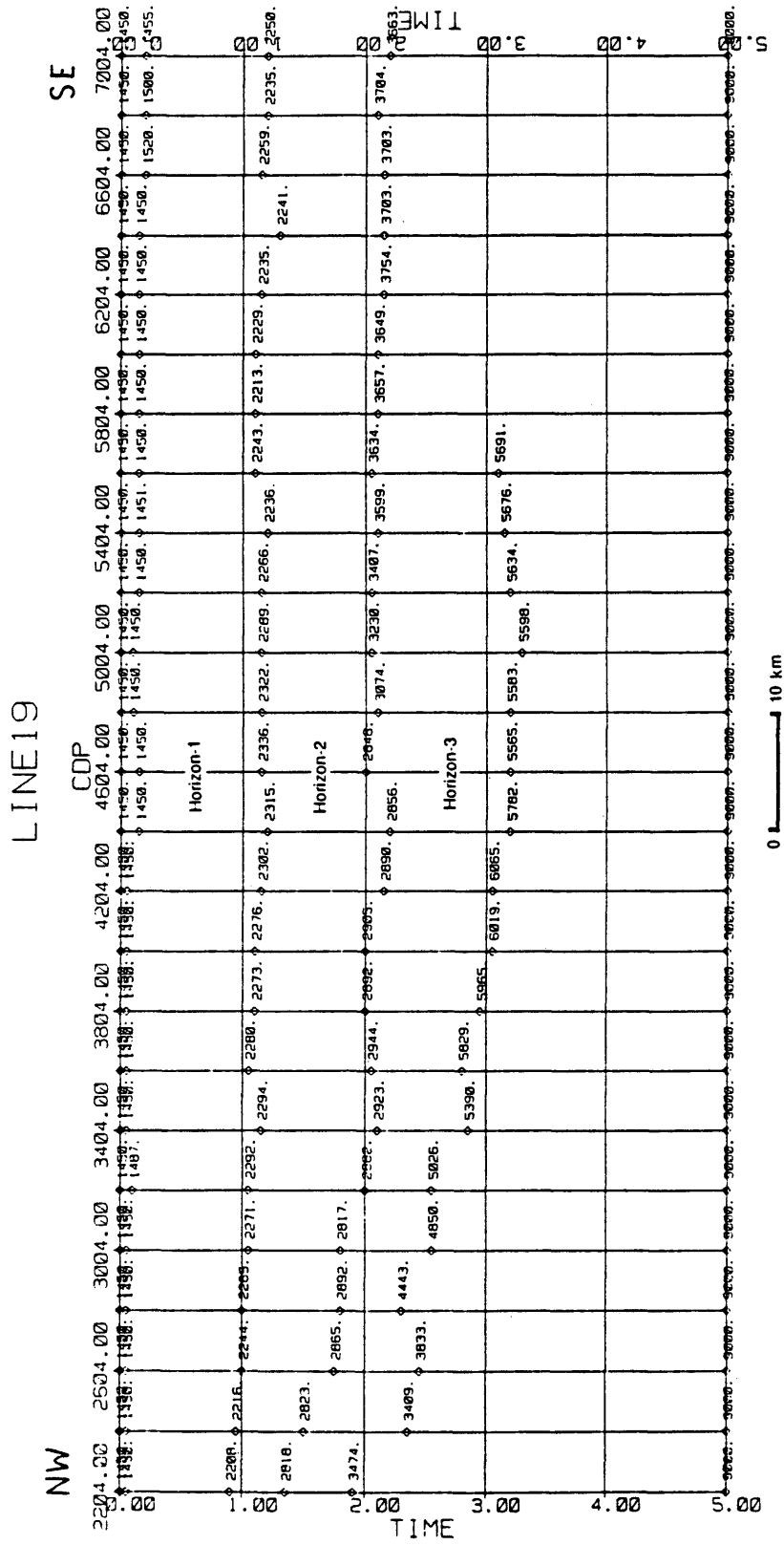


Figure 5.2: Average interval velocities (CDP moveout) across the shelf along USGS seismic line 19 (averaged over 5 points).

present in the plot, the interpreter conclude that errors were possibly made in the processing of the data or that the velocity analyses performed on the data could not give a reliable estimate of the stacking velocity. However, if the interpreter is sure that the velocity functions input to the program are valid, then the presence of isovelocity anomalies can be quite significant to his interpretation.

Another advantage of an isovelocity plot is one of interest to the processor. The processor is familiar with the velocity functions since he chooses them from velocity analysis displays. Thus, he should have a general idea of the appearance of the isovelocity plots before it is generated. Therefore, after looking at the plot generated from his input data, he can quickly determine if he has made any input errors by noting anomalies or the absence of them in the plot. Correcting those functions which were in error will save processing time since NMO corrections are quite time consuming and will be useless if made with incorrect velocity functions. The interval velocities from the CDP moveout velocities of line 209 and 19 along with their standard deviations are presented in appendix A-1 and A-2 respectively.

INTERPRETATION

6.1: Seismic stratigraphic interpretation

Five basin wide unconformities have been delineated on both of the seismic lines 209 and 19 in the Georges Bank (Plate 1 and 2). They are: 1) at the base of Tertiary, 2) at the base of Upper Cretaceous, 3) at the base of Lower Cretaceous, 4) at the base of Upper Jurassic, and 5) at the base of Middle Jurassic (i.e., Postrift unconformity). The postrift unconformity, separates the synrift and the postrift sediments. It appears at the northwestern corner of seismic line 19 as an angular unconformity. However, this unconformity is conformable seaward of the mid shelf region and is not very clear (probably reflected energy is masked by limestone and evaporites). For the purpose of this study, only three major lithostratigraphic units represented by strong reflection events across the entire seismic section are considered for the velocity gradients. These units are mostly, 1) Tertiary and Cretaceous, 2) Upper Jurassic, and 3) Middle Jurassic formations.

The unconformities have been identified on the basis of borehole information (Poag and Valentine, 1988) and by

projecting the continuity of the seismic events along the seismic sections. A comparison of the synthetic seismogram generated from the sonic and density logs of COST G-2 well is shown in figure 4.3 where the five unconformities have been correlated with line 209.

Seismic line 19 passes across from the inner shelf to the continental rise, whereas line 209 passes across from the midshelf region to the continental rise in the Georges Bank. It may be observed on both the lines that the Jurassic section thins slightly toward the shelf edge where the carbonate platform is the most dominant feature, but some of this thinning may be due to a velocity pull up.

The unconformity at the base of Lower Jurassic is probably the postrift (Schlee and Klitgord, 1988 ; sometimes refered to as the "breakup unconformity", Falvey, 1974 ; Montadert et al., 1979) and is a conspicuous acoustic reflector that marks a major change in depositional pattern during basin evolution. This unconformity separates synrift sedimentary rock from overlying postrift sedimentary rock (figure 6.1 and 6.2). This boundary is caused by a change in tectonic regime from block faulting during rifting to broad

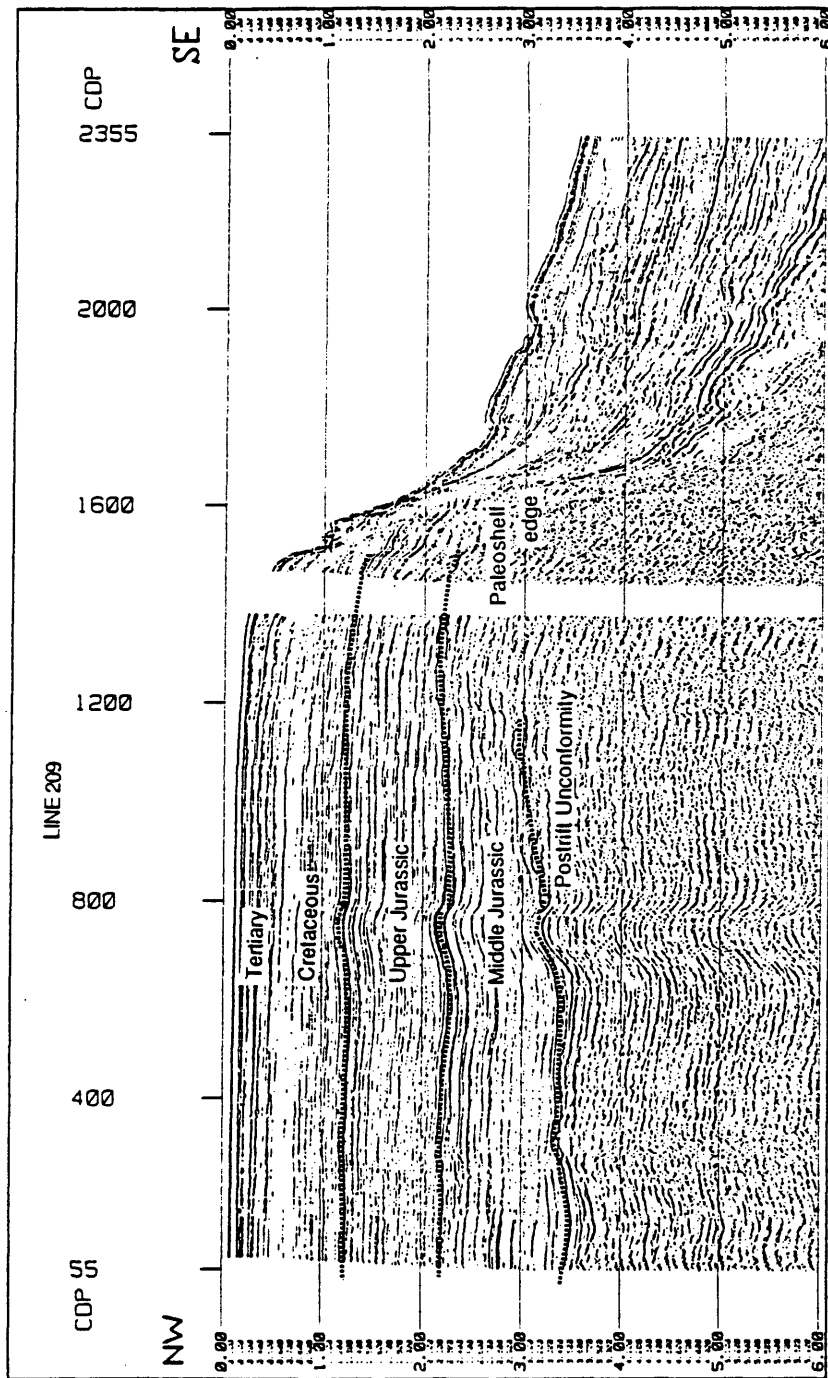


Figure 6.1: Interpreted seismic section of USGS seismic line 209 (only the major postrift sedimentary horizons are shown).

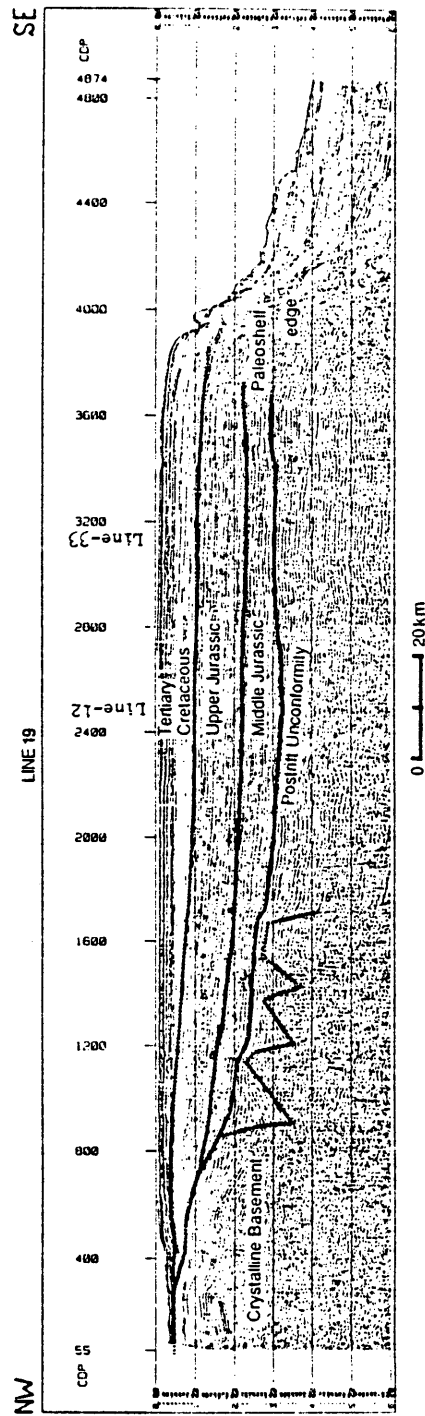


Figure 6.2: Interpreted seismic section of USGS seismic line 19 (only the major postrift sedimentary horizons are shown).

crustal subsidence during the passive tectonic phase as the axis of seafloor spreading migrated seaward.

The COST G-1 well (figure 2.3) was drilled near a basement high at the western edge of the main basin, in an area where a seismic profile reveals a rapidly thinning sequence marked by alternating continuous high amplitude reflections (interbedded and non-marine strata, Schlee and Klitgord, 1988). The postrift unconformity is interpreted as the acoustic reflector at the top of a conglomerate layer at COST G-1; it can be traced acoustically to a conglomerate layer at COST G-2 well, where it coincides with a thin red siltstone-sandstone layer above a salt layer sampled in the bottom of the COST G-2 well. Some patches of mounded chaotic reflectors (plate 1 and 2) beneath postrift unconformity have been interpreted as carbonate mounds (Poag, 1982a, Schlee and Fritsch, 1982). The COST G-2 well penetrated only the upper 12 m of the salt, but seismic evidence suggests that basement is at least 500 m below the top of the salt (Schlee and Klitgord, 1988). The salt has not been dated at the COST G-2 site; it may be as old as Late Triassic to late Early Jurassic.

Normal faults within synrift deposits and possibly crystalline rock can be inferred from acoustic records (figure 6.2). On both the profiles over the main basin, crystalline basement is buried beneath a salt layer that masks the return of acoustic energy. Seaward dipping reflectors beneath the postrift unconformity along the landward edge of the main basin could be from crystalline basement, overlain by a thick layer of synrift sediments.

6.1.1: Early Postrift Deposits (Jurassic)

The change to a regime of broad basin subsidence was attended by the formation of a broad carbonate bank, along the outer continental shelf edge, as open marine conditions became more prevalent. The carbonate bank may have been built from coalescing carbonate banks above elevated basement blocks or possibly salt swells. Earliest stages were probably marked by patch reefs and banks that were separated by moats and deep water channels (Eulik, 1978).

The character of the early postrift deposits changes from a dominantly clastic section in the northwest section of the basin (COST G-1) to a dominantly carbonate section

in the east (COST G-2) figure 6.3. The lowermost section of the postrift Early Jurassic(?) rocks or lower most Middle Jurassic? (Poag and Valentine, 1988) at the COST G-1 well is 400 m of dolomite and sandstone interbedded with minor shale and anhydrite. This unit corresponds to a 580 m section of limestone, dolomite, and anhydrite at COST G-2 site (figure 6.3).

Seismic data in the area between the two wells are characterized by zones of very weak discontinuous subparallel reflections and zones of continuous parallel high amplitude reflections (figure 6.4 (a and b)), probably the wide spread carbonate section so prevalent in the main basin. The beds of sandstone and shale at the COST G-1 site are not found at COST G-2 . Toward the shelf edge and toward the COST G-2 well, reflections become more coherent, continuous, parallel, and have high amplitudes all characteristics that suggests a broad open marine shelf type of depositional environment (Schlee and Fritsch, 1982; and plates 1 and 2). Further, the widespread distribution of high interval velocities (>5km/sec) associated with these reflections, suggests that the limestone and dolomite penetrated in the boreholes cover much of the basin complex. Their uniform lithology in the lower part of the section

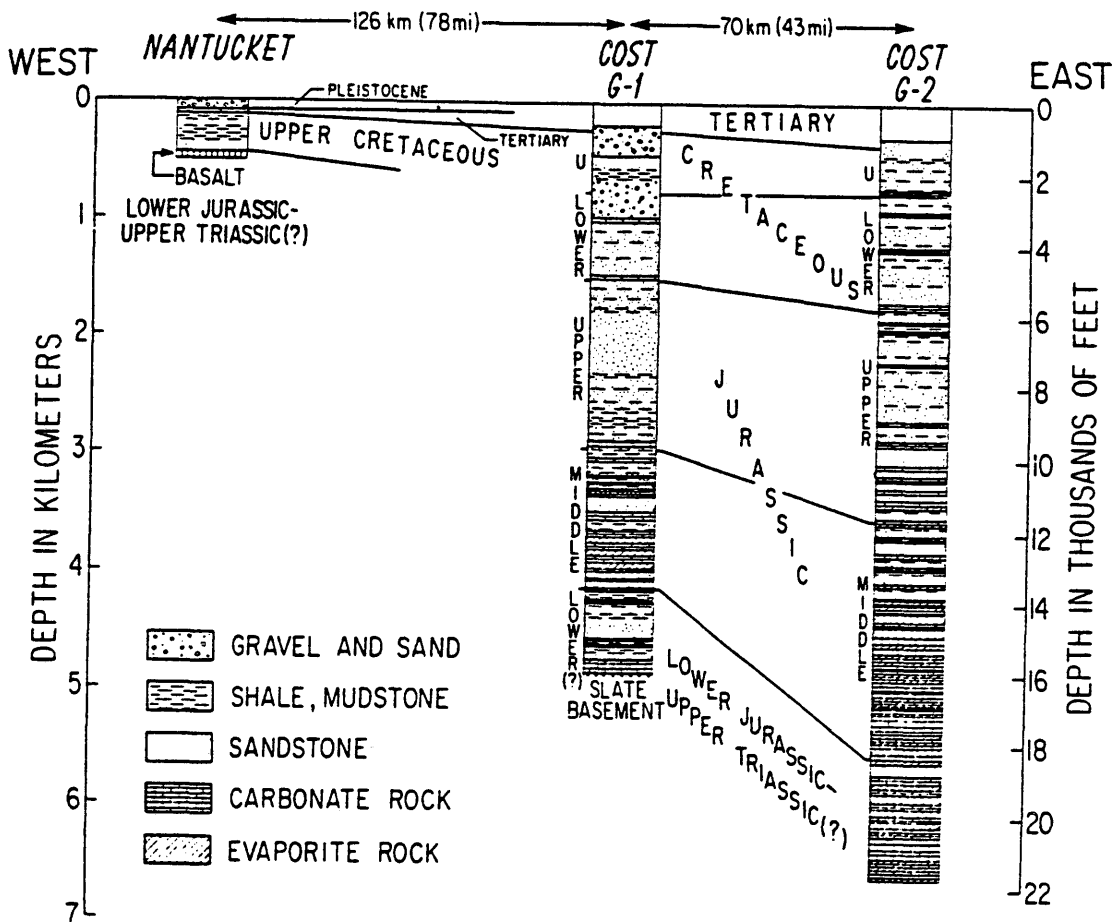


Figure 6.3: Strata penetrated in COST G-1 and COST G-2 wells in the Georges Bank (from Schlee and Klitgord, 1988).

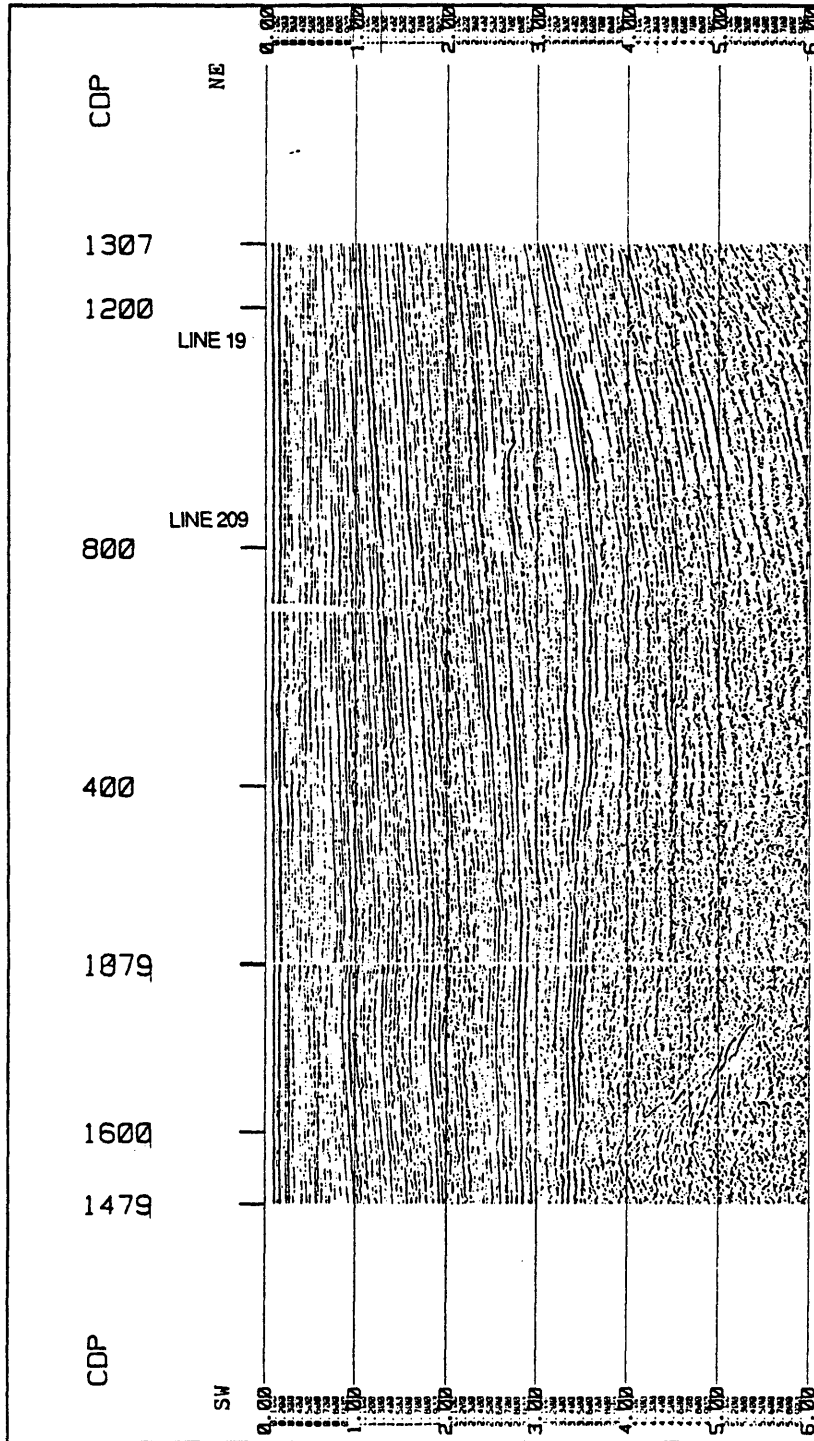


Figure 6.4(a): Part of the final stacked section of seismic line 12I and 12J that joins line 209 and 19 in the mid-shelf region.

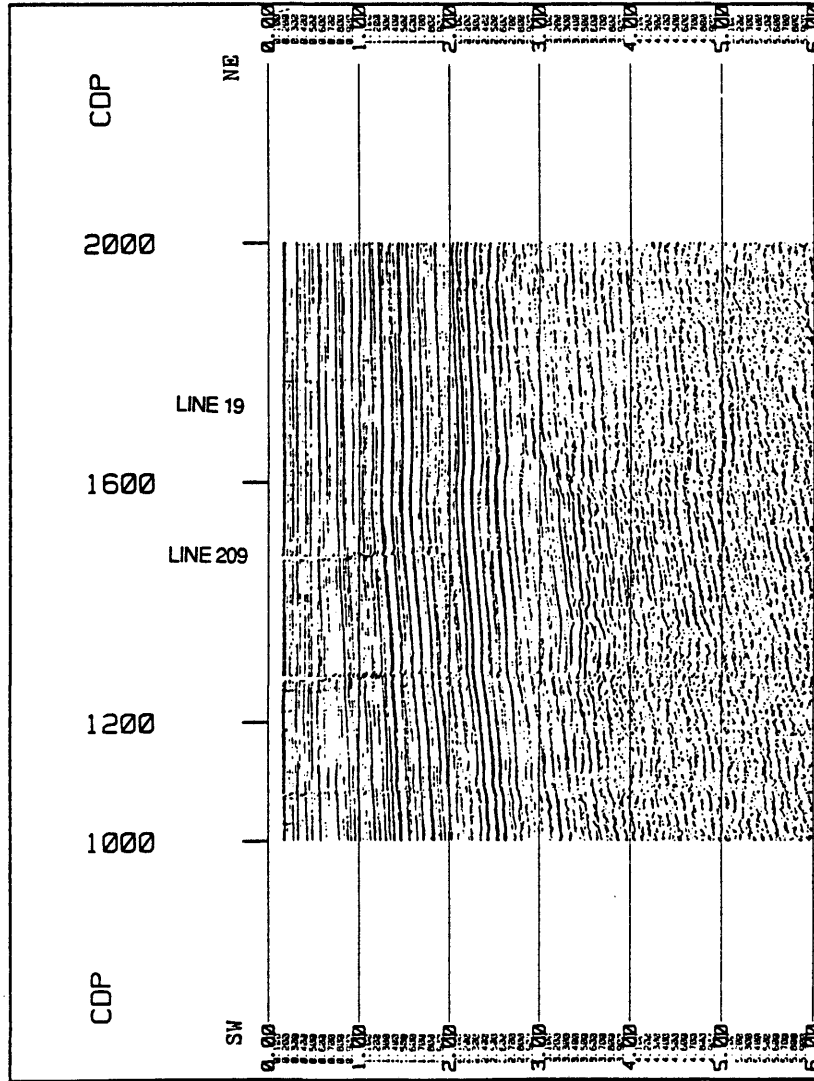


Figure 6.4(b): Part of the final stacked section of seismic line 33 that joins line 209 and 19 in the mid-shelf region.

results acoustically in a loss of continuity at a time depth of 3 seconds from mid shelf toward the shelf edge.

The next overlying sequence of Middle Jurassic(?) rocks grade from approximately 980 m of interbedded sandstones, shales, and limestones at COST G-1 to approximately 1350m of limestone minor amounts of sandstone and shale at COST G-2 (Poag, 1982a).

The Upper Jurassic section in COST G-1 (1000 m thick and at a depth of 2000-3000m) is mainly shale and sandstone of the Mohawk and Mic Mac formations together with abundant lignite and some coal near the top of the section (Poag,1982a; Arthur,1982). The Upper Jurassic rocks are abundant 1300m thick in COST G-2 (depth 1700 - 3000m) and, for the first time, contain abundant sandstone,shale,siltstone, and mudstone and a few oolitic and algal limestone beds. During the early Late-Jurassic(?), both well sites were characterized by fluctuation of alluvial, nearshore, and inner-shelf environments (Poag, 1892a; Schlee and Fritsch, 1982). The COST G-2 site returned to an inner-shelf environment by the end of the Late Jurassic. Sediment accumulation rates were less than

during the Early and Middle Jurassic, reflecting the slower subsidence of the margin. Seaward of the COST G-2 well (figure 2.3 and 6.1), reflection profiles indicate that the Upper Jurassic section is characterized by zones of highly continuous parallel reflections interleaved with a few zones of less continuous parallel reflections of moderate amplitude. Toward the present shelf edge, the acoustic character changes as the parallel arrangement of reflections becomes faint and their amplitude variable. This is the main area of carbonate paleoplatform development.

6.1.2: Late Postrift Deposits (Cretaceous-Tertiary)

Postrift Cretaceous rocks on Georges Bank are less than half as thick as the post-rift Jurassic section (in COST G-1, about 1300m versus 2500m, and in COST G-2, about 1450m versus 3900m). Subsidence on the margin slowed during the Cretaceous and Tertiary and became more uniform over the entire margin, so that little thickening took place. Further, the Cretaceous and Tertiary marked a change over to dominantly noncarbonate marine sedimentation.

Lower Cretaceous rocks are 900m thick in COST G-1 and consist of loosely cemented sandstone and shale containing beds of coal, dolomite, and lignite. The equivalent section in the COST G-2 is about 1050m thick; although some thick limestone beds are present, sand containing beds of coal, shale and mudstone dominates. Strata at both sites were deposited in a shallow nearshore to coastal alluvial environment. The first strata traceable on seismic profiles over the carbonate buildup that formed a paleoshelf edge (figures 6.1 and 6.2) are within this section (Hauterivian in age; Poag,1982b).

The Upper Cretaceous section is thin in COST G-1, about 450m, and comprises sand, shale, and gravel, together with glauconite and lignite. In COST G-2, the same section thins to about 350m and is mainly calcareous sand, claystone, and siltstone; it is marked by several conspicuous unconformities (Poag and Schlee,1984). Seaward, the Upper Cretaceous section thickens rapidly under southwest Georges Bank to more than 1km, and several units reappear. At the eastern end of Georges Bank, extensive erosion and outbuilding in the Tertiary cut back the Upper Cretaceous section, so that Middle Eocene chalk unconformity overlies Neocomian limestone in Heezen Canyon(Ryan and Millar, 1981).

The Tertiary section is estimated to about 250 m thick in both COST G-1 and G-2 wells. It contains mostly unconsolidated sand, abundant shale, glauconite, and lignite. Thin Paleocene strata are present in both COST G-1 and G-2 wells. Pleistocene to rocks are present in the COST G-2 well.

6.1.3: Ancient Carbonate Platform

A conspicuous feature of the Atlantic margin is a buried limestone platform of Jurassic age (figures 2.2, 6.1 and 6.2). From Nova Scotia to the Gulf of Mexico, the carbonate platform and the slope seaward of it formed a major physiographic province; the platform, banks, and atolls probably flourished as a semicontinuous feature that stretched along most of eastern North America (Schlee et al., 1979; Klitgord et al., 1982; and Schlee and Fritsch, 1982).

6.2: Interval velocity interpretation

Compressional velocities within sedimentary rocks vary as functions of lithology, age, depth of burial, and diagenetic history. Analysis of velocity data derived from multichannel seismic profiles permits the continuous mapping of vertical and horizontal velocity variations. In cases where age and depth of burial are known to be constant, velocity variations can be restricted to differences in either lithology or diagenetic history. Analysis of these velocity variations on the U.S. Atlantic margins has revealed certain major trends. For example, Schlee et al., (1976) and Grow et al., (1979) observed in both Georges Bank and Baltimore Canyon Trough, that sedimentary horizons between 2 and 4 km depth increased in velocity from near shore to off-shore. This is interpreted as indicating a trend from near shore clastic facies to more limestone-rich facies offshore such as a carbonate bank or reef complex.

6.2.1: Common Depth Point (CDP) moveout velocities

Velocity analyses were made at every 2.5 km along the entire length of the line 209 and 19. The stacking velocities were smoothed by removing the handpicked velocities other than at the three main interfaces. These interfaces are 1) at the base of Cretaceous, 2) at the base of Upper Jurassic, and 3) at the base of Middle Jurassic. Formations lying between these interfaces will be referred to as horizon 1 ,2 and 3 respectively. These horizons are shown in figures 6.1 and 6.2 respectively. Interval velocities were derived from root-mean-square or stacking velocities according to the method of Dix (1955). The interval velocities along key reflecting horizons were averaged over 10 km length (5 point average) and plotted as a function of time along the profiles. Figures 5.1 and 5.2 show the average interval velocities across line 209 and line 19.

Across horizon-1 along line 209 and 19 (figures 5.1 and 5.2), velocities are nearly uniform (2200 to 2300 m/sec) in a NW-SE direction. The formation is characterized by 250 m thick Tertiary section of unconsolidated sand, shale, glauconite, and lignite at the COST G-1 site and

poorly consolidated calcareous sandstone shale (Arthur, 1982) at COST G-2 site (figure 6.3).

The middle part of horizon 1 (U.Cret.) contain 450 m sand, shale, and gravel, together with glauconite and lignite at COST G-1 site. In COST G-2 site, this section thins to about 350 m and is mainly calcareous sand, claystone, and siltstone (Schlee and Poag, 1984). The Lower Cretaceous rocks are 900 m thick in COST G-1 and consists of loosely cemented sandstone, and shale containing beds of coal, dolomite, and lignite. The equivalent section at COST G-2 is about 1050 m thick; although some thick limestone beds are present, sand containing beds of coal, shale, and mudstone, dominates (Poag, 1982b).

Interval velocities for horizon 2 varies between 2800 to 4104 m/sec, from the inner shelf to the outer shelf along line- 209 and 19 (figures 5.1 and 5.2). The formation is characterized by 1000 m thick Upper Jurassic section of shale and sandstone at COST G-1 and 1300 m thick sandstone, shale, siltstone, and mudstone and some limestone at COST G-2 site (Poag, 1982a, Arthur, 1982). Therefore horizon-2 shows nearly a 50% increase in velocity from the inner shelf to the outer shelf.

The interval velocities for horizon 3 along the shelf varies between 3400 m/sec to 6200m/sec, along line 209 and 19 (figures 5.1 and 5.2), where there is a trend of increasing interval velocities from inner shelf to outer shelf in a NW-SE direction, reflecting a systematic change in lithology to carbonate bank or reef facies. It was observed from COST G-1 and COST G-2 wells that this horizon comprises of 980 m of interbedded sandstone, shale, and limestone at COST G-1 site to approximately 1300 m of limestone and minor amounts of sandstone and shale at COST G-2 site (Poag, 1982a).

Early refraction studies of the Atlantic shelf revealed four mappable velocity units (Drake et al., 1959). Velocities less than 2 km/sec were generally found at depths less than 1 km, and were assumed to represent "unconsolidated sediments". Velocities between 2.0 to 3.0 km/sec generally were found at depths between 1 and 2 km and were assumed to represent " semiconsolidated sediments". Velocities between 3.0 to 4.5 km/sec were found at depths of 2 to 3 km along the outer shelf; these velocities were assumed to represent "consolidated sediments". Material with velocities over 4.5 km/sec underlay the consolidated sediment and, since these correlate with basement velocities

on shore beneath coastal plain, they were also assumed to represent on basement the outer continental shelf. More recent interpretations have assumed that the high velocity refracting horizons at depths of 2 to 5 km on the middle and outer shelf are limestone units (Emery and Uchupi, 1972; Berhendt et al., 1974; Mayhew, 1974; Sheridan,1974; Schlee et at., 1976).

6.2.2: Sonic log velocities

The sonic logs from nine different wells in the Georges Bank (COST G-1, COST G-2 , Exxon-153, Exxon-170, Conoco-179, Tenneco-182, Mobil-196, Shell-210, and Shell-218) are converted into velocity logs (from microseconds/ft to feet/sec and then meters/sec). Average interval velocities are obtained from these velocity logs at a 500 m interval. Short wavelength velocity inversions are numerous on the sonic logs, while the 500 m averaged interval velocities display a systematic increase with depth. Figure 6.5 displays sonic velocity and averaged interval velocity log from COST G-2 well. Sonic velocity and averaged interval velocity logs from the other wells are presented in the appendix B.

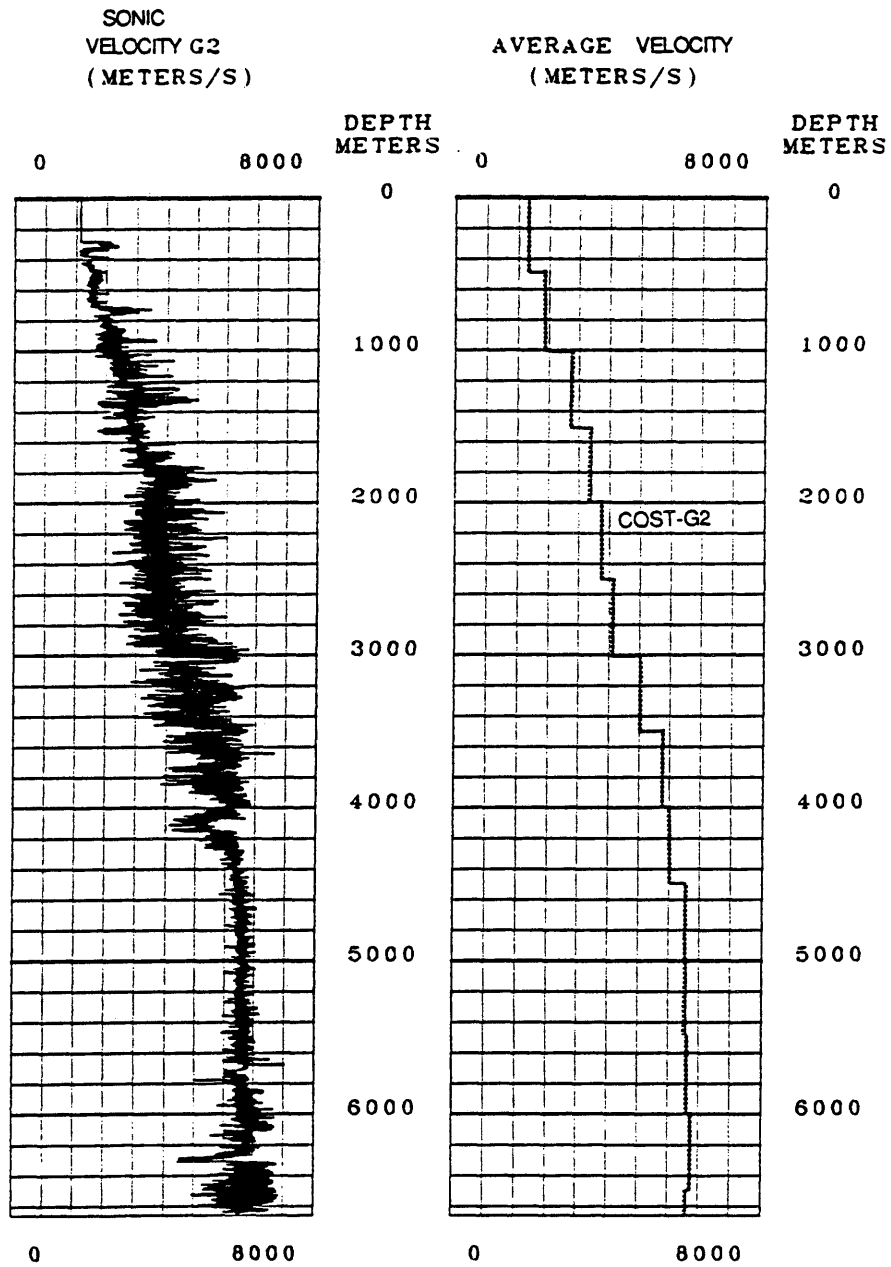


Figure 6.5: Velocity and the averaged interval velocity (500 m) logs obtained from the sonic log of COST G-2 well.

Figure 6.6 show a composite of the interval velocity curves obtained from the sonic logs. All of these curves display a similar increasing trend in velocity with depth although their ranges differ from each other depending upon the location of the wells. Since too many curves make it difficult to distinguish a velocity gradient from inner shelf to the outer shelf and along the margin, a separate comparison along certain profiles are made and will be discussed later.

6.2.3: Checkshot velocities

Interval velocities at a 500 m intervals were computed from the time-depth curves from the ten wells (Shell-200 and nine other wells mentioned in the earlier section). In general, checkshot interval velocities (for intervals greater than 100 m) are considered to be more accurate than the sonic interval velocities. A comparison of the checkshot and the sonic interval velocities for COST G-2 well is shown in figure 6.7. It is very clear that they agree very well throughout the depth of the log data. Similar comparison for the other wells are presented in the appendix C. Although the difference is very little between these two sets of curves, sonic velocities sometimes show a slower velocity

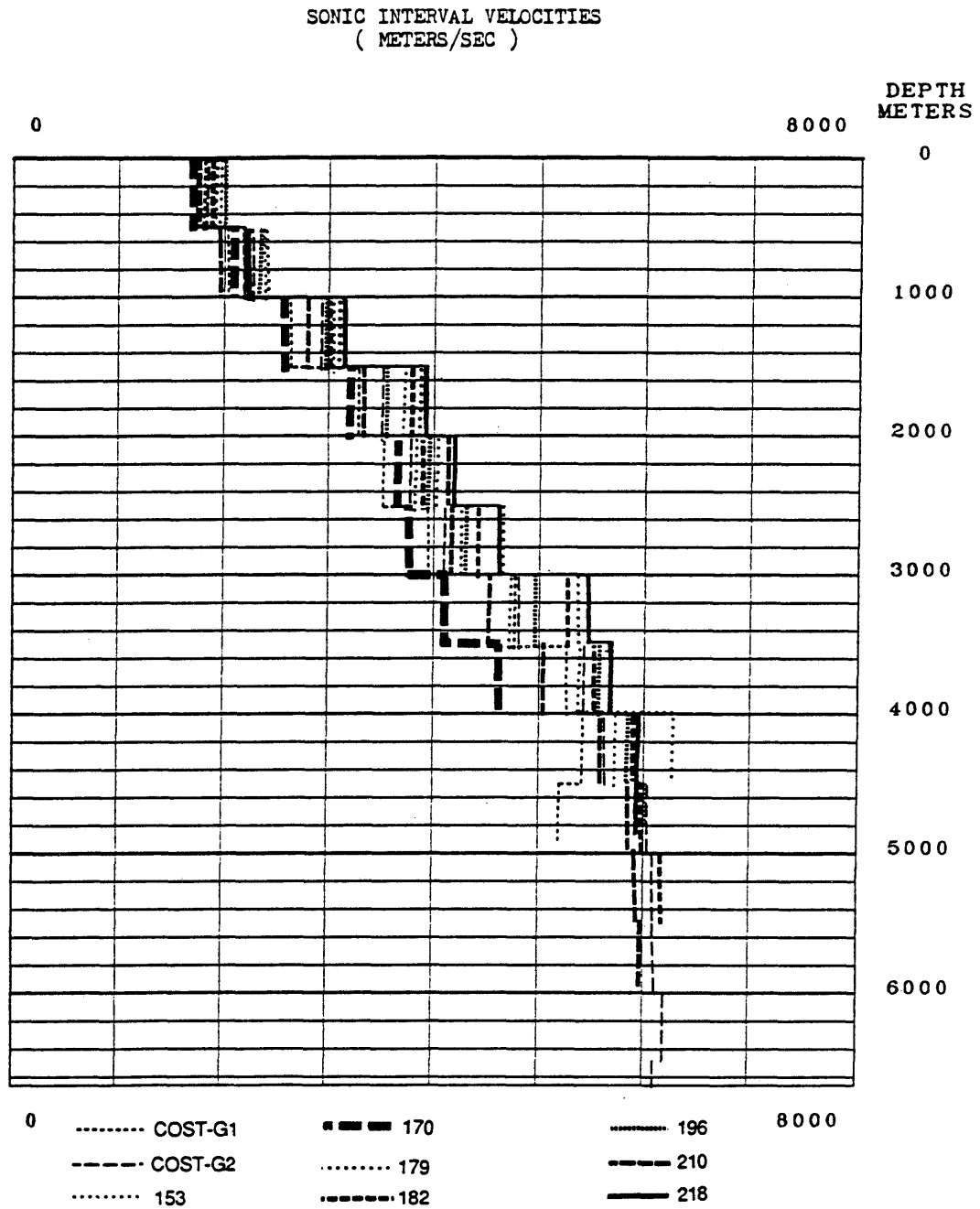


Figure 6.6: Averaged interval velocity logs from sonic logs (at 500 m interval) from the nine wells in the Georges Bank Basin.

SONIC AND CHECKSHOT INTERVAL VELOCITIES
(METERS/SEC)

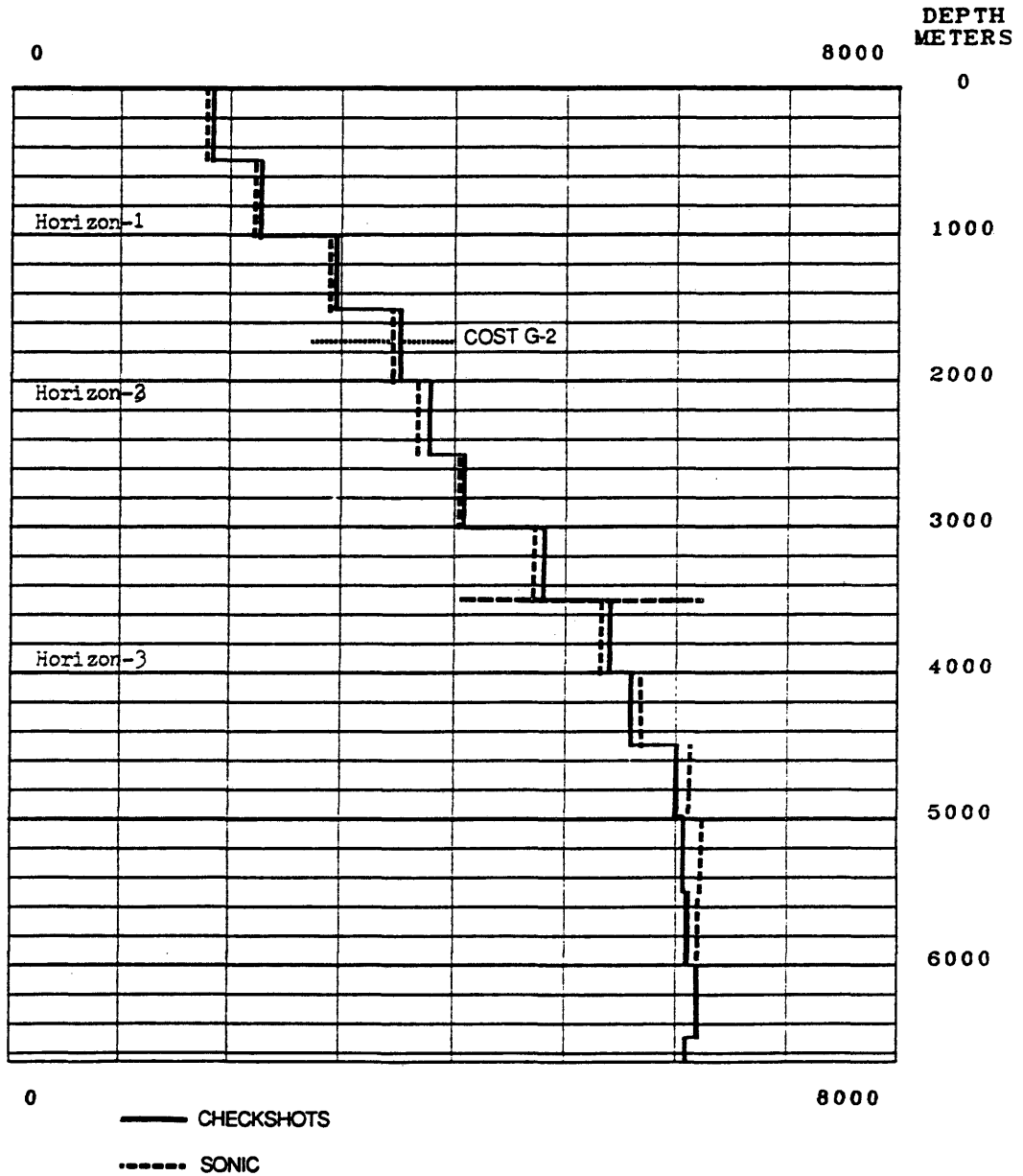


Figure 6.7: A comparison of checkshot and sonic interval velocities (at 500 m interval) at the COST G-2 site.

throughout the curve, for example Exxon-170. It has been observed that the drift between these two sets of curves show a little asymmetry, while the mean remains very close to zero, and 80% of the drift is within 0 to (plus/minus) 200 m/sec (appendix D-10). Their general agreement also proves the reliability of the interval velocities computed from sonic logs. A comparison of the interval velocities from CDP moveout velocities with sonic and checkshot interval velocities is presented in appendix D-11. Because of the extremely good general agreement between the checkshot and sonic velocities, and that the checkshot data are less incomplete (do not represent the entire depth of the wells) I will use the averaged interval velocities based on the sonic logs for the subsequent discussion of lateral velocity gradients.

6.2.4: Velocity gradients across the shelf.

Figure 6.8(a) show a comparison of the interval velocities at a 500m interval, obtained from the sonic logs of COST G-1, Exxon-170, Mobil-196, and Shell-218 in a northwest to southeast direction across the shelf. It is clear that the interval velocities show a systematic increase from Exxon-170 at the inner shelf to Shell-218 at

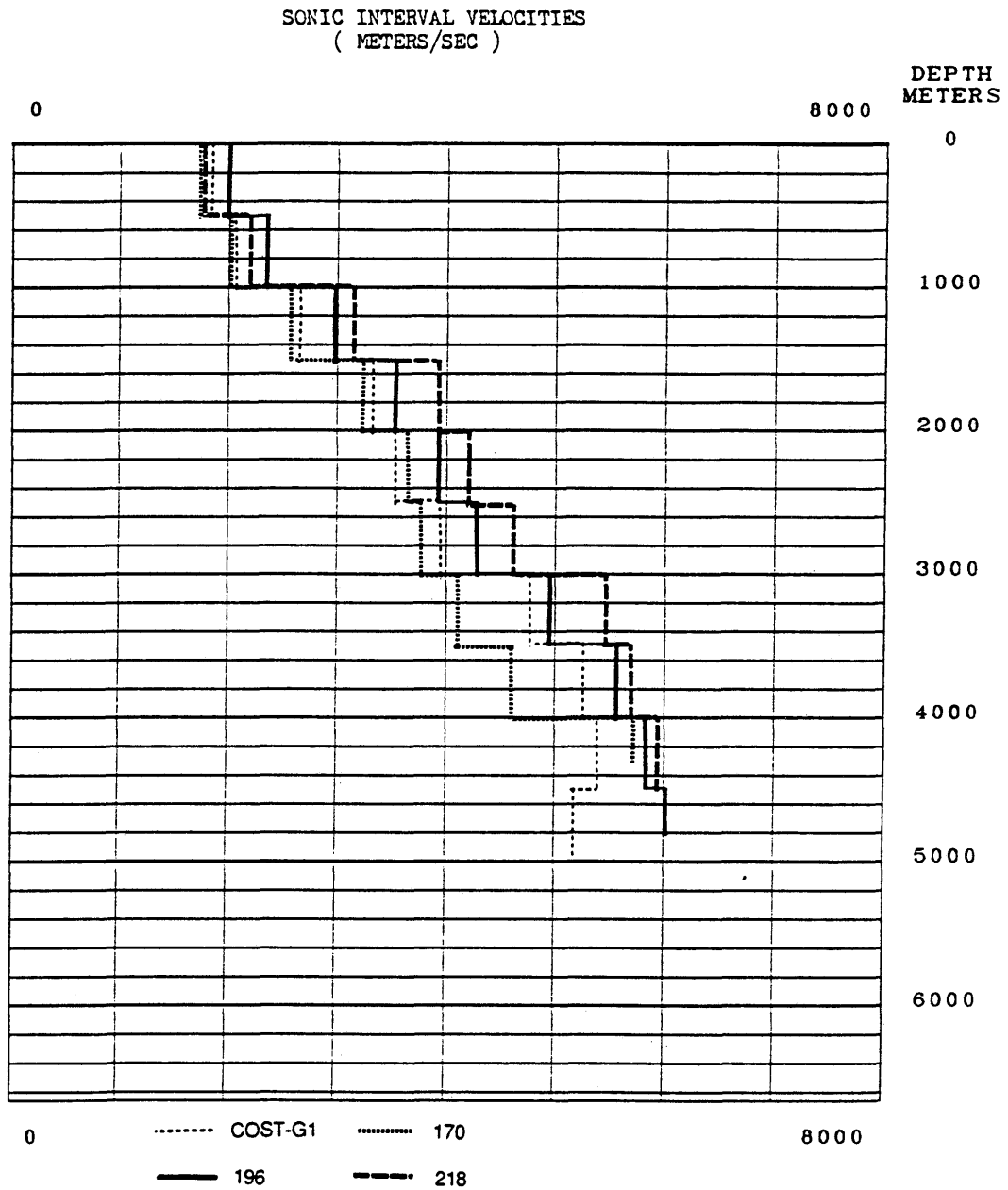


Figure 6.8(a): A comparison of the averaged sonic velocities along a NW-SE section through COST G-1, Exxon-170, Mobil-196, and Shell-218 wells.

the outer shelf through Mobil-196 at the mid shelf region. Which is a definite indication of a gradual change in lithology from a clastic to a more carbonate facies. COST G-1 has higher velocity trend than Exxon-170, but it is still relatively low.

Another northwest to southeast cross section through Exxon-153, COST G-2, Tenneco-182, and Shell-218 is shown in figure 6.8(b), and passes from inner shelf to the outer shelf region. It is clear that the range of velocities remain close in the upper 1500 m and then they show a gradual increase in the velocity until a depth of 4000 m. Beyond 4000 m there is very little increase in velocity. However, the higher velocity values of Tenneco-182 and Conoco-179 with respect to COST G-2 and Exxon-153 between 1500 and 4000 m depth imply a systematic change in lithology from clastic to a more carbonate rock at the outer shelf. Velocities in excess of 5500 m/sec beneath the middle and outer continental shelf indicates dense limestones, while velocities in excess of 6000 m/sec require the dominance of dolomites and anhydrites (appendix E).

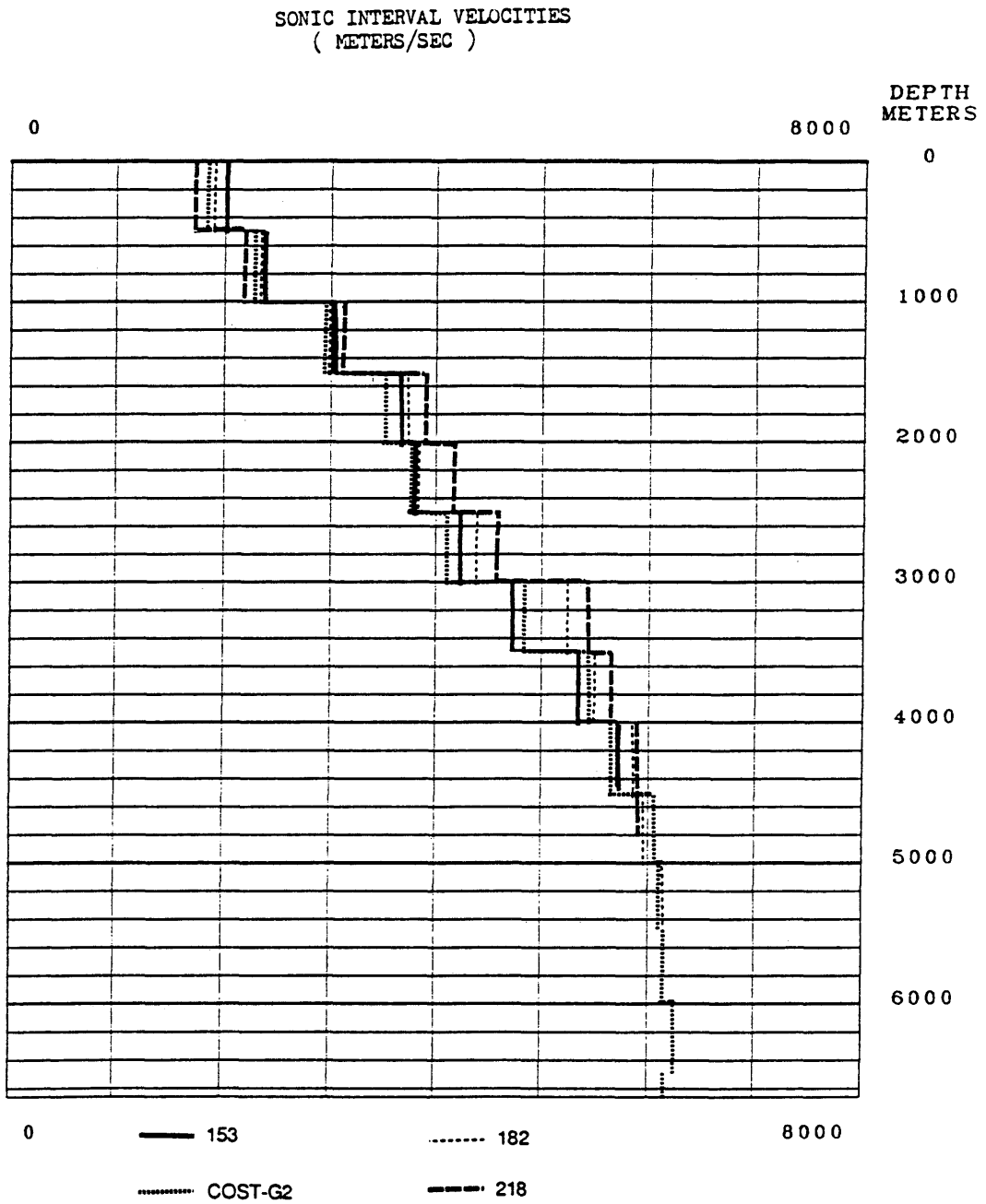


Figure 6.8(b): A comparison of the averaged sonic velocities along a NW-SE section through Exxon-153, COST G-2, Tenneco-182, and Shell-218 wells.

6.2.5: Velocity gradients along the margin.

Figure 6.8(c) shows a comparison of the sonic interval velocities obtained from the COST G-1, Exxon-170, and Exxon-153 wells along the margin in a southwest to northeast direction. An increase in velocity through the entire depth range of the data is clear, which definitely indicates a change in lithology from Exxon-170 to the Exxon-153 site. Exxon's OCS-170 shows the lowest overall velocities in the entire set of wells. A comparison of COST G-1 and Exxon-153 velocities (figure 6.8(d)) shows a moderate difference suggesting a velocity difference probably due to differential compaction along the margin, rather than a significant lithological change. The lower interval velocity range shown by Exxon-170 may be due to a higher percentage of shale and sand in the section, although no detailed lithologic descriptions of the Exxon-170 lithologies has been published to date.

Another southwest to northeast section through the wells Shell-210, Mobil-196, Tenneco-182, and Conoco-179 is shown in figure 6.8(e). Shell-210 show a lower range of velocities throughout the depth of the well. However, the remaining three wells show an increase in velocity along the

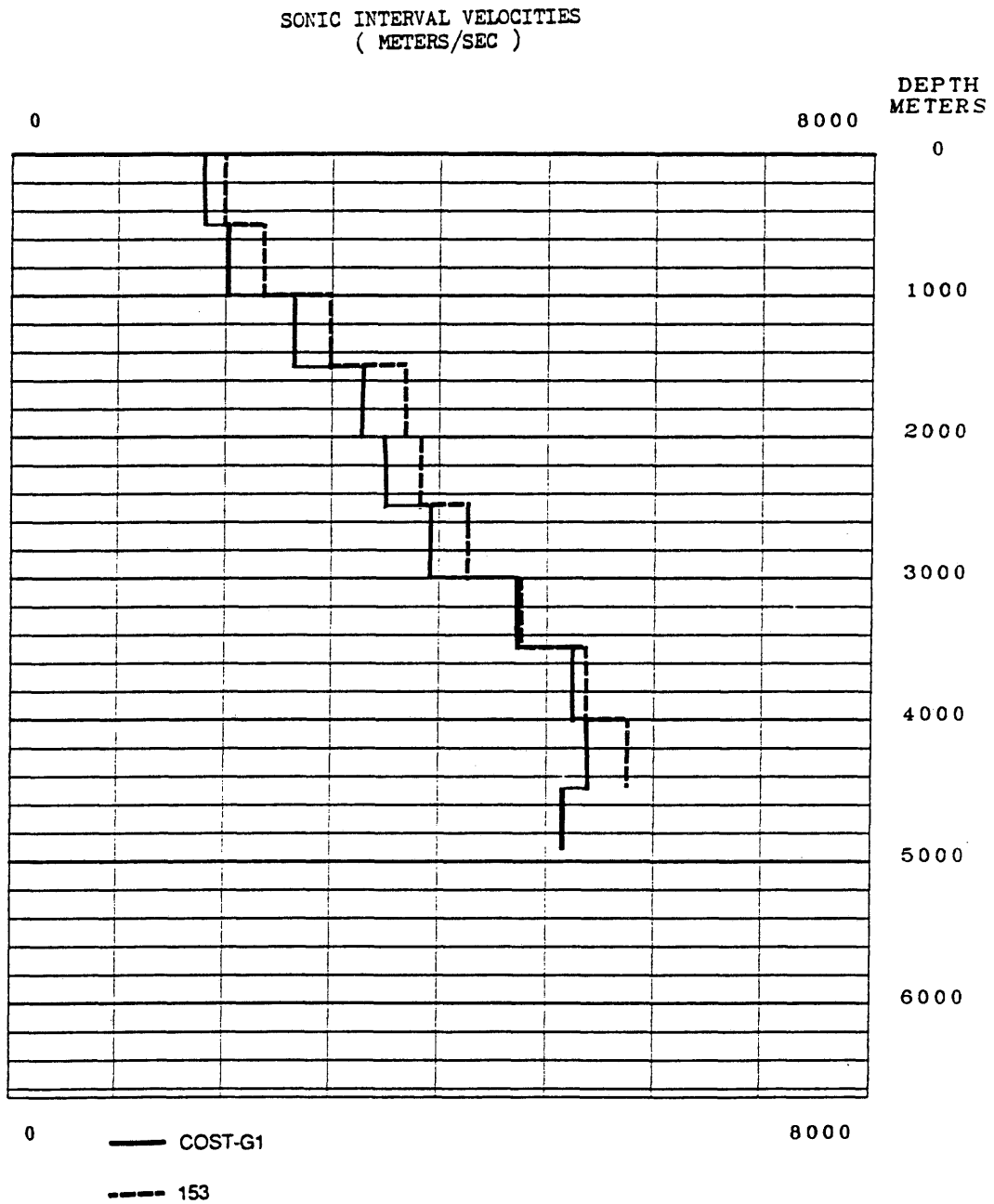


Figure 6.8(d): A comparison of the averaged sonic velocities along a west-east section through COST G-1 and Exxon-153 wells.

margin from southwest to northeast. This velocity change due primarily to thinning of the section to the northeast as indicated in the in the above paragraph by COST G-1 and Exxon-153 wells.

Part of the final stacked sections of line 12I, 12J, and 33 that joins line 209 and 19 in the mid shelf region is shown in figures 6.9 and 6.10 respectively. Averaged sonic velocities from the nearby wells have been projected on the respective horizons of these two lines. A moderate increase in velocity in the Jurassic formations may be noted on line 12 between Exxon-170 and Exxon=153 wells, where the formation average velocities ranges from 3566 to 3930 m/sec in the Upper Jurassic section and 4800 to 5266 m/sec in the Middle Jurassic section respectively (figure 6.9). Therefore, there is a 10% increase in velocity between Exxon-170 to Exxon-153 locations. On line 33, averaged sonic velocities from Mobil-196, Tenneco-182, and Conoco-179 have been projected (figure 6.10). Although these averaged sonic velocities show a slight change along the seismic section, a significant increase is observed in the Upper Jurassic section, from 3500 /3600 m/sec on line 12 (figure- 6.9) to 4100 /4200 m/sec on line 33 (figure 6.10), and from 4800/5100 to 5600/5800 m/sec in the Middle Jurassic

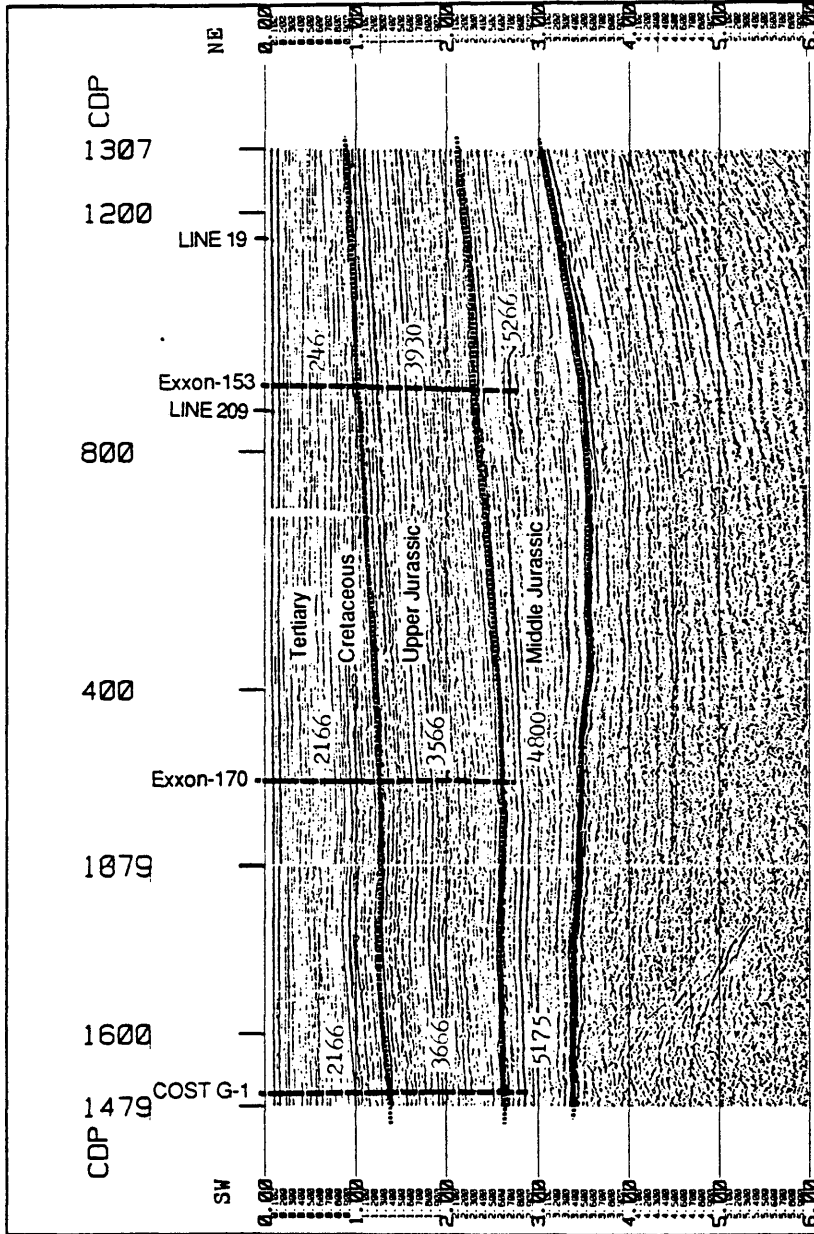


Figure 6.9: Part of the final stacked section of seismic line 12I and 12J , that joins line 209 and 19 in the mid-shelf region, on which averaged sonic velocities have been projected.

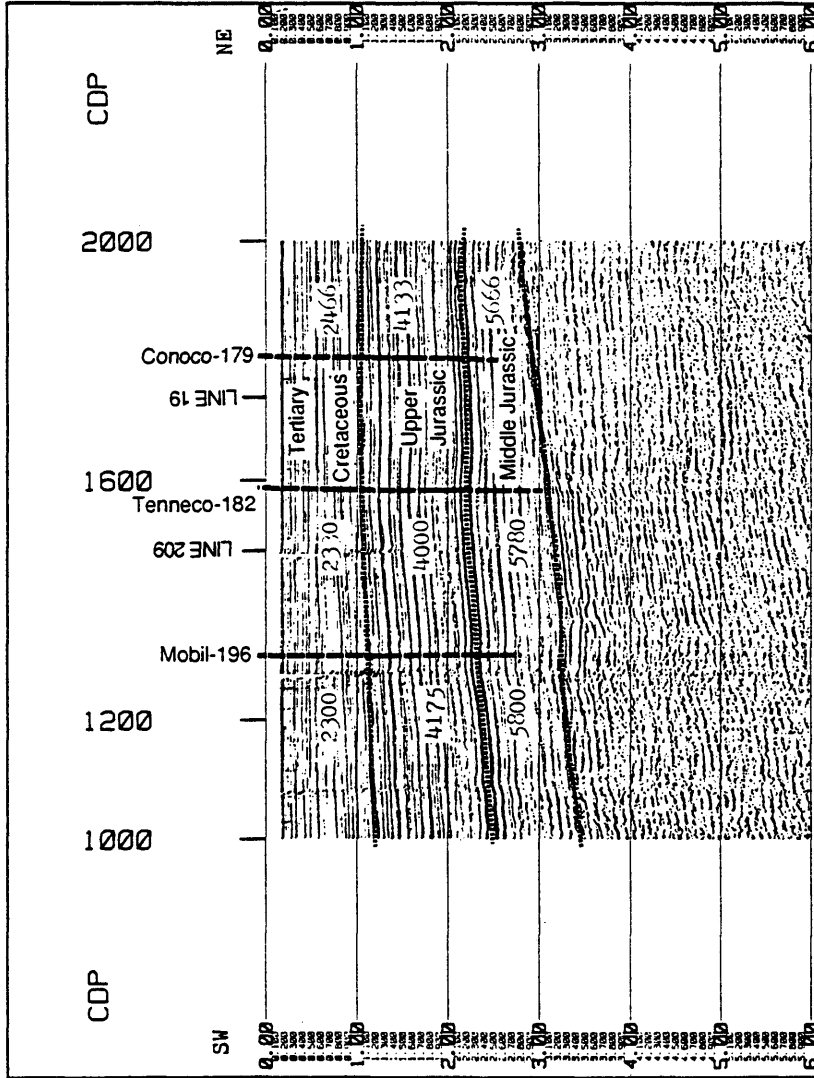


Figure 6.10: Part of the final stacked section of seismic line 33, that joins line 209 and 19 in the mid-shelf region, on which averaged sonic velocities have been projected.

section may be noted. The increase in velocity from 4800 m/sec to 5800 m/sec is a definite indication of an increase in carbonate sequence in the Middle Jurassic section along the shelf region of the Georges Bank basin. The slight lateral change in velocity (figure 6.10) shown by the averaged sonic velocities while the individual sonic averaged velocities do show some increase along line 33 may be interpreted to be due to the shallowing and thinning of the Jurassic section towards the northeastern end of the profile.

CONCLUSIONS

1) It has been observed along the seismic line 209 and line 19 that the interval velocities obtained from the CDP moveout velocity analysis show a gradual increase in the interval velocities from inner shelf to the outer shelf in the Jurassic section, while the Cretaceous and Tertiary units have more nearly uniform velocities. This increase is probably due to a lithologic change from a dominantly clastic to more carbonate sequences in the outer shelf, where the development of reef or carbonate banks has been demonstrated in the drilling data (Poag and Valentine, 1988).

2) A general agreement between checkshot and sonic interval velocities attests to the reliability of the computed velocities from these two sets of data. The checkshot and sonic velocities also confirm that the interval velocities obtained from the CDP moveout velocity analyses are reliable for thick intervals (i.e., greater than 1000 m).

3) Interval velocities obtained from the checkshots and the sonic logs of ten wells on Georges Bank also show a similar trend of gradual increase in the interval velocities

from the inner shelf to the outer shelf, confirming a lithologic change from a clastic to carbonate sequence in the Jurassic section.

4) The interval velocities from the checkshots and sonic logs also show a gradual increase in the interval velocities along the margin from southwest to northeast, which is probably due to a differential compaction rather than a dominant lithologic change along the shelf.

5) The velocities along the outer shelf edge at depths from 4000 m to 6700 m range from 5600 m/sec to 6200 m/sec indicating massive limestone and dolomites. This type of carbonate sequence development along the outer shelf of Georges Bank is not unique and also been observed in the Baltimore Canyon Trough (Grow et al., 1988). This is probably true for the Carolina Trough and Blake Plateau Basin which lack deep exploration wells (Dillon and Popenoe, 1988).

6) Although the interval velocities obtained from the checkshots and the sonic logs are more reliable, carefully picked CDP moveout velocities also show a very good

correlation with them and is very useful in identifying the lithologic changes along the seismic lines. Therefore a careful CDP velocity analyses, which can be done on any high quality multichannel seismic data, has been demonstrated to be a very reliable tool for predicting lateral velocity variations in sedimentary rocks in frontier continental margins before drill hole velocity surveys become available.

REFERENCES

- Anderson, R.C., and Taylor, D.J., (1981): Very high amplitude seismic anomaly in Georges Bank Trough, Atlantic continental margin; AAPG Bulletin, V.65, No. 1, P. 133-144.
- Amato, R.V., and Bebout, J.W., (1980): Geologic and operational summary, COST No. G-1 well, Georges Bank area, North Atlantic OCS: U.S. Geological Survey Open-file report 80-208, p.112.
- Arthur, M.A., (1982): Lithology and petrography of the COST Nos. G-1 and G-2 wells. United States North Atlantic Outer Continental Shelf: U.S. Geological Survey Circular 861, p. 11-13.
- Bally, A.W., (1981): Atlantic type margins, in Bally, A.W., ed., Geology of passive continental margins: AAPG education course notes, series 19, p. 1-1-1-48.
- Behrendt, J.C., et al., (1974): Seismic evidence of a thick section of sedimentary rock on the Atlantic outer continental shelf and slope of the United States [abs.]: EOS Transaction of the American Geophysical Union, V.55, p.278.
- Brustad, J.T., (1953): Curve path Delta-T analysis: Geophysics, V.18, p.738 (Abstract).
- Cornet, B., (1977): Palynostratigraphy and age of Newark super group (Ph.D. Thesis): University Park, Pennsylvania State University, p. 506.
- Dix, C.H., (1955): Seismic velocities from surface measurements: Geophysics, V.20, p. 68.
- Dillon, W.P., and Popenoe, P., (1988): The Blake Plateau Basin and Carolina Trough. The Geology of North America, V. I-2, The Atlantic Continental Margin:

U.S., The Geological Society of America, 1988. p. 291-328.

Drake, C.L., et al., (1959): Continental margins and geosynclines; The East coast of North America north of Cape Hatteras, Physics and Chemistry of the Earth: London, Pergamon Press, V.3, p. 110-198.

Emery, K.O., et al., (1970): Continental rise off eastern North America: AAPG Bulletin, V. 54, p. 44-108.

Emery, K.O., and Uchupi, E., (1972): Western North Atlantic Ocean; Topography, rocks, structure, waterlife, and sediments: AAPG Memoir 17, p. 532.

Eulik, L.S., (1978): The Abenaki formation, Nova Scotia shelf, Canada; A depositional and diagenetic model for a Mesozoic carbonate platform; Bulletin of Canadian Journal of Earth Sciences, V.9, p. 54-70.

Falvey, D.A., (1974): The development of continental margins in plate tectonic theory: Australian Petroleum Exploration Association Journal, V. 14, p. 95-106.

Gardnar, L.W., (1947): Vertical velocities from reflection shooting: Geophysics, V.12, p. 221.

Green, C.H., (1938): Velocity determinations by means of reflection profiles: Geophysics, V.3, p. 295.

Grow et al., (1988): Structure and evolution of Baltimore Canyon Trough, The Geology of North America, V. I-2, The Atlantic Continental Margin: U.S., The Geological Society of America, 1988, p. 296-290.

Grow, J.A., et al., (1979): Multichannel seismic depth sections and interval velocities over continental shelf and upper continental slope between Cape Hatteras and Cape Cod, AAPG Memoir 29, p. 65-83.

- Grow, J.A., and Sheridan, R.E., (1988): U.S. Atlantic Continental Margin; A typical Atlantic-type or passive continental margin, The Geology of North America, V. I-2., The Atlantic Continental Margin: U.S., The Geological Society of America, 1988.
- Hallam, A., (1971): Mesozoic geology and the opening of the North Atlantic: Journal of Geology, V.79, p. 129-157.
- Jansa, L.E., and Wade, J.A., (1975): Paleogeography and sedimentation in the Mesozoic and Cenozoic, southeastern continental margins and offshore petroleum exploration: Canadian Society of Petroleum Geologists Memoir 4, p. 79-102.
- Jaworski, B.L., et al., (1976): Airgun sonobuoy refraction measurements on Georges Bank (abs.); EOS, V.57, No.4 p. 265.
- Klitgord, K.D., and Behrendt, J.C., (1979): Basin structure of the U.S. Atlantic Margin, in Geological and Geophysical investigations of continental margins: AAPG Memoir 29, p. 85-112.
- Klitgord et al., (1982): Basement structure, sedimentation, and tectonic history of the Georges Bank Basin, in Scholle, P.A., and Wenkham, C.R., eds. United States North Atlantic Outer Continental Shelf; Geological Studies of the COST Nos G-1 and G-2 Wells: U.S. Geological Survey Circular 861, p. 160-186.
- Maher, J.C. and Applin, E.R., (1974): Geologic framework and petroleum potential of the Atlantic coastal plain and continental shelf: U.S. Geological Survey prof. paper 659, p. 98.
- Mattick et al., (1975): Sediments, structural, framework, petroleum potential, environmental conditions, and operational conditions of the United States North Atlantic outer continental shelf: U.S. Geological Survey open-file report 75-353, p. 179.

- Manspeizer et al., (1978): Separation of Morocco and eastern North America; A Triassic-Liassic stratigraphic record: Geological Society of America Bulletin, V. 89, p. 901-920.
- Mayhew, M.A., (1974): Geophysics of the Atlantic North America, in C.A. Burk and C.L. Drake, eds. Geology of continental margins: New York, Springer-Verlag, p. 409-427.
- Mayne, W.H., (1962): Common reflection point horizontal stacking technique: Geophysics, V. 27, p. 927.
- McIver, N.L., (1972): Cenozoic and Mesozoic stratigraphy of the Nova Scotia shelf: Canadian Journal of Earth Sciences, V. 9, p. 54-70.
- Montadert, L. et al., (1979): Rifting and subsidence of the northern continental margin of the Bay of Biscay, DSDP, Washington D.C., U.S. Govt. Printing Office, V. 48, p. 1025-1066.
- Morgan, L., and Dowdell, W., (1981): The Atlantic continental margin, a picture and work atlas: Seismic Expression of Structural Styles, AAPG, Studies in Geological Science No. 15, p. 30-35.
- Musgrave, A.W., (1962): Applications of expanding reflection spread: Geophysics, V. 27, p. 981.
- Pfleuger, J.E., (1954): Delta-T formula for obtaining average seismic velocity to a dipping reflection bed: Geophysics, V. 19, p. 339.
- Poag, C.W., (1982b): Stratigraphic reference section for Georges Bank Basin; Depositional model for New England passive margin: American Association of Petroleum Geologists Bulletin, V. 66, p. 1021-1041.

- Poag, C.W., (1982a): Foraminiferal and seismic stratigraphy, paleoenvironments, and depositional cycles in the Georges Bank Basin, Geological studies of the COST G-1 and G-2 wells, United States North Atlantic outer continental shelf: U.S. Geological Survey circular 861, p. 43-92.
- Poag, C.W., and Schlee, J.S., (1984): Depositional sequence and stratigraphical gaps on the submerged U.S. Atlantic margin, AAPG Memoir 36, p. 165-182.
- Poag, C.W., and Valentine, R.C., (1988): Mesozoic and Cenozoic stratigraphy of the United States Atlantic continental shelf and slope, The Geology of North America, V.1-2, The Atlantic Continental Margin: U.S., The Geological Society of America, 1988.
- Ryan, W.B.F., and Millar, E.L., (1981): Evidence of a carbonate platform beneath Georges Bank: Marine Geology, V. 44, p. 213-228.
- Schultz, L.K., and Grover, R.C., (1974): Geology of Georges Bank Basin: AAPG Bulletin, V.58, NO. 6, pt.2, p. 1159-1160.
- Schlee, J.C. and Cheetham, A.H., (1967): Rocks of Eocene age on Fippennies Ledge, Gulf of Maine: GSA Bulletin, V. 78, p. 681-684.
- Schlee, J. et al., (1976): Regional geologic framework off North-eastern United States, AAPG Bulletin, V.60, No.6, p. 926-951.
- Schlee, J., (1977): Stratigraphy and Tertiary development of the continental margin east of Florida: U.S. Geological Survey professional paper 581-F, p. 25.
- Schlee et al., (1979): Structure of the Continental slope off the Eastern United States, in Doyle, L.J., and Pilkey, O.H.; eds., Geology of Continental Slopes: Society of Economic Paleontologists and Mineralogists Special Papers 27, p. 95-118.

- Schlee, J. and Klitgord, K.D., (1981): Regional geology and geophysics in the vicinity of Georges Bank basin, U.S. Geological Survey open-file report 81-1352, p. 17-36.
- Schlee, J. and Klitgord, K.D., (1988): Georges Bank Basin: A regional synthesis, The Geology of North America, V. I-2, The Atlantic Continental Margin: U.S., The Geological Society of America, 1988.
- Schlee, J. and Fritsch, J., (1982): Seismic stratigraphy of the Georges Bank basin, studies in continental margin geology: AAPG Memoir 34, p. 223-251.
- Sengbush, R.L., (1961): Interpretation of synthetic seismograms: Geophysics, V. 26, No. 2, p. 138-157.
- Slotnik, M.M., (1959): Lessons in seismic computing: Tulsa, SEG.
- Sheridan, R.E., (1974): Atlantic Continental margin of North America, The Geology of Continental Margins: New York, Springer-Verlag, p. 391-407.
- Sheridan, R.E., (1976): Sedimentary basins of the Atlantic margin of North America: Tectonophysics, V. 36, p. 113-132.
- Sherwin, D.F., (1975): Scotian shelf and Grand Banks, in R.G. McGrossan, ed., Future petroleum provinces of Canada- their geology and potential: Canadian Society of Petroleum Geologists Memoir 1, p. 519-559.
- Steele, W.E., Jr., (1941): Comparison of well survey and reflection "time-delta-time" velocities: Geophysics, V.6, p. 370.
- Swift, A., et al., (1987): Subsidence, crustal structure, and thermal evolution of Georges Bank Basin: American Association of Petroleum Geologists Bulletin, V. 71, p. 702-718.

APPENDIXES

APPENDIX A. Standard deviations of CDP moveout velocities.

APPENDIX B. Checkshot time-depth curves.

APPENDIX C. Sonic and interval velocity logs.

APPENDIX D. Checkshot and sonic interval velocities.

APPENDIX E. Velocity-density relationships.

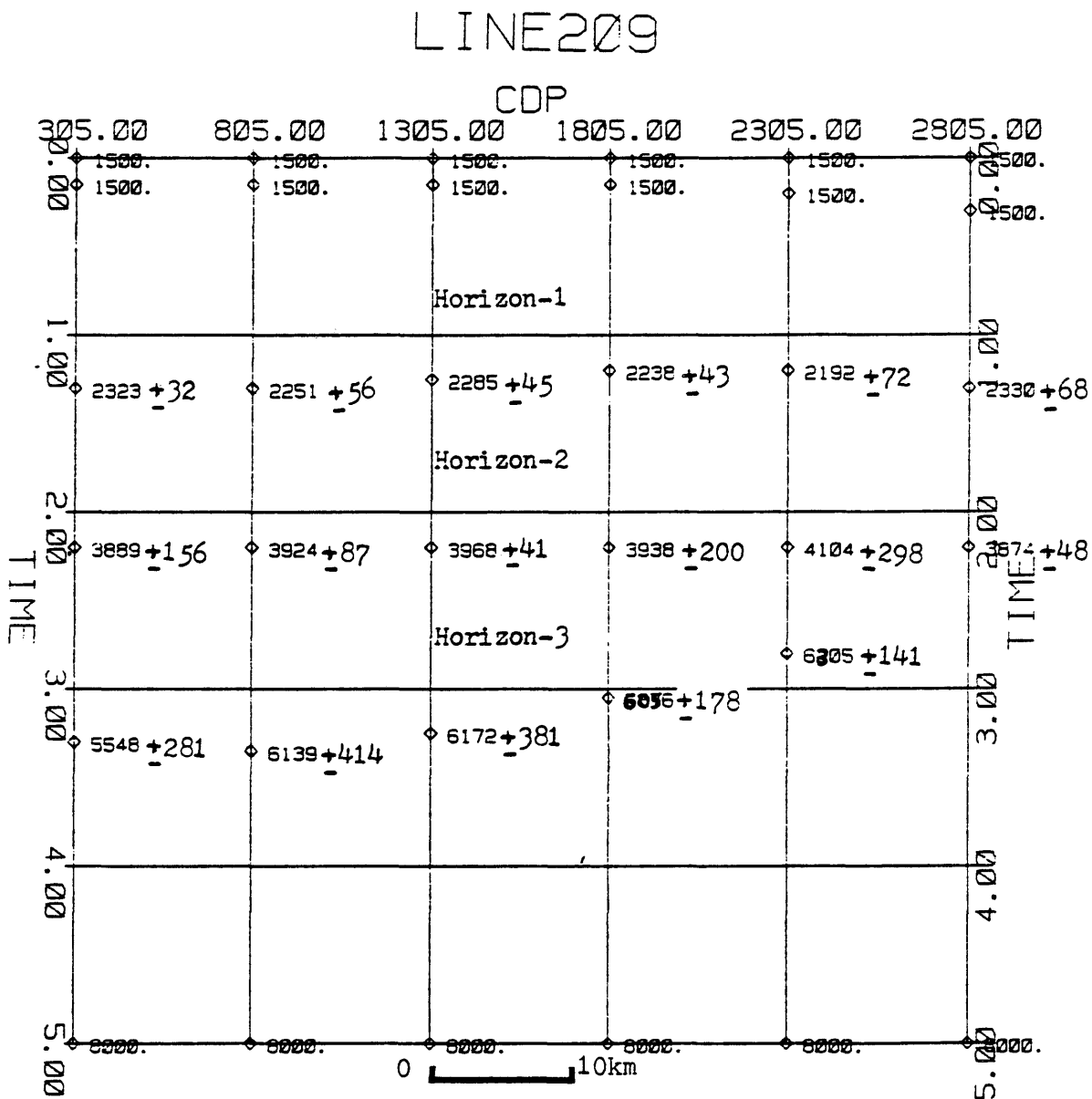


Figure A-1. Average interval velocities (5 point average of CDP moveout velocities) of seismic line 209 with their standard deviations.

LINE19

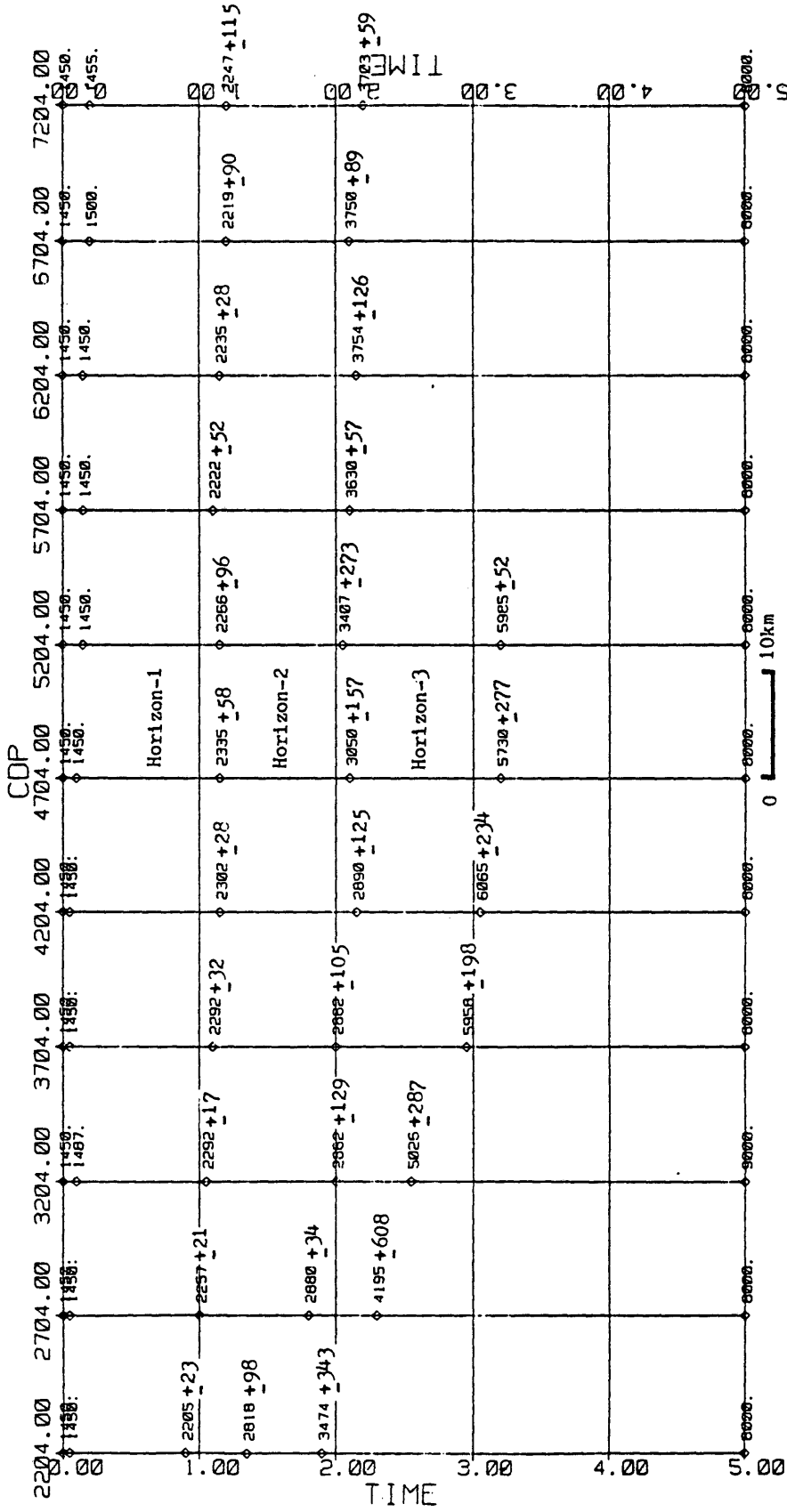


Figure A-2. Average interval velocities (5 point average of CDP moveout velocities) of seismic line 19 with their standard deviations.

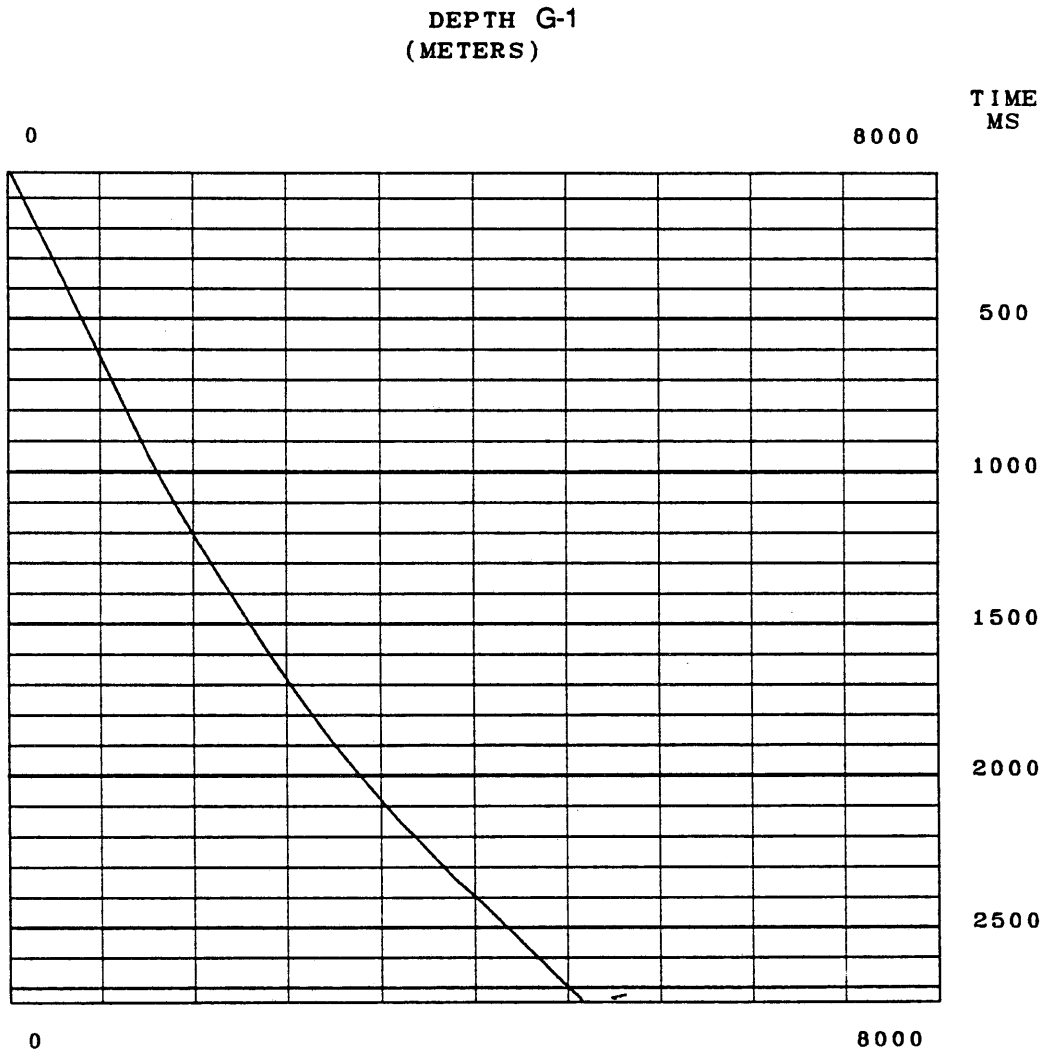


Figure B-1. Time-depth curve obtained from the checkshots of COST G-1 well in the Georges Bank Basin.

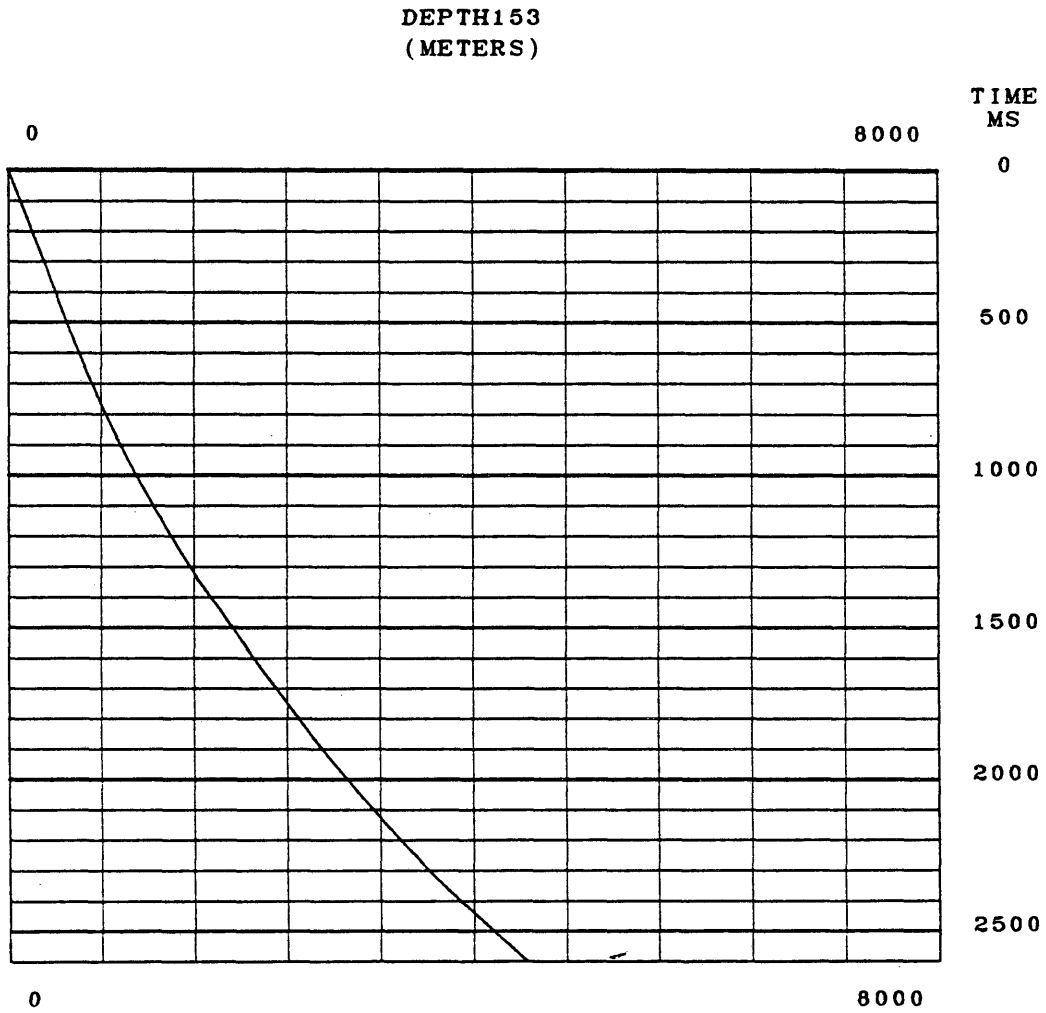


Figure B-2. Time-depth curve obtained from the checkshots of Exxon-153 well in the Georges Bank Basin.

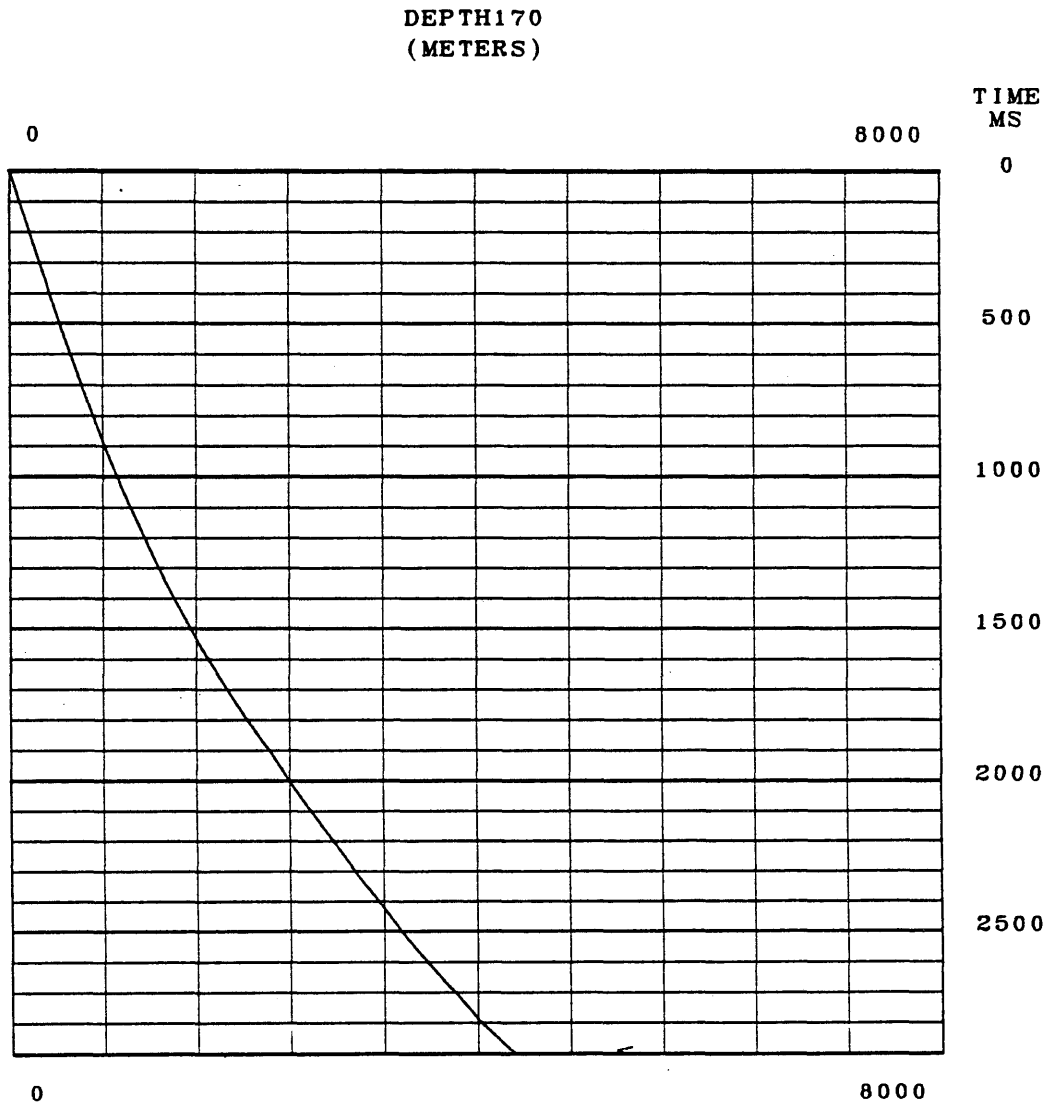


Figure B-3. Time-depth curve obtained from the checkshots of Exxon-170 well in the Georgse Bank Basin.

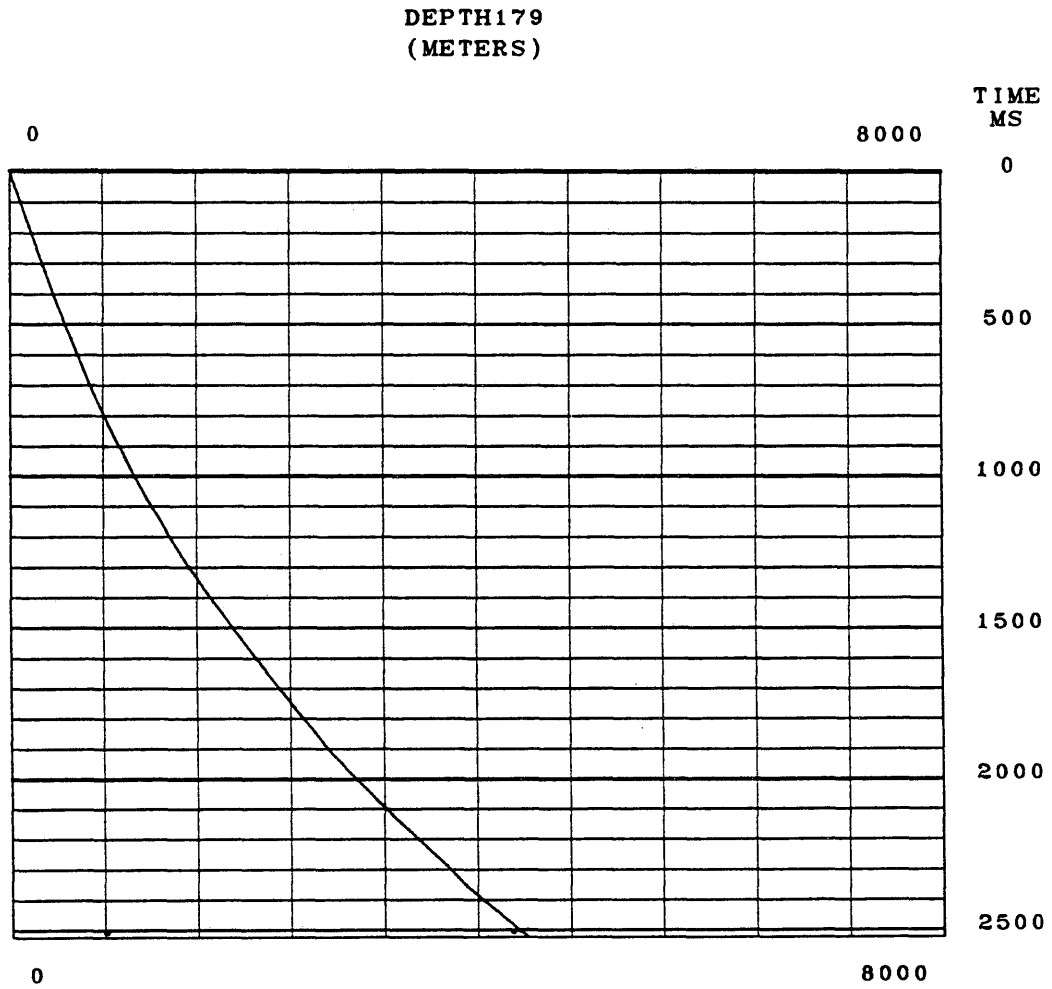


Figure B-4. Time-depth curve obtained from the checkshots of Conoco-179 well in the Georges Bank Basin.

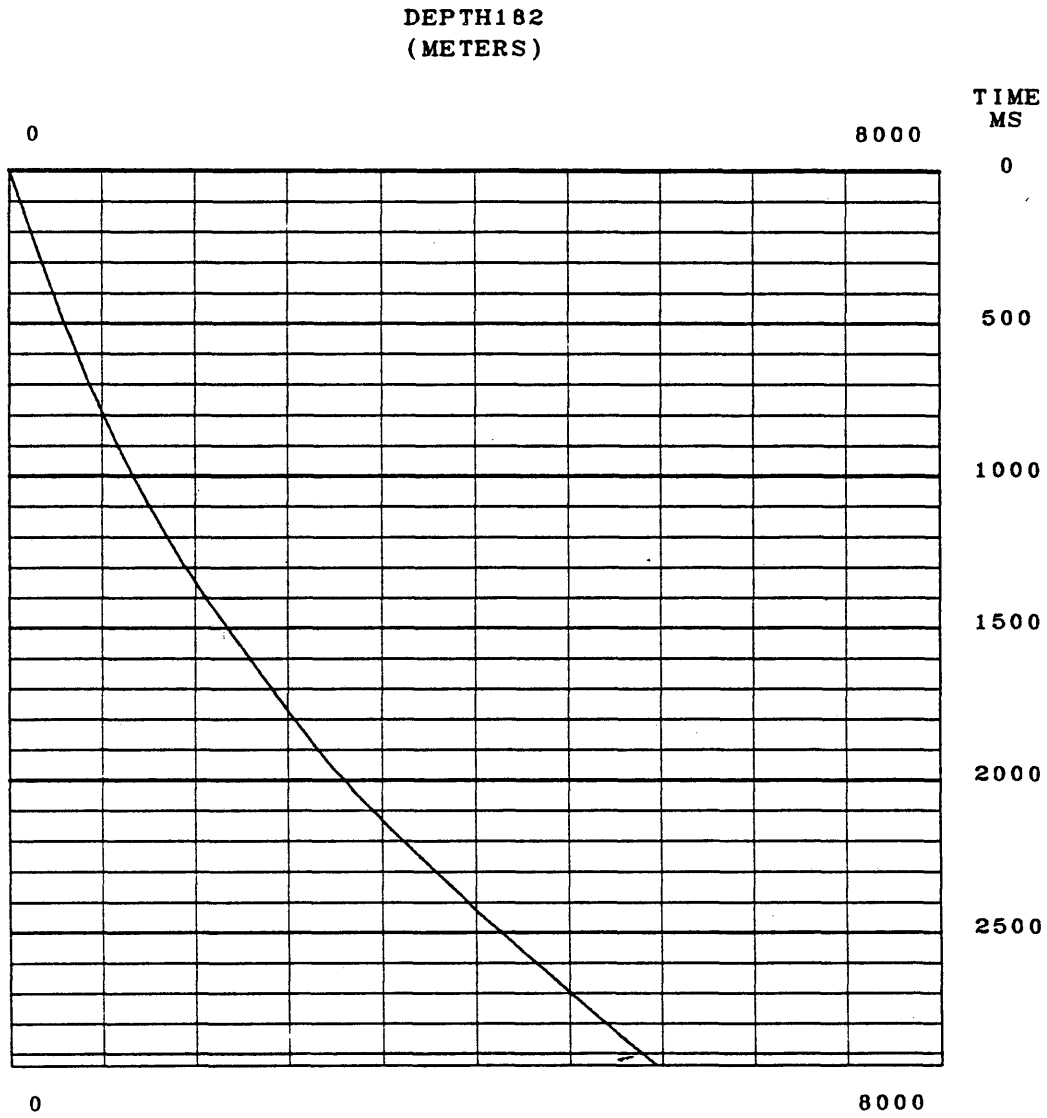


Figure B-5. Time-depth curve obtained from the checkshots of tenneco-182 well in the Georges Bank Basin.

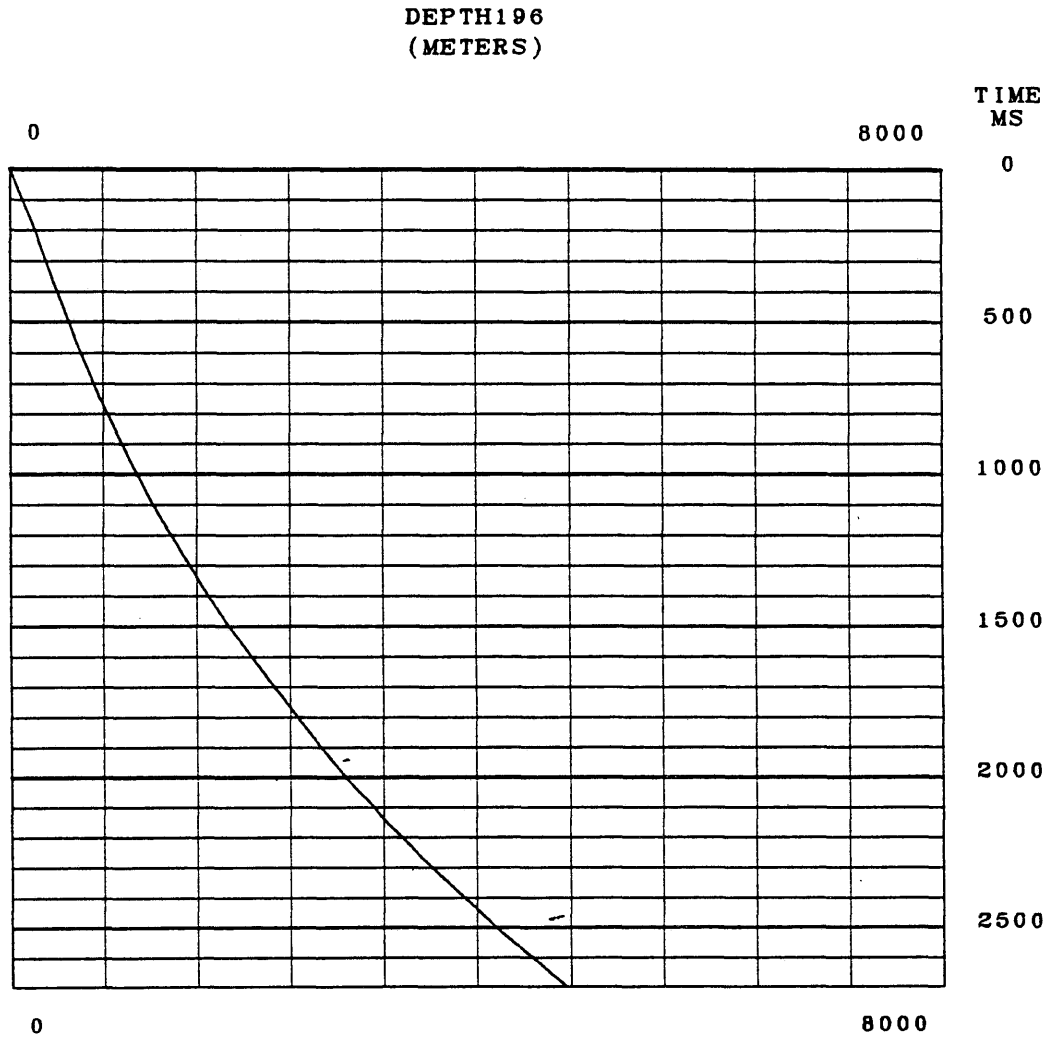


Figure B-6. Time-depth curve obtained from the checkshots of Mobil-196 well in the Georges Bank Basin.

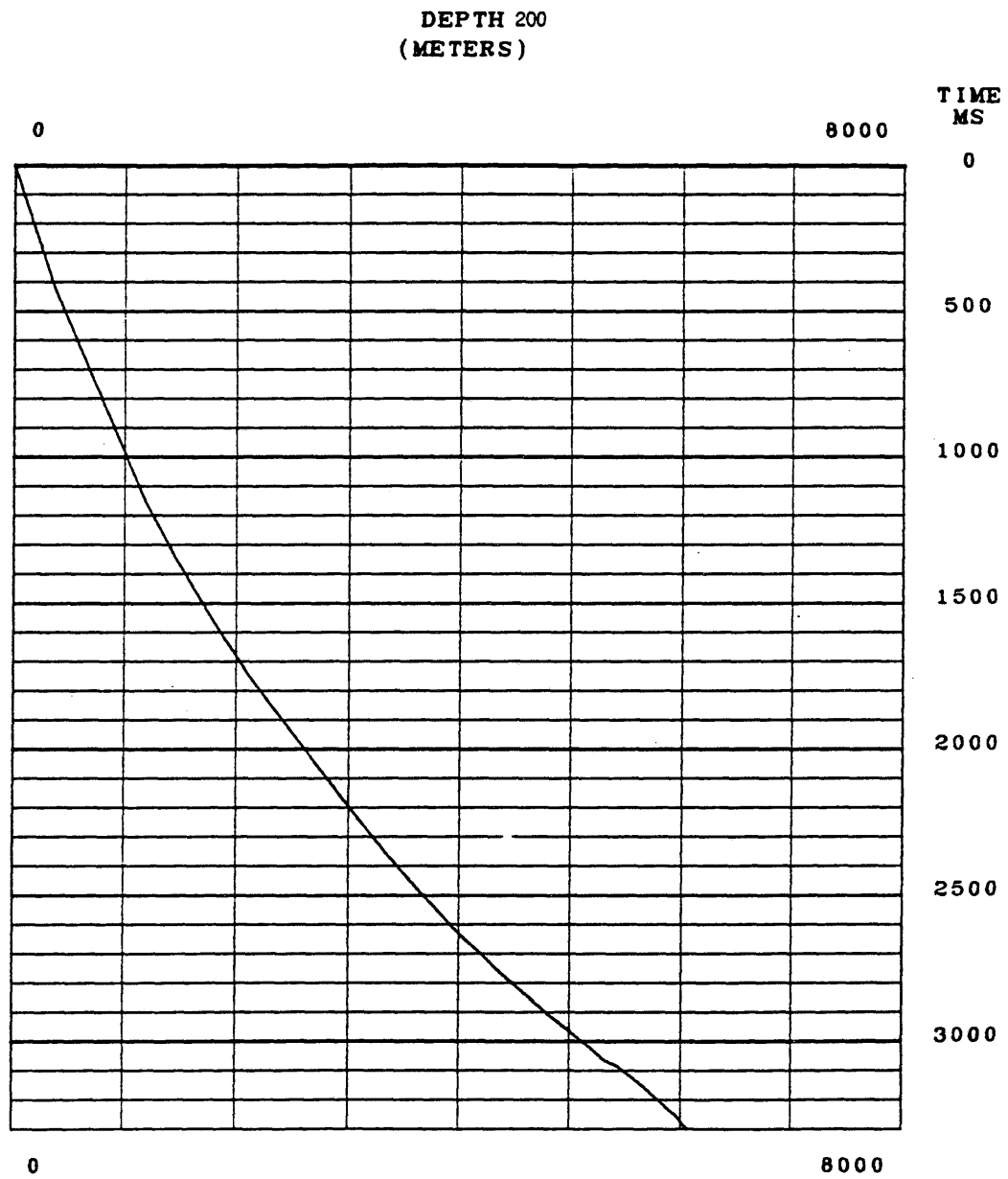


Figure B-7. Time-depth curve obtained from the checkshots of Shell-200 well in the Georges Bank Basin.

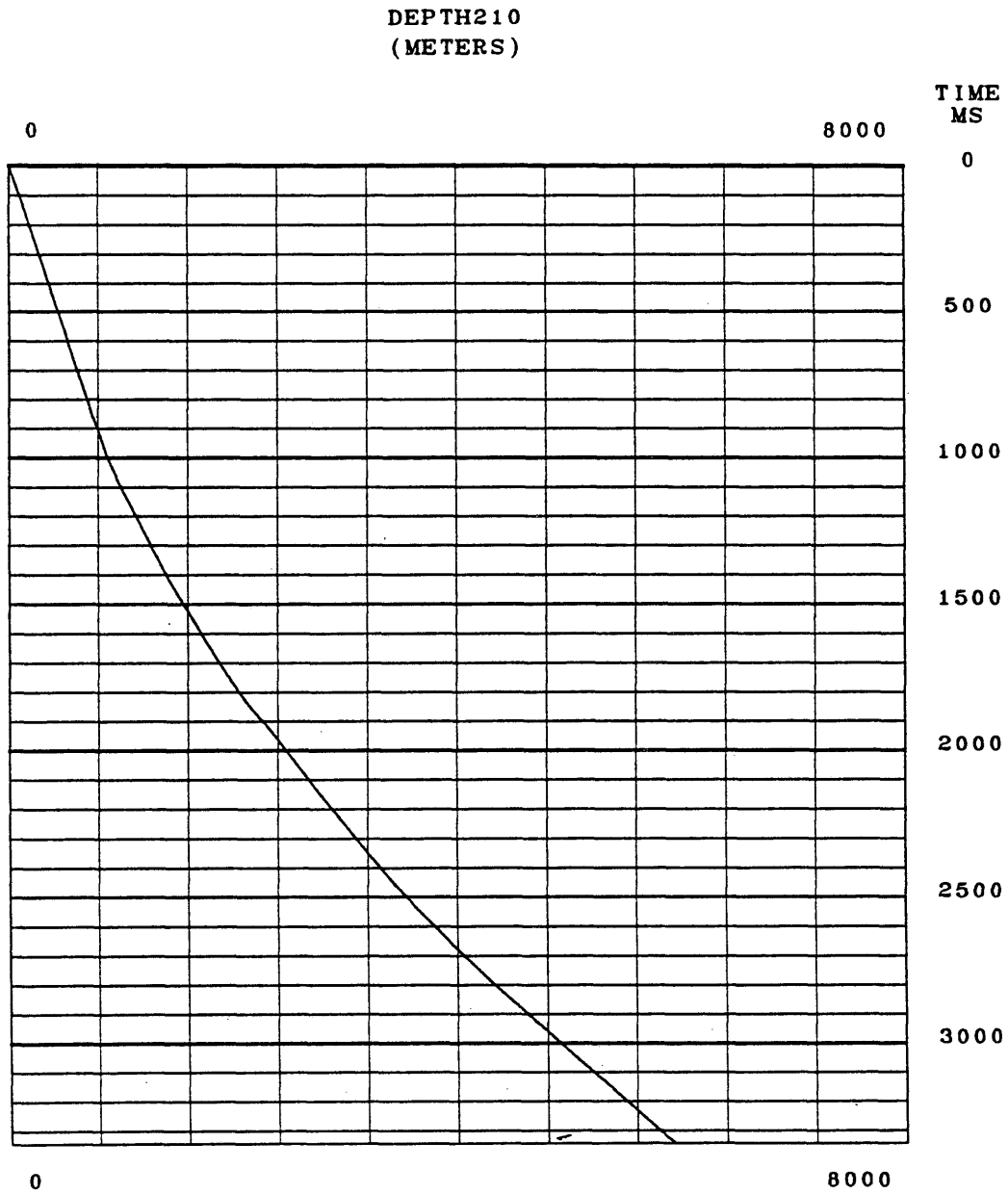


Figure B-8. Time-depth curve obtained from the checkshots of Shell-210 well in the Georges Bank Basin.

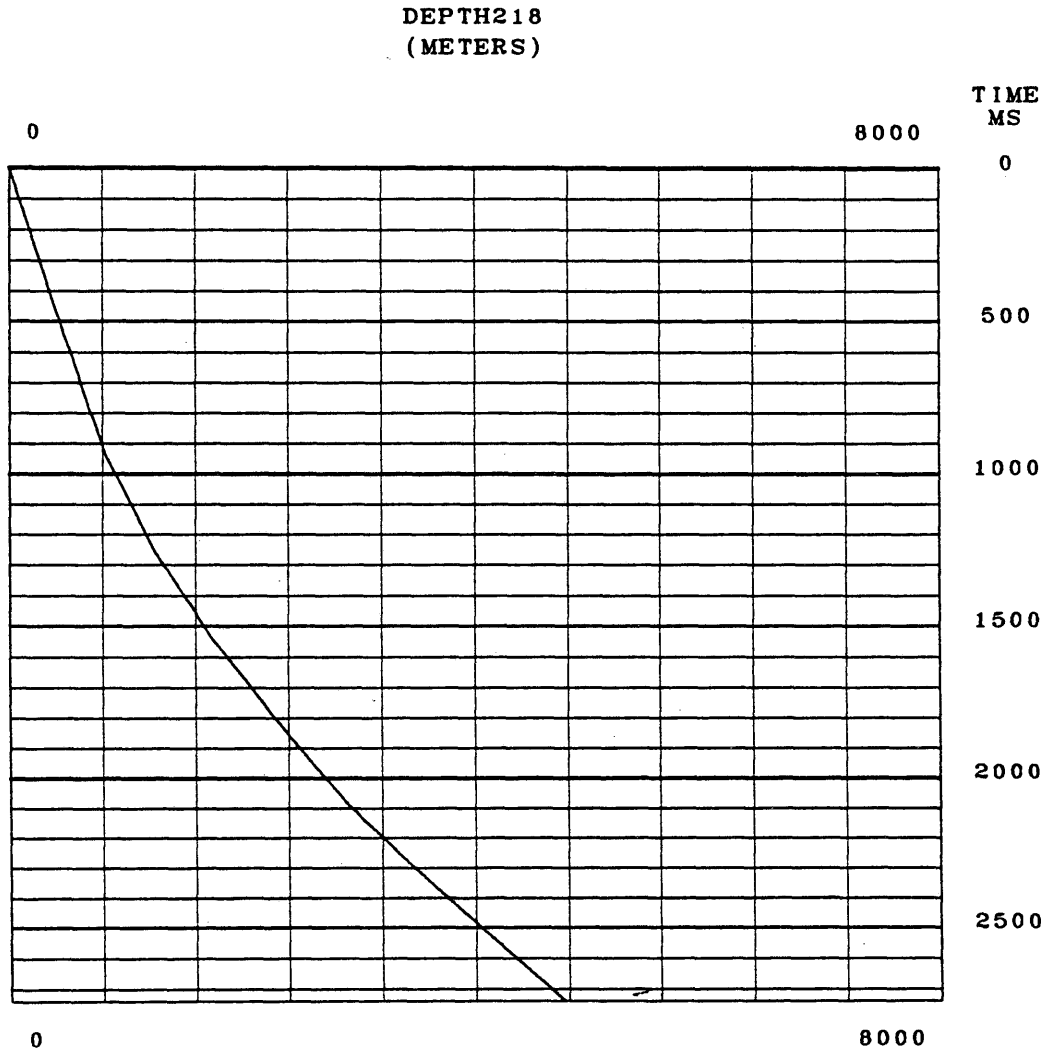


Figure B-9. Time-depth curve obtained from the checkshots of Shell-218 well in the Georges Bank Basin.

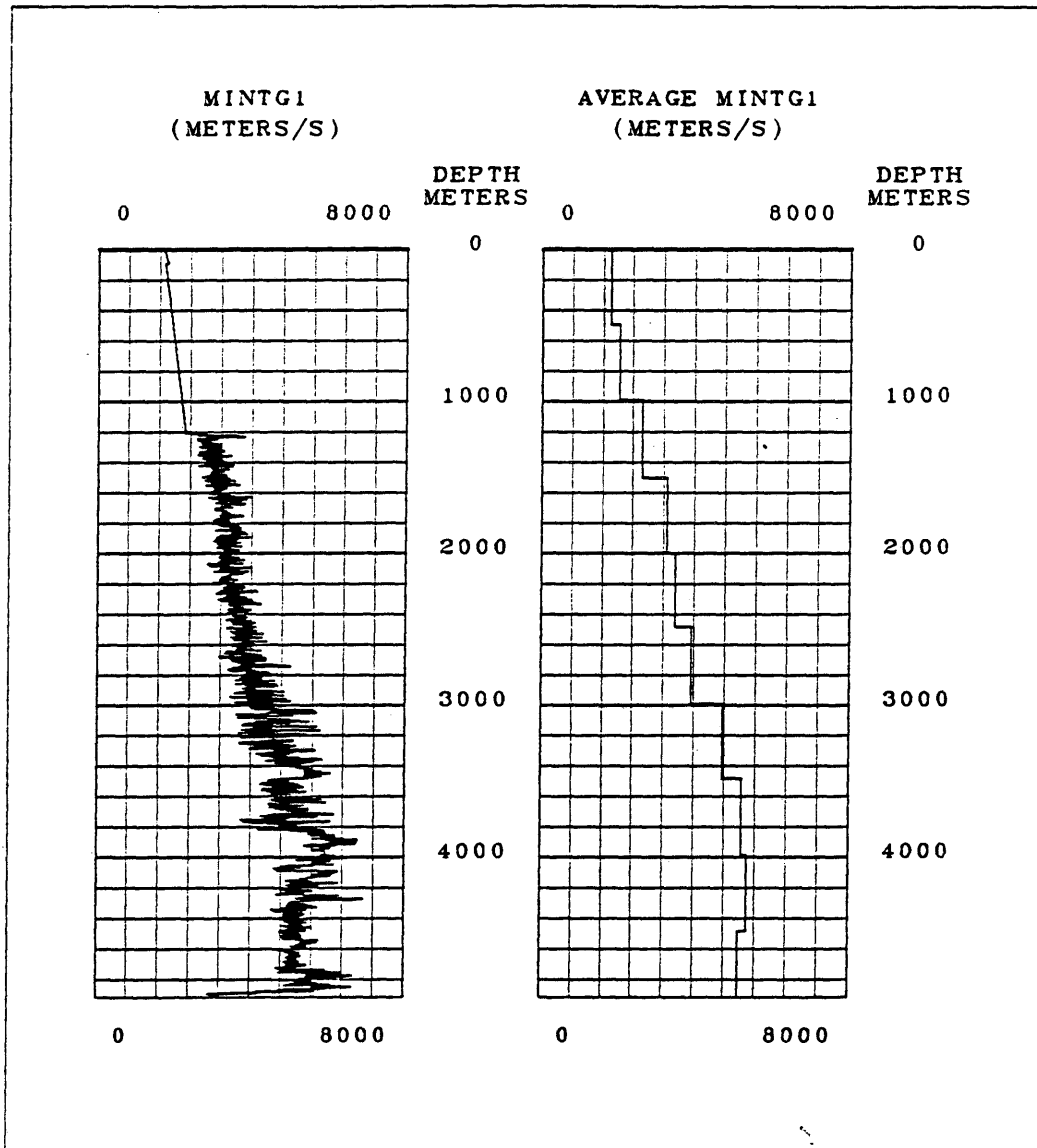


Figure C-1. Velocity and averaged interval velocity logs (at 500 m interval) obtained from the sonic log of COST G-1 well in the Georges Bank Basin.

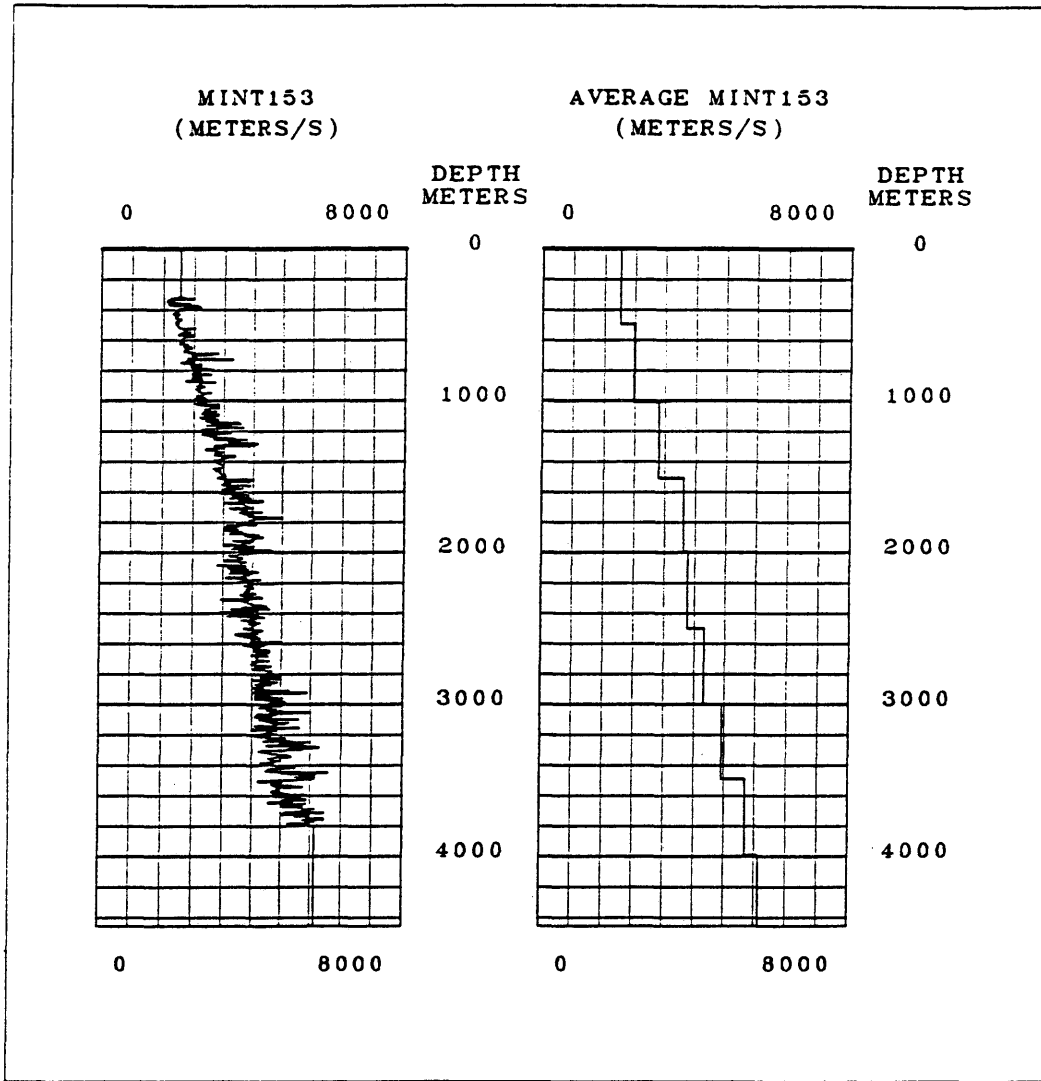


Figure C-2. Velocity and averaged interval velocity logs (at 500 m interval) obtained from the sonic log of Exxon-153 well in the Georges Bank Basin.

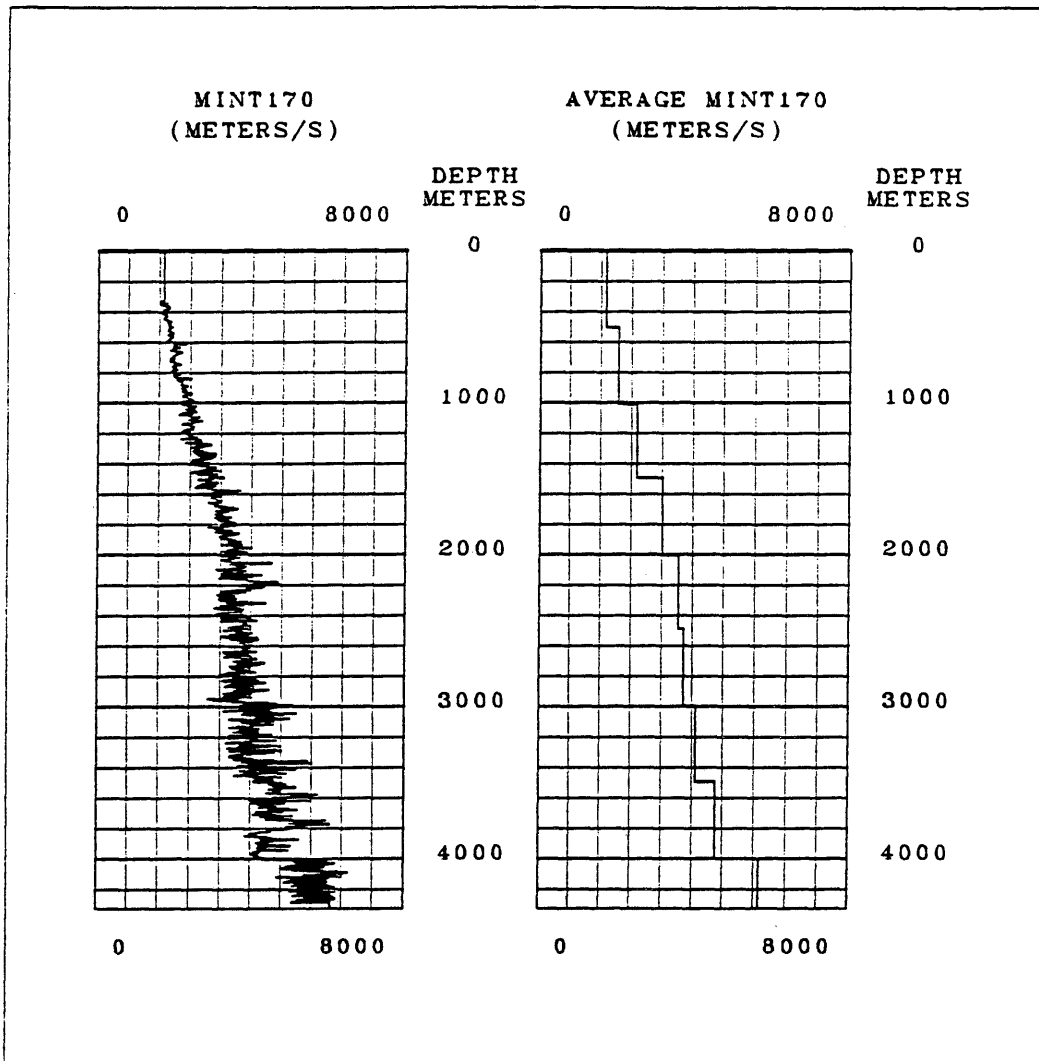


Figure C-3. Velocity and averaged interval velocity logs (at 500 m interval) obtained from the sonic log of Exxon-170 well in the Georges Bank Basin.

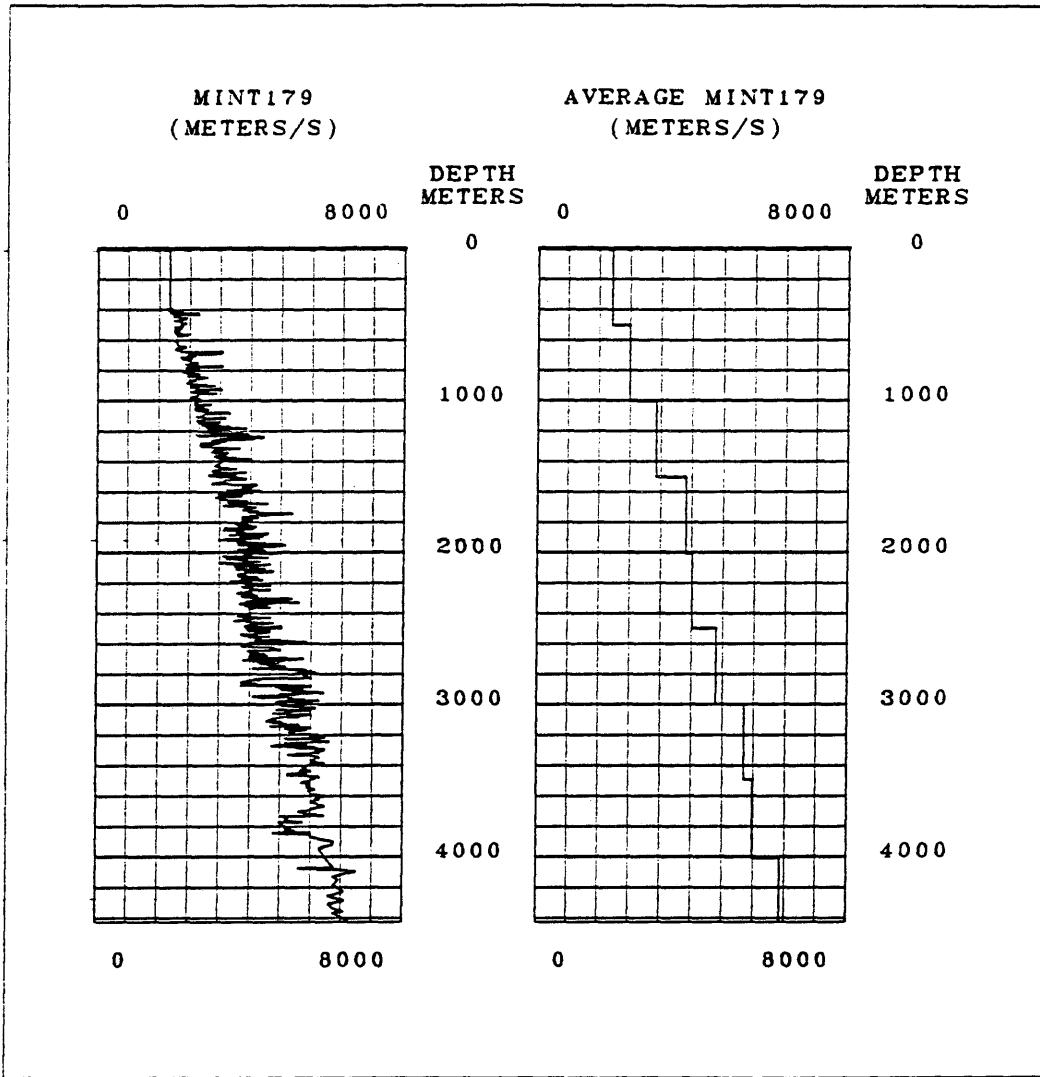


Figure C-4. Velocity and averaged interval velocity logs (at 500 m interval) obtained from the sonic log of Conoco-179 well in the Georges Bank Basin.

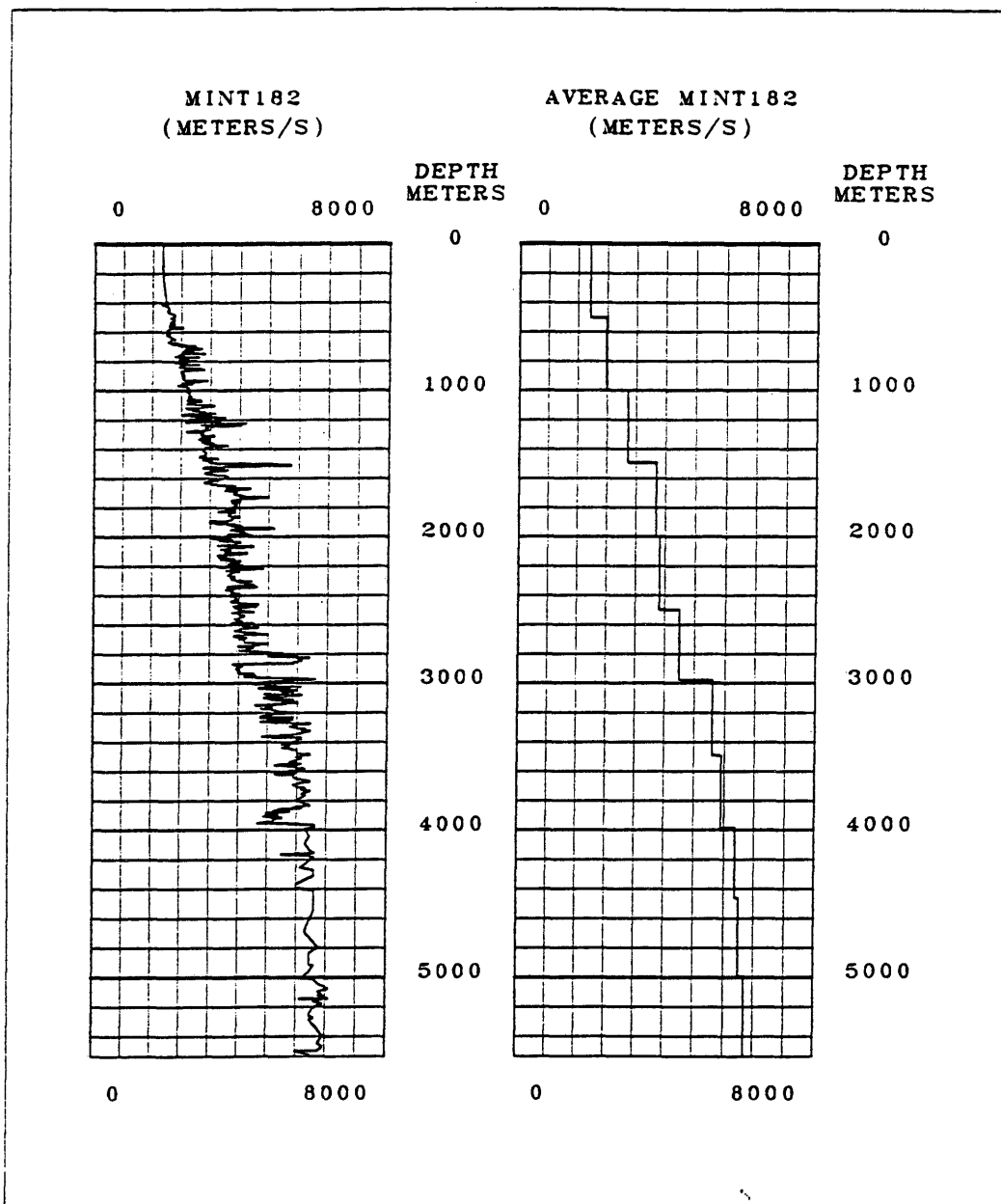


Figure C-5. Velocity and averaged interval velocity logs (at 500 m interval) obtained from the sonic log of Tenneco-182 well in the Georges Bank Basin.

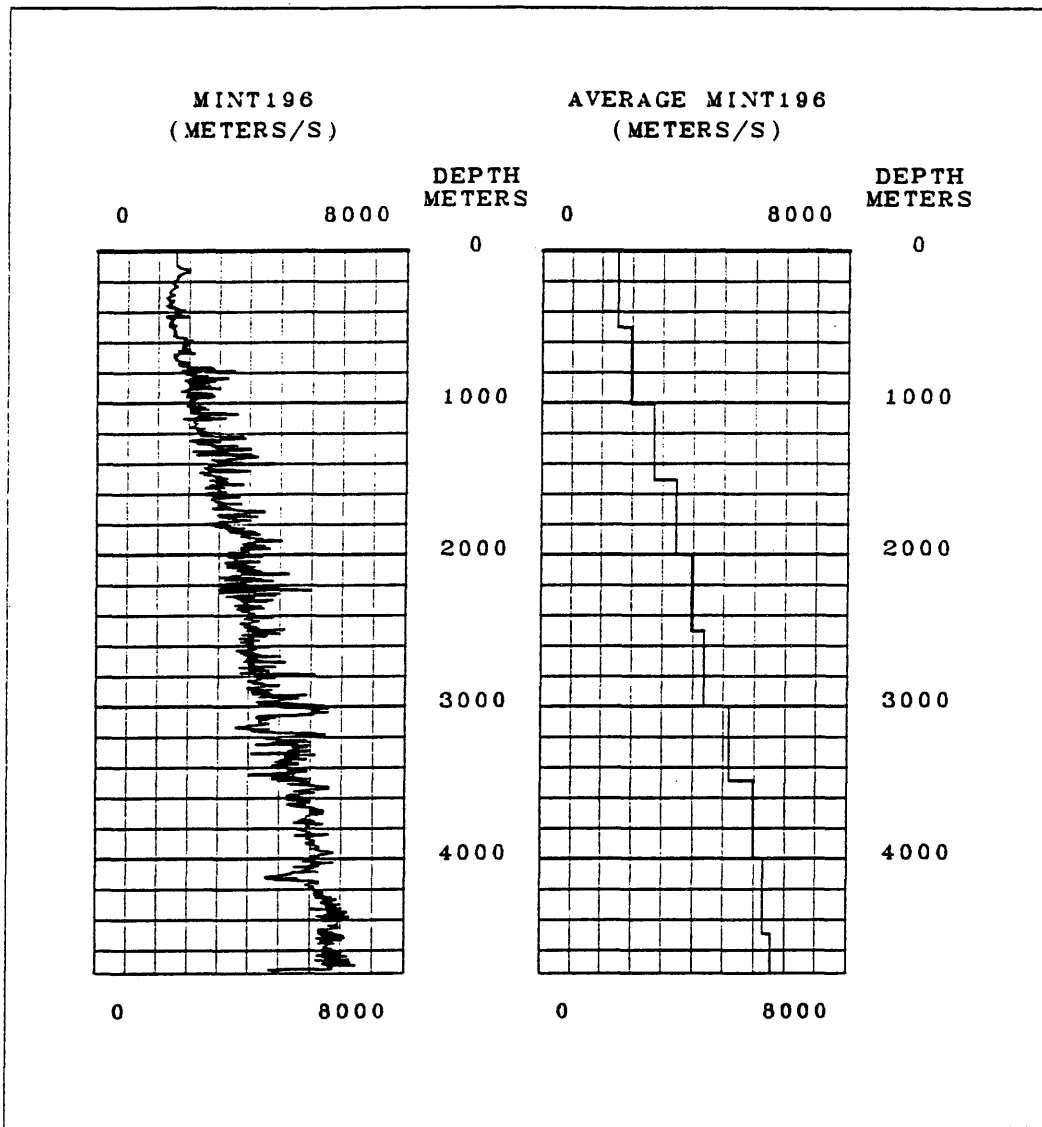


Figure C-6. Velocity and averaged interval velocity logs (at 500 m interval) obtained from the sonic log of Mobil-196 well in the Georges Bank Basin.

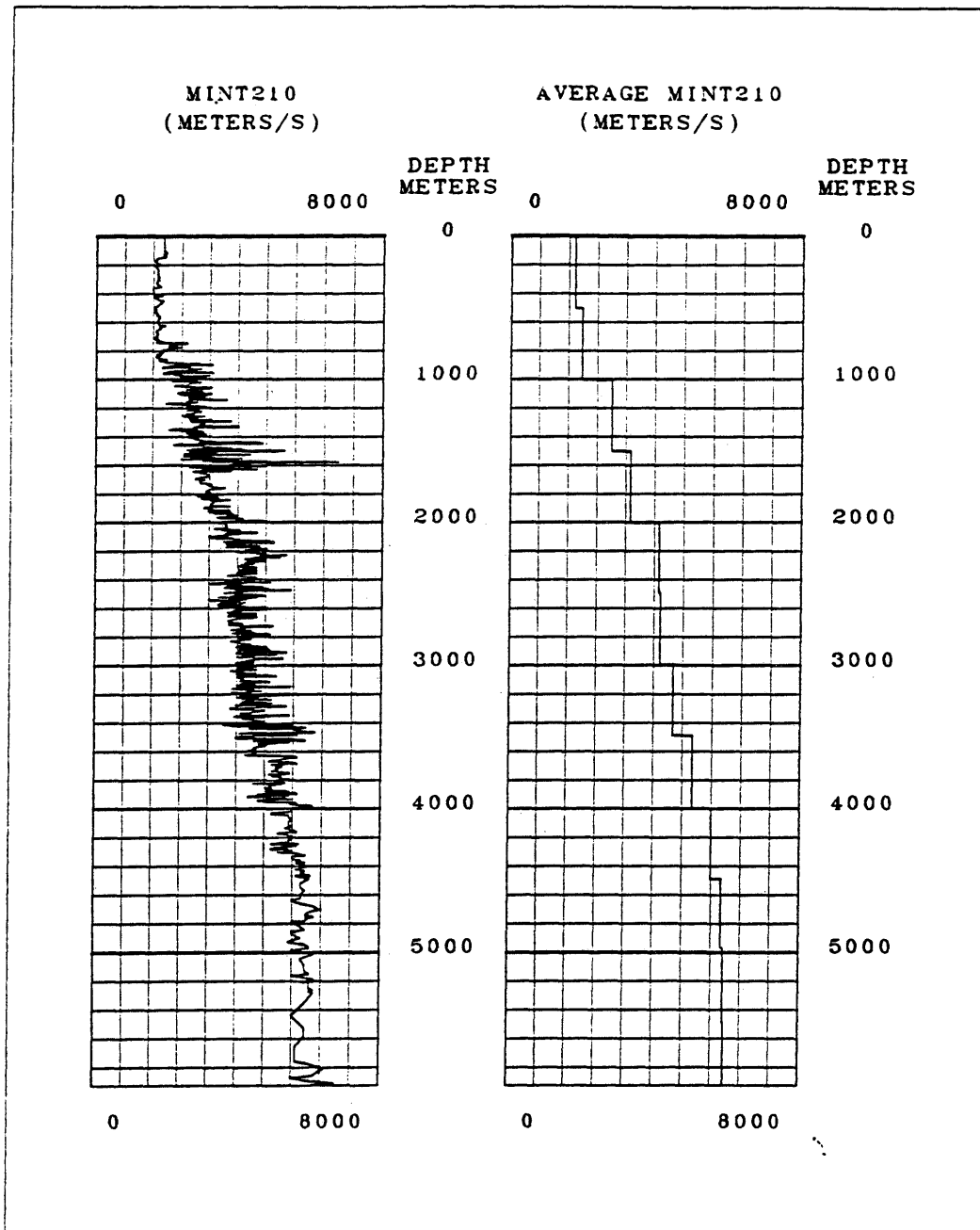


Figure C-7. Velocity and averaged interval velocity logs (at 500 m interval) obtained from the sonic log of Shell-210 well in the Georges Bank Basin.

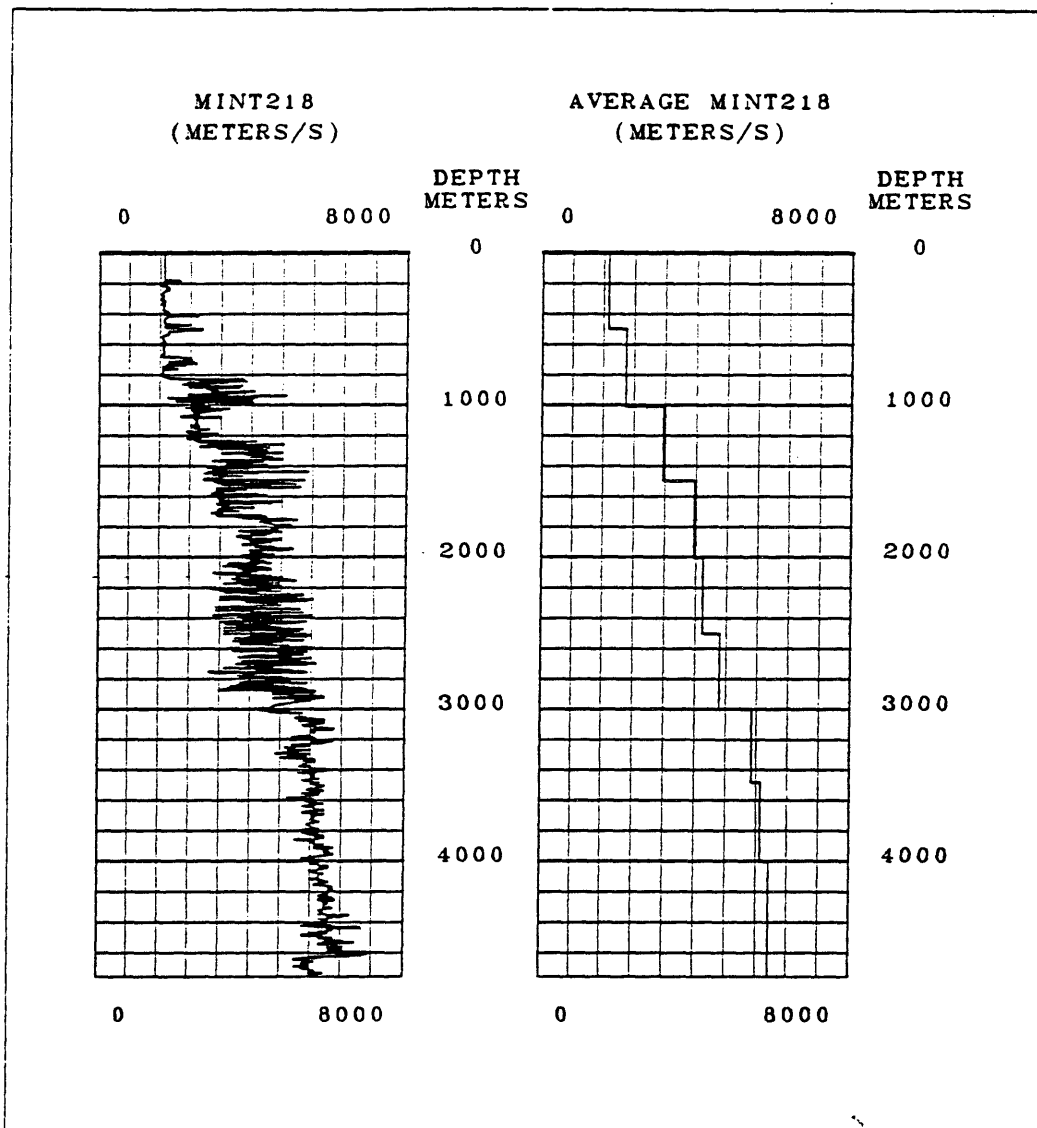


Figure C-8. Velocity and averaged interval velocity logs (at 500 m interval) obtained from the sonic log of Shell-218 well in the Georges Bank Basin.

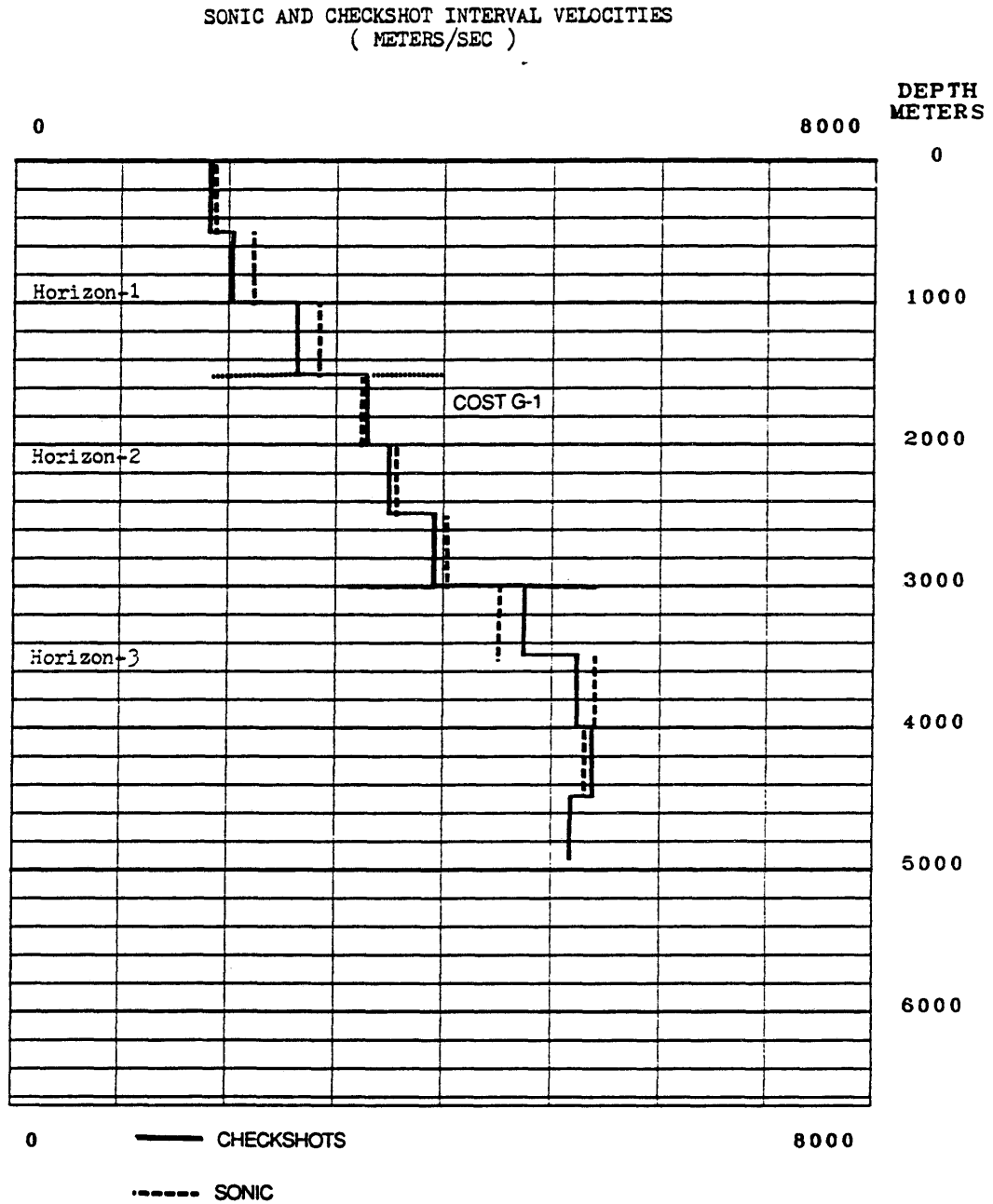


Figure D-1. A comparison of the checkshot and sonic interval velocities (at 500 m interval) at COST G-1 well site in the Georges Bank Basin.

SONIC AND CHECKSHOT INTERVAL VELOCITIES
(METERS/SEC)

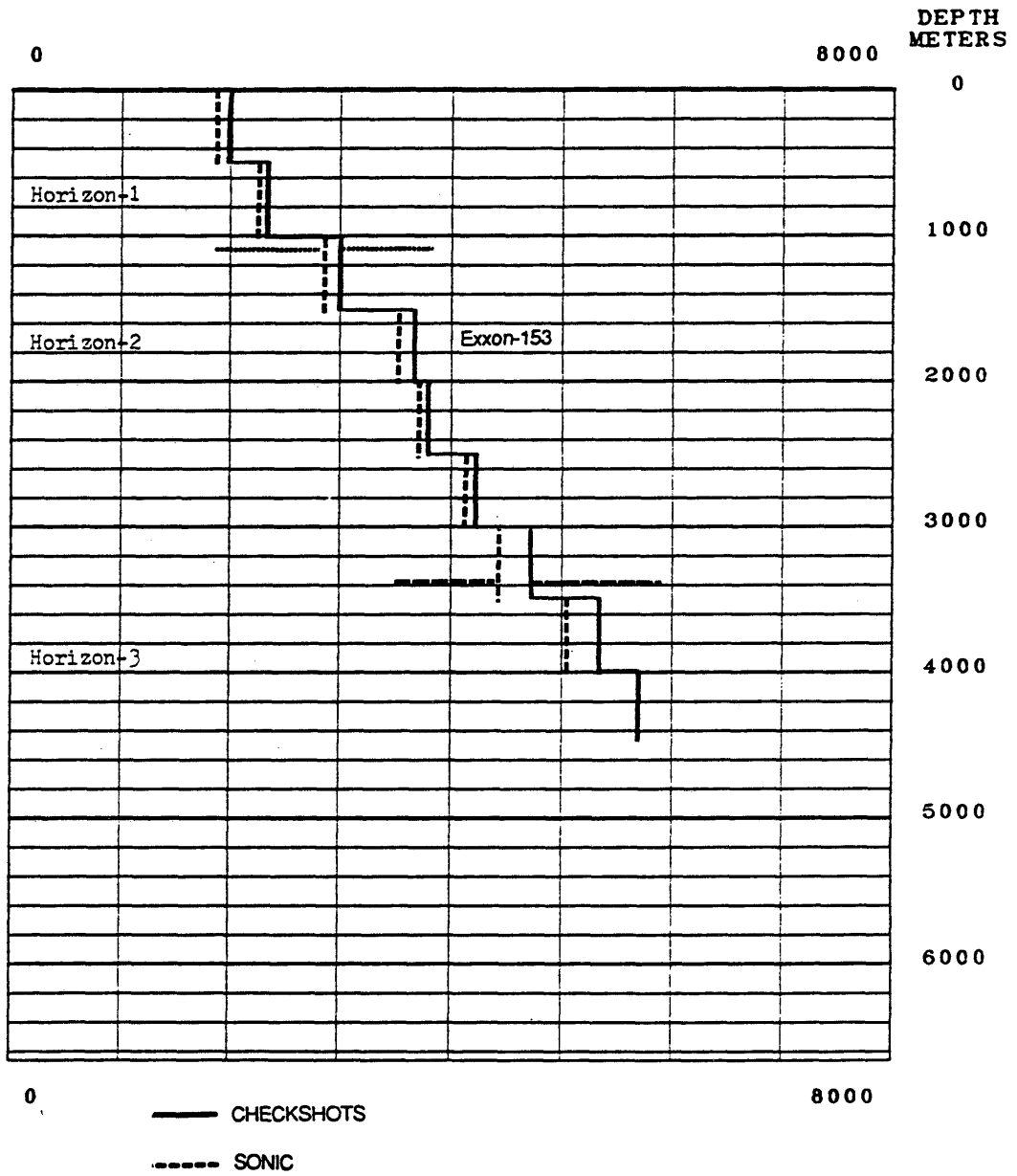


Figure D-2. A comparison of the checkshot and sonic interval velocities (at 500 m interval) at Exxon-153 well site in the Georges Bank Basin.

SONIC AND CHECKSHOT INTERVAL VELOCITIES
(METERS/SEC)

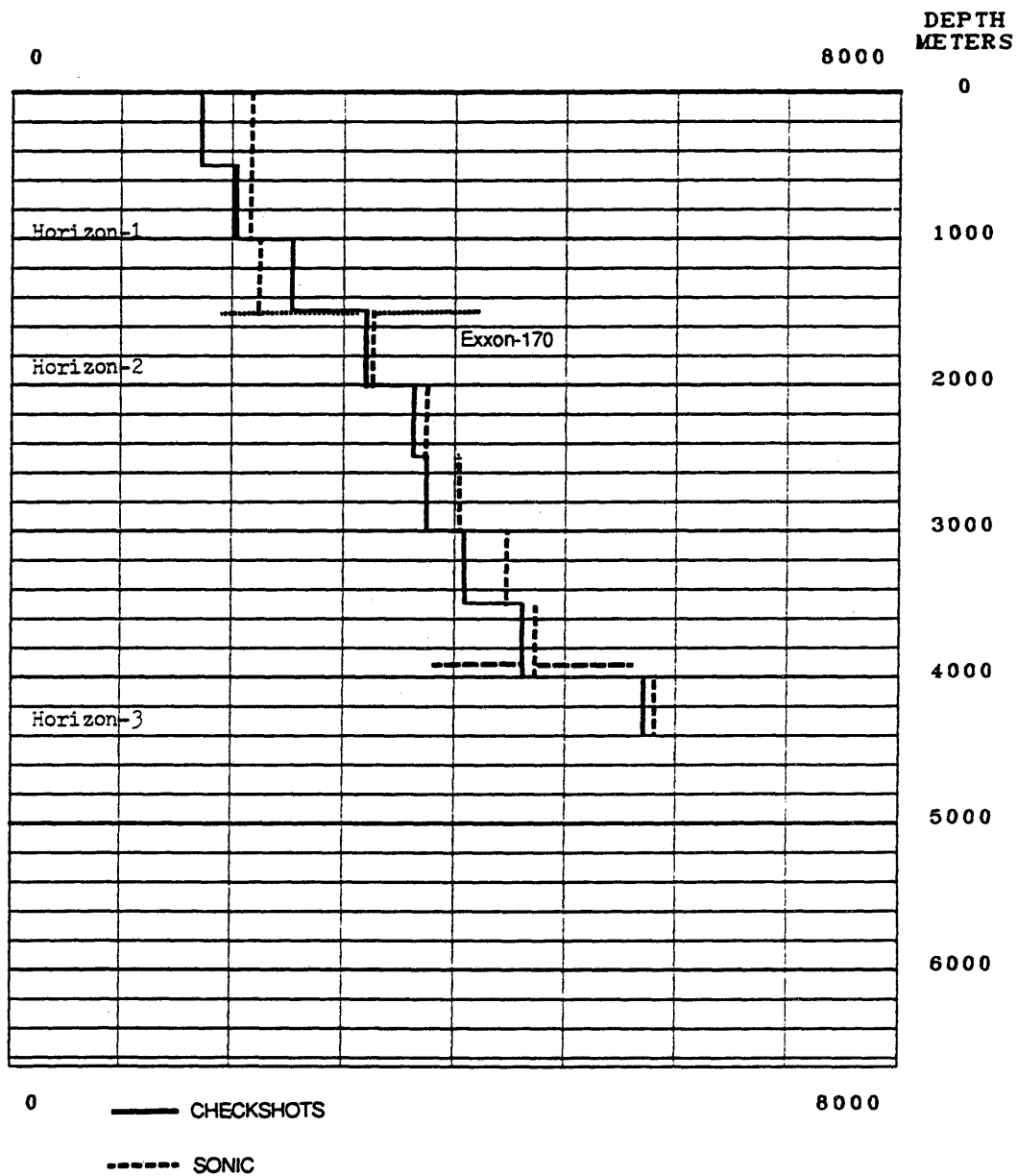


Figure D-3. A comparison of the checkshot and sonic interval velocities (at 500 m interval) at Exxon-170 well site in the Georges Bank Basin.

SONIC AND CHECKSHOT INTERVAL VELOCITIES
(METERS/SEC)

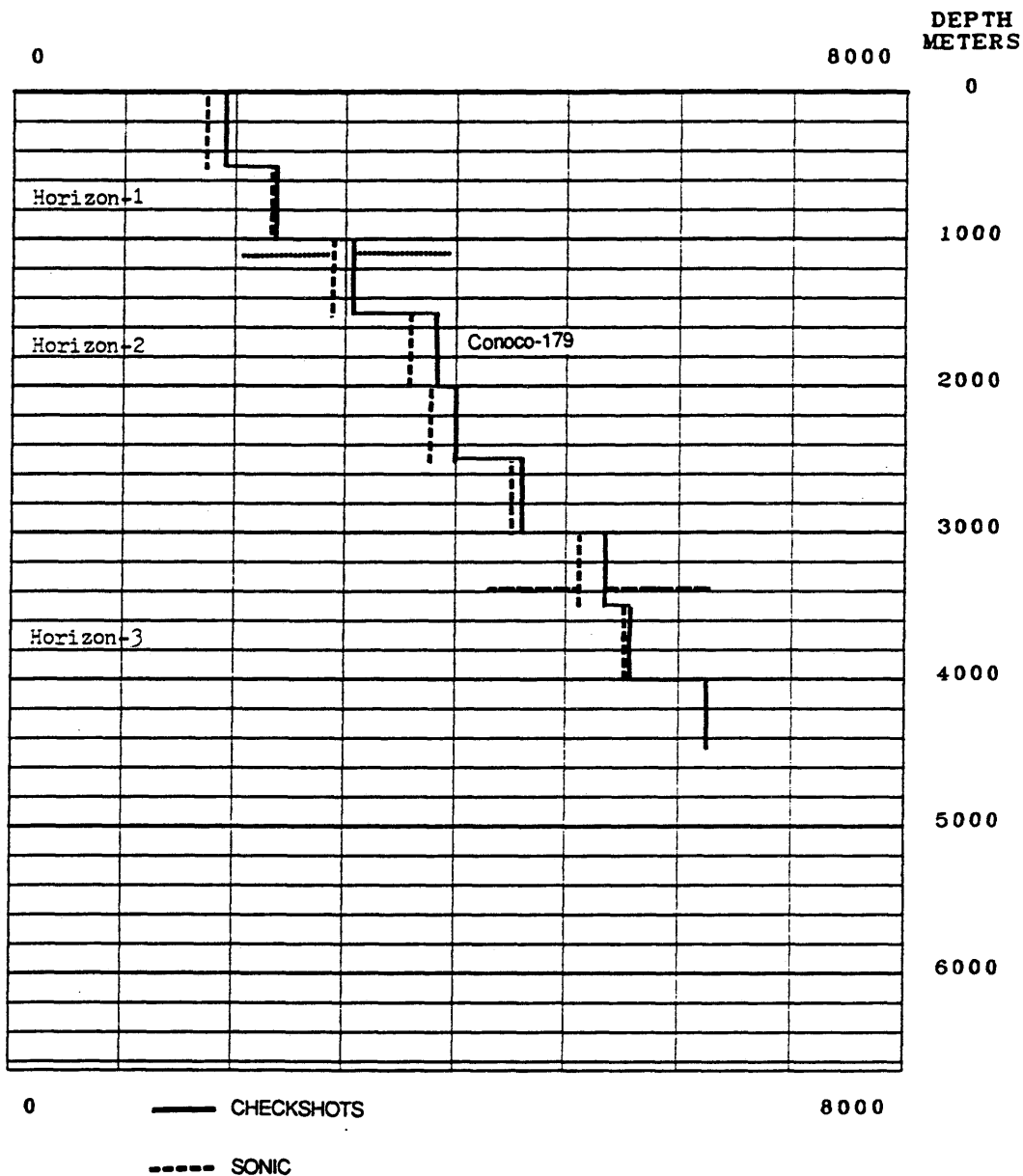


Figure D-4. A comparison of the checkshot and sonic interval velocities (at 500 m interval) at Conoco-179 well site in the Georges Bank Basin.

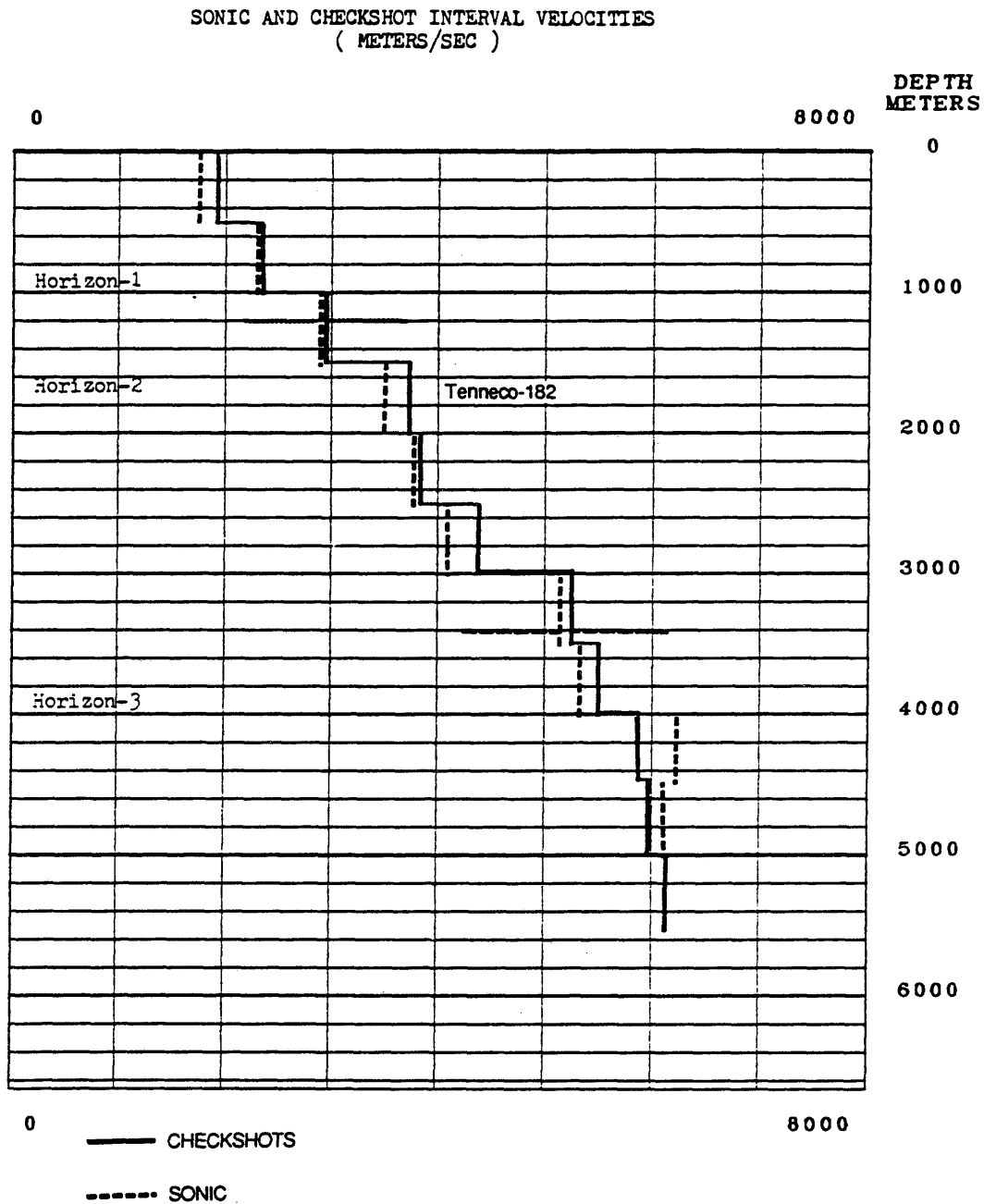


Figure D-5. A comparison of the checkshot and sonic interval velocities (at 500 m interval) at Tenneco-182 well site in the Georges Bank Basin.

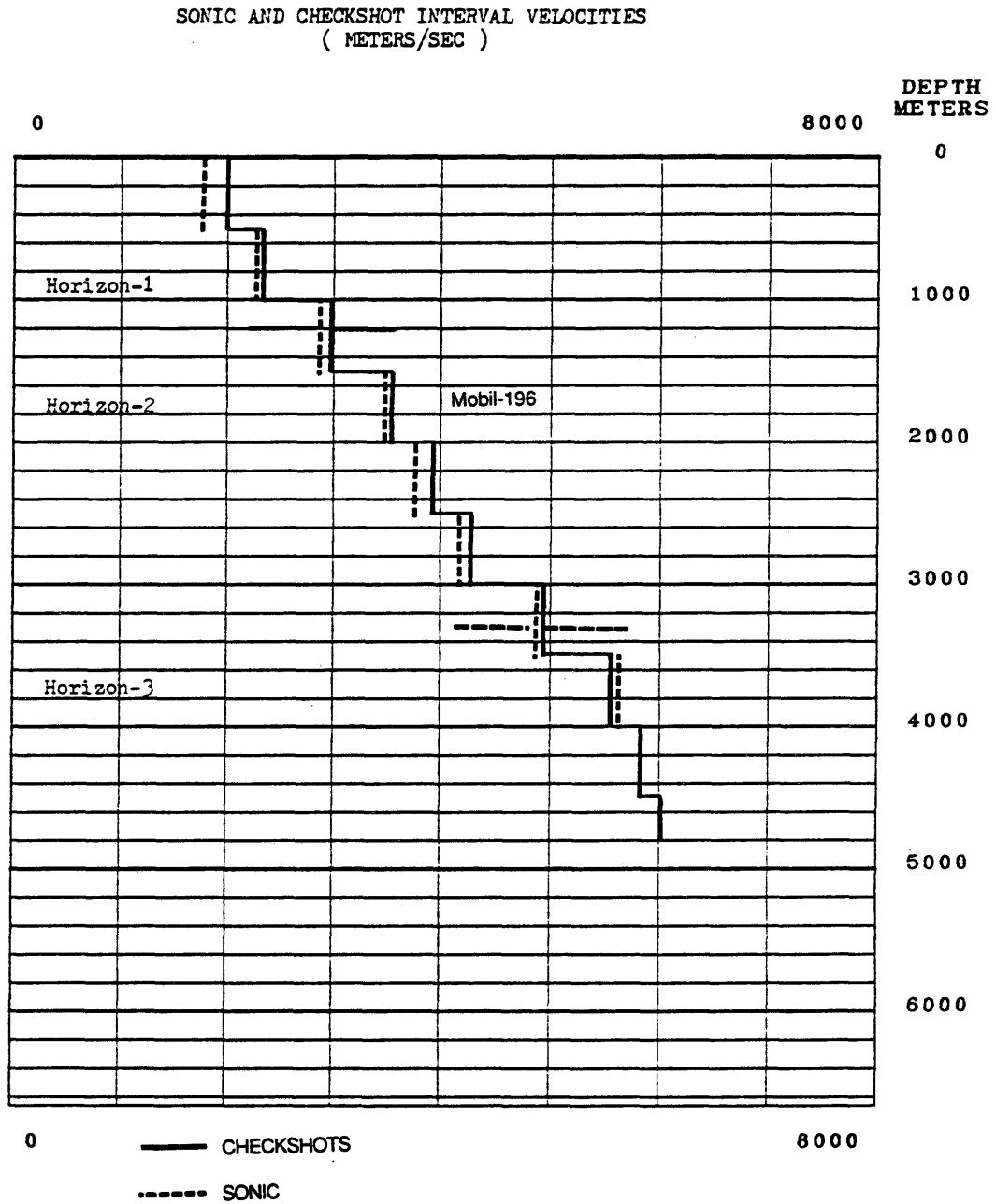


Figure D-6. A comparison of the checkshot and sonic interval velocities (at 500 m interval) at Mobil-196 well site in the Georges Bank Basin.

SONIC AND CHECKSHOT INTERVAL VELOCITIES
(METERS/SEC)

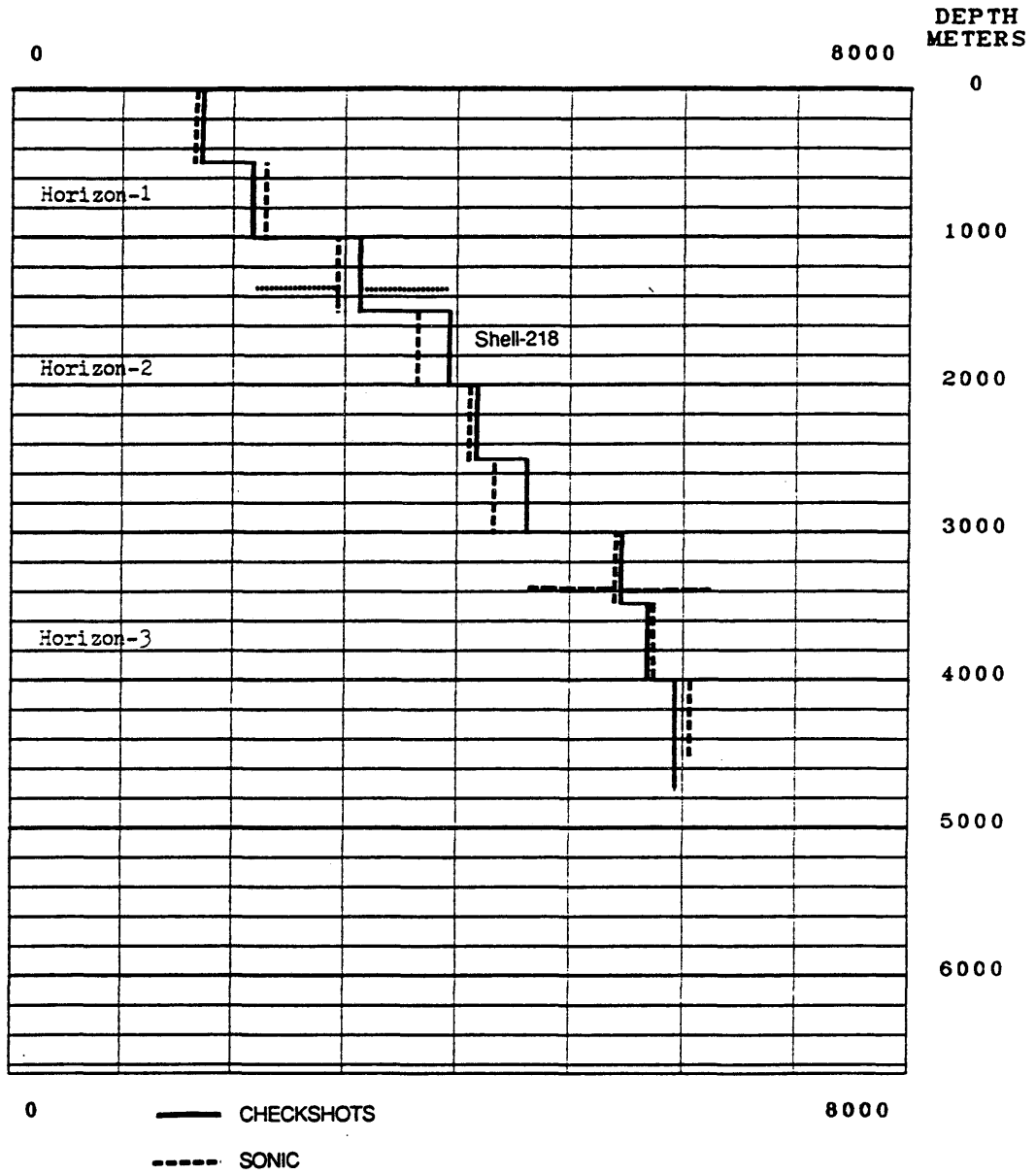


Figure D-8. A comparison of the checkshot and sonic interval velocities (at 500 m interval) at Shell-218 well site in the Georges Bank Basin.

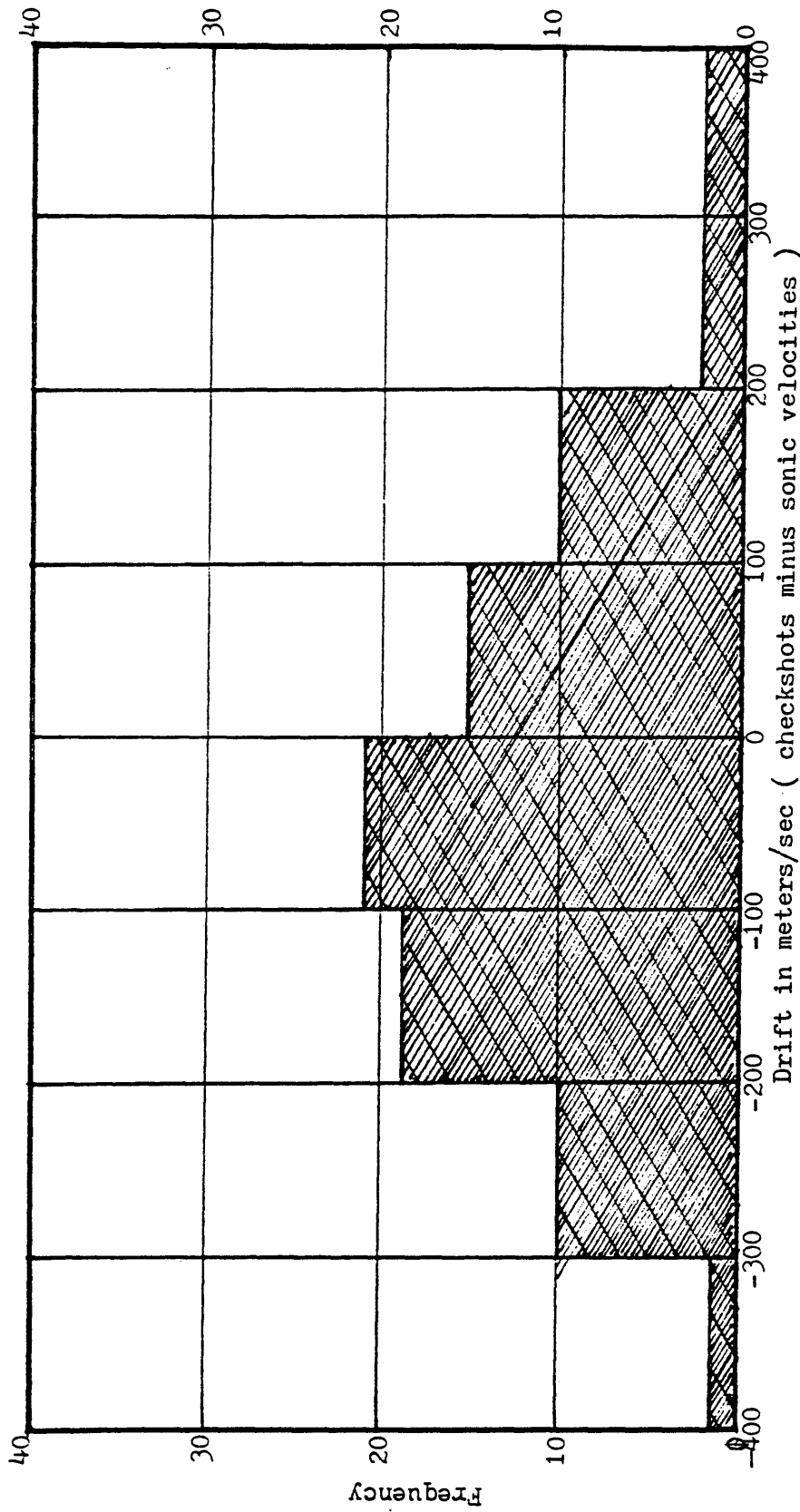


Figure D-10. A bar graph showing distribution of the drift of sonic interval velocities from the checkshot interval velocities (at 500 m interval) of nine wells in the Georges Bank Basin.

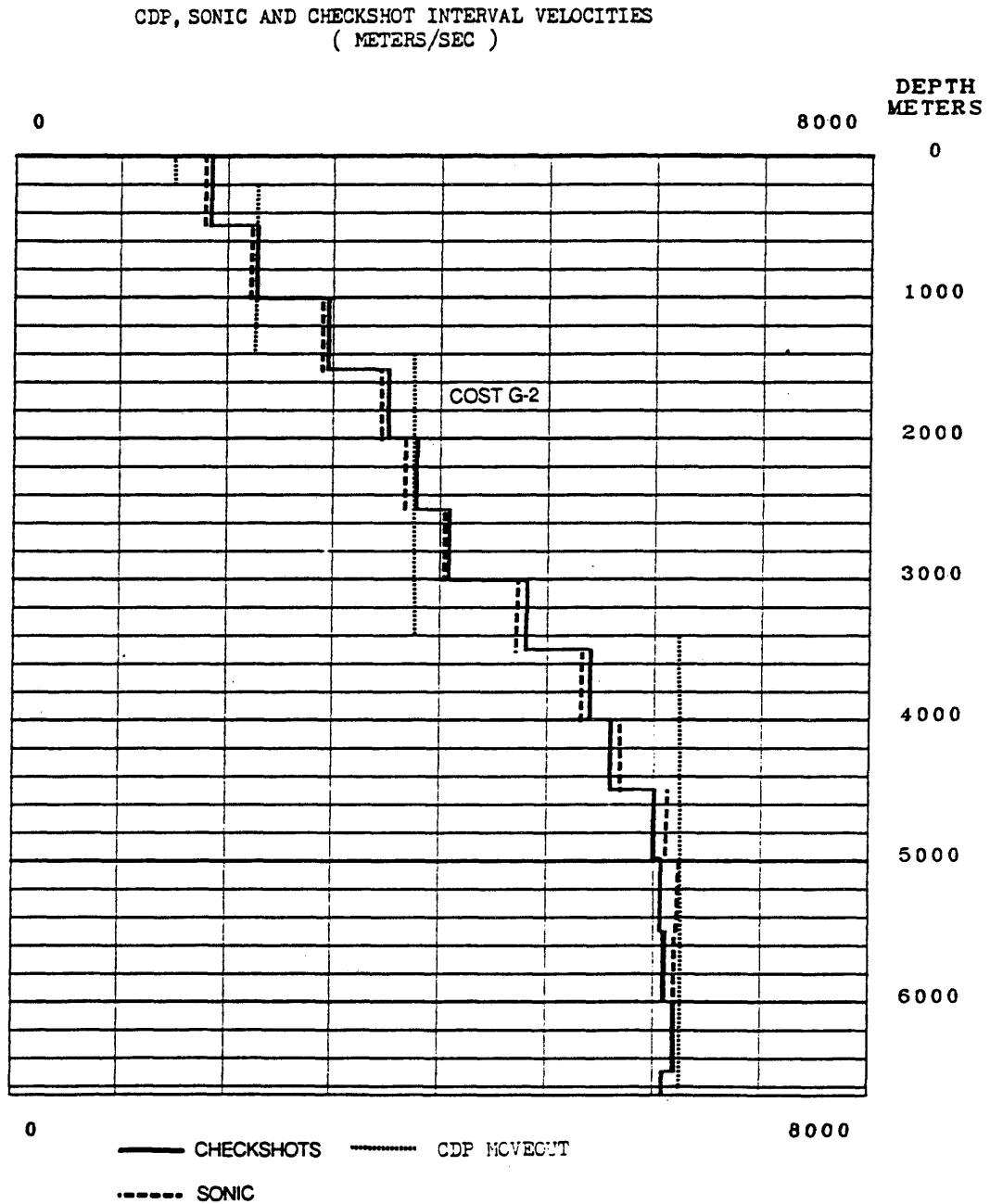


Figure D-11. A comparison of the interval velocities from CDP moveout velocities with sonic and checkshot interval velocities at the COST G-2 site.

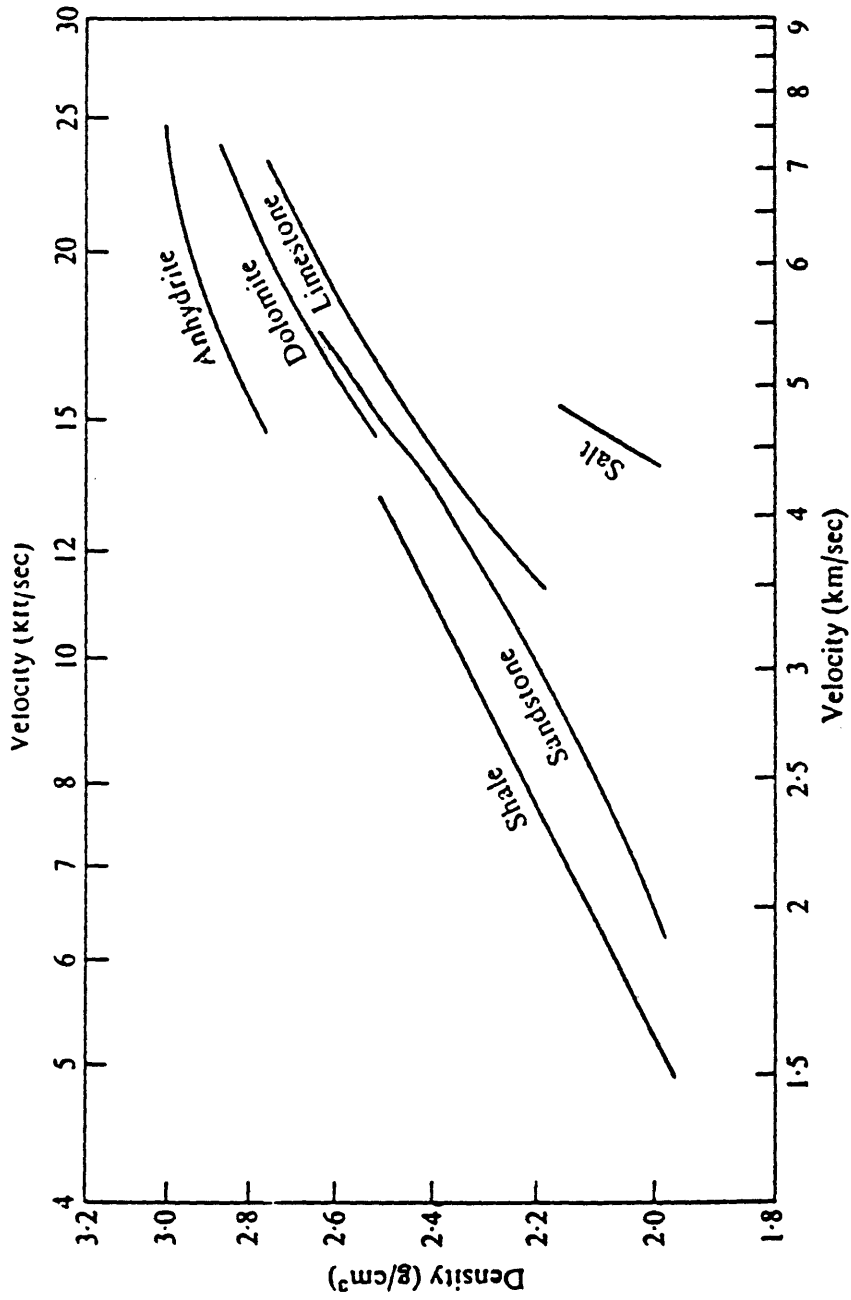


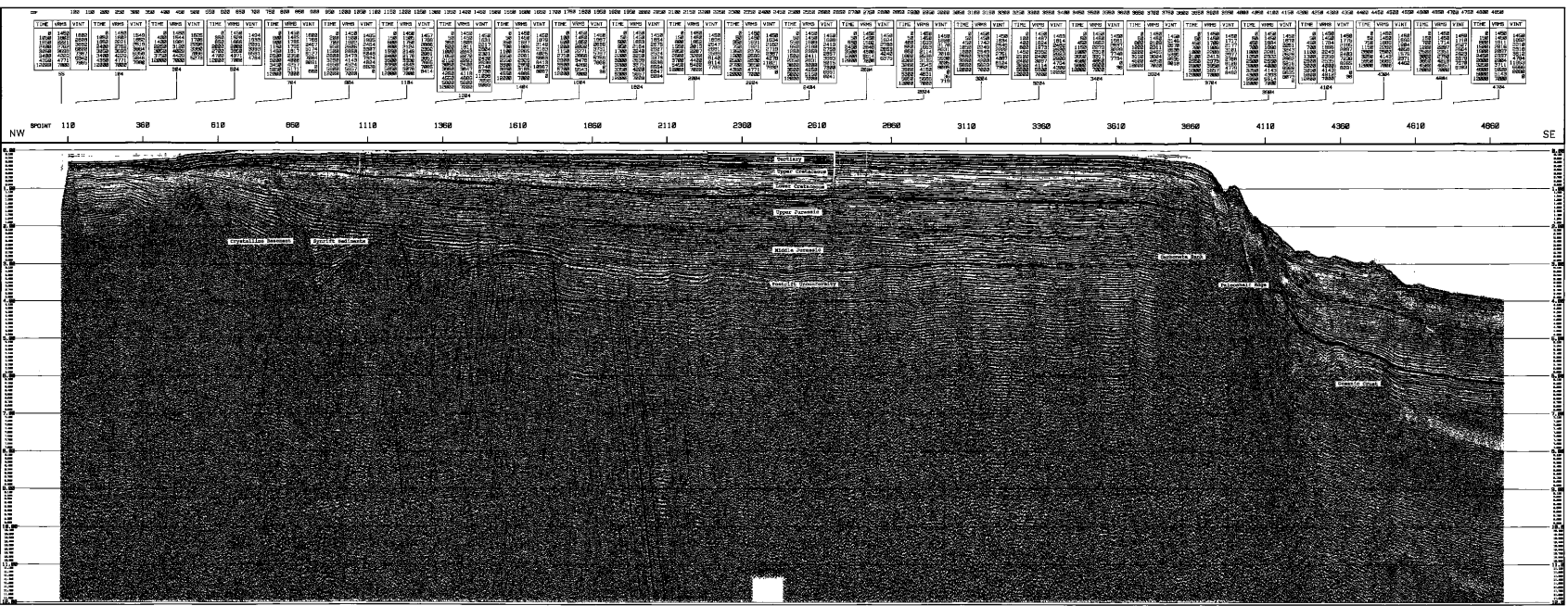
Figure E-1. Velocity-density relationships for different lithologies (log-log scale). (From Gardner et al., 1974.)

UNITED STATES
GEOLOGICAL SURVEY
GEORGES BANK
LINE: 19
REPROCESSED FINAL STACK, FILTERED
EAST
PROCESSED AT: U.S.G.S.
PETROLEUM GEOLOGY BRANCH
DOWNER FEDERAL CENTER
BY: M. LINDOR ALBA

RECORDING PARAMETERS
 RECORD BY: G. L. ...
 SURVEY NO.: ...
 DATE: ...
 TIME: ...
 LOCATION: ...
 INSTRUMENT: ...
 CHANNELS: ...
 SAMPLE RATE: ...
 GAIN: ...
 FILTER: ...
 GEOPHYSICIST: ...
 CHECKED BY: ...

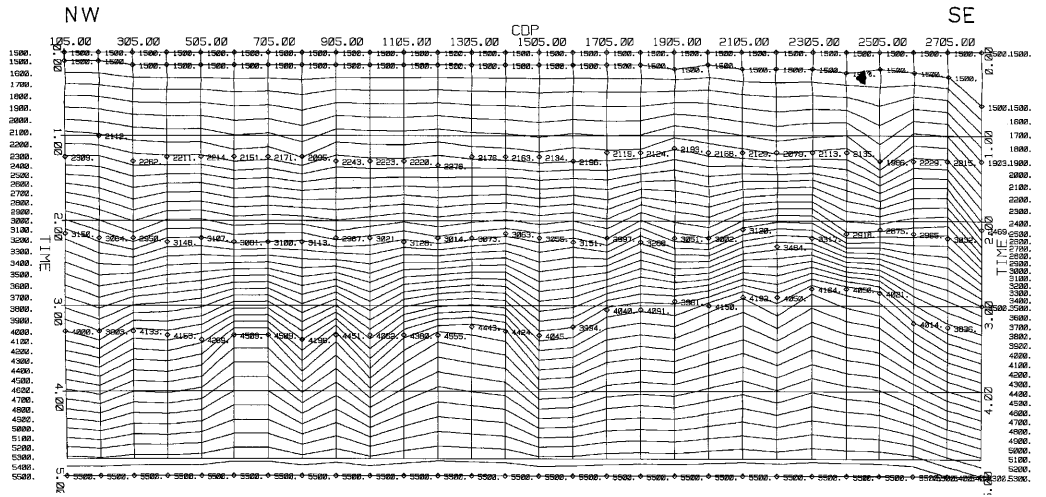
PROCESSING SEQUENCE
 01 DEBLITZING
 02 GEOMETRIC CORRECTION
 03 VELOCITY CORRECTION
 04 TIME CORRECTION
 05 ANTI-DIP CORRECTION
 06 STACKING
 07 SCALED
 08 SILENCING
 09 GAIN
 10 FILTER
 11 SCALED
 12 SILENCING
 13 GAIN
 14 FILTER
 15 SCALED
 16 SILENCING
 17 GAIN
 18 FILTER
 19 SCALED
 20 SILENCING
 21 GAIN
 22 FILTER
 23 SCALED
 24 SILENCING
 25 GAIN
 26 FILTER
 27 SCALED
 28 SILENCING
 29 GAIN
 30 FILTER

DISPLAY PARAMETERS
 TRACKS PER TRAIL: 100
 HORIZONTAL SCALE: 1 IN = 5000 FT
 VERTICAL SCALE: 1 IN = 100 MS
 POLARITY: NORMAL
 DISPLAY OPTION: NONE
 DISPLAY DATE: OCT 22, 1990



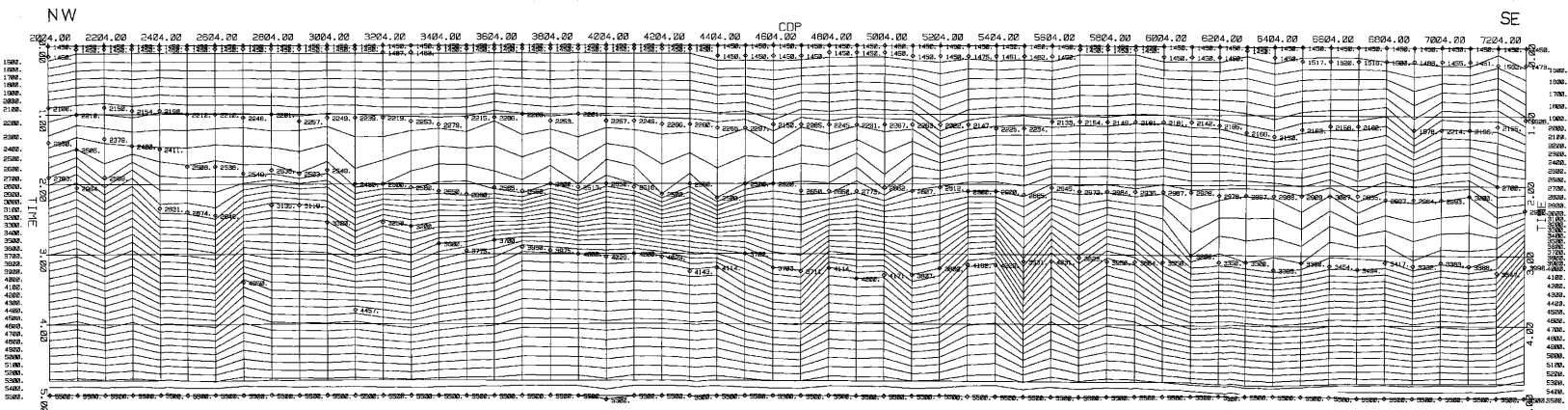
UNITED STATES GEOLOGICAL SURVEY
 PETROLEUM GEOLOGY BRANCH
 DOWNER FEDERAL CENTER
 WASHINGTON, D.C. 20548
 OCT 22, 1990

ISO-VELOCITY CONTOURS
PROJECT: POWDER
IDENT: SMO 209
LINE NAME LINE209
DATE 11/4 /88



DATE: 4/10/88 15:59
FLUT JOBID: 16 51 1 CT 1
USER: ALM

ISO-VELOCITY CONTOURS
PROJECT: POWDER
IDENT: SMO 19
LINE NAME LINE19
DATE 11/4 /88



DATE: 4/10/88 15:59
FLUT JOBID: 16 51 1 CT 1
USER: ALM